

---

Masters

Science

---

2018-6

## Modulation of Primary Amine Oxidase by Phytochemicals

Padraig Shanahan

*Dublin Institute of Technology*, padraigshanahan@icloud.com

Follow this and additional works at: <https://arrow.tudublin.ie/scienmas>

 Part of the [Medicine and Health Sciences Commons](#)

---

### Recommended Citation

Shanahan, P. (2018) Modulation of Primary Amine Oxidase by Phytochemicals, MA, Technological University Dublin. doi.org/10.21427/m580-nk39

This Theses, Masters is brought to you for free and open access by the Science at ARROW@TU Dublin. It has been accepted for inclusion in Masters by an authorized administrator of ARROW@TU Dublin. For more information, please contact [yvonne.desmond@tudublin.ie](mailto:yvonne.desmond@tudublin.ie), [arrow.admin@tudublin.ie](mailto:arrow.admin@tudublin.ie), [brian.widdis@tudublin.ie](mailto:brian.widdis@tudublin.ie).



This work is licensed under a [Creative Commons Attribution-Noncommercial-Share Alike 3.0 License](#)

# Modulation of Primary Amine Oxidase by Phytochemicals.

**Padraig Shanahan B.Sc.**



**Department of Food Science & Environmental Health  
Dublin Institute of Technology**

A thesis submitted to Dublin Institute of Technology for the award of Master of  
Philosophy

**Research Supervisors:**

Professor Gary T.M. Henehan

Dr. Barry Ryan

Dr. Gemma K Kinsella

**June 2018**

## **Declaration**

I certify that this thesis which I now submit for examination for the award of M.Phil, is entirely my own work and has not been taken from the work of others, save and to the extent that such work has been cited and acknowledged within the text of my work. This thesis was prepared according to the regulations for graduate study by research of the Dublin Institute of Technology and has not been submitted in whole or in part for another award in any other third level institution.

The work reported on in this thesis conforms to the principles and requirements of the DIT's guidelines for ethics in research.

DIT has permission to keep, lend or copy this thesis in whole or in part, on condition that any such use of the material of the thesis be duly acknowledged.

\_\_\_\_\_ Date \_\_\_\_\_

Padraig Shanahan

## **Acknowledgements**

I would like to firstly thank all my supervisors for their hard work and patience in getting this thesis over the line. Prof. Gary Henehan, Dr. Barry Ryan, Dr. Gemma Kinsella and Dr. Jeff O’Sullivan, who all worked hard and were generous in giving their time, advice and support throughout this thesis. There were definitely a few bumps along the way but I appreciate the fact you all stuck it out till the end so I could finally manage to submit it!

I would like to thank all the staff in DIT for all their help and support especially Tony Hutchinson who was a great help on the 4<sup>th</sup> floor and also the staff in Trinity College who kindly took me in and gave me use of their facilities.

I would also like to thank Dr. Rachel Hearne for all her time, support and advice in helping to proof read and amend this thesis. You were pivotal in getting this thesis submitted which I greatly appreciate.

I would finally like to thank all my family and friends who gave encouragement and good advice when needed most.

## **Abstract**

Primary Amine Oxidase (PrAO) is an enzyme with a variety of physiological roles. It catalyses the oxidative deamination of primary amines to the corresponding aldehydes. PrAO converts amines such as methylamine and aminoacetone to reactive compounds that can damage small blood vessel proteins. It also acts as a vascular adhesion protein (VAP-1) where it is essential for the migration of leukocytes through the vascular endothelium. Inhibitors of PrAO have been reported to have anti-cancer, anti-diabetic and anti-inflammatory action. In this study we explore the interaction between dietary phytochemicals and Bovine PrAO.

Methylxanthines (MXs) are food alkaloids having a positive association with good health. Of several MXs we examined, only caffeine and theobromine were found to be inhibitors of PrAO. Structure activity relationships along with *in silico* modelling and inhibition studies allowed us to identify a unique site for MX binding to PrAO.

Green Tea extracts also inhibited PrAO but these reactive compounds were shown to give complex inhibition patterns due to the formation of non-enzymatic reaction products and interference in assay procedures. Despite these difficulties we found some evidence of direct inhibition of PrAO by Green Tea catechins. A number of other compounds tested showed a similar ability to inhibit PrAO.

Taken together these studies show the potential for a variety of dietary compounds to inhibit the activity of this key enzyme. The role of PrAO inhibition by such phytochemicals in health and disease is discussed.

## Table of Contents

<b>Acknowledgements</b> .....	<b>iii</b>
<b>Abstract</b> .....	<b>iv</b>
<b>Table of Contents</b> .....	<b>v</b>
<b>List of Abbreviations</b> .....	<b>viii</b>
<b>List of Figures</b> .....	<b>x</b>
<b>List of Tables</b> .....	<b>xii</b>
<b>Chapter 1 Introduction</b> .....	<b>1</b>
1.0 Diet and health benefits .....	2
1.1 Amine Oxidases.....	5
1.2 PrAO: An Introduction .....	7
1.2.1 PrAO Molecular Structure.....	9
1.2.2 Inter species variation in PrAO active site ligand access. ....	10
1.3 Physiological role of PrAO.....	13
1.4 PrAO catalysed Oxidation of Amines .....	16
1.5 PrAO Substrates .....	18
1.5.1 Sources of Amines.....	19
1.6 PrAO and Disease.....	21
1.6.1 Elevated PrAO Activity and Disease.....	22
1.6.2 VAP-1 and Inflammation .....	23
1.7 Inhibitors of PrAO .....	24
1.7.1 Inhibition of PrAO.....	26
1.8 Dietary components in Health and disease .....	27
1.8.1 Caffeine and Related Methylxanthines.....	28
1.8.2 Green Tea .....	31
1.8.3 Amino Acids.....	34
1.8.4 Vitamins and Health Benefits.....	35
1.9 Computational Modelling.....	36
1.9.1 Molecular Docking.....	37
1.9.2 Molecular Docking with AutoDock Tools .....	40
1.10 Proposed Research and Aims .....	42
<b>Chapter 2 Materials &amp; Methods</b> .....	<b>44</b>
2.1 List of Reagents .....	45
2.2 List of Instrumentation & Equipment.....	47
2.3 Preparation of PrAO for Storage and Use .....	48
2.4 Preparation of Substrates, Controls and Inhibitor Solutions.....	48

2.5	U.V. Spectrophotometric assay of PrAO; Benzaldehyde Production at 254 nm.....	49
2.5.1	Holt Coupled-Assay of PrAO Monitoring Hydrogen Peroxide Production .....	50
2.5.2	Preparation of Chromogenic Solution for H <sub>2</sub> O <sub>2</sub> .....	51
2.5.3	HPLC Assay for Monitoring Inhibition of Benzaldehyde at 254 nm.....	51
2.6	Green Tea Extraction.....	52
2.7	IC <sub>50</sub> Inhibition Plots.....	53
2.8	Lineweaver Burk Plots and Ki Estimation .....	53
2.9	PrAO Computational Docking Studies.....	54
2.9.1	Grid File Generation.....	55
2.9.2	Grid Size Determination.....	55
2.9.3	Docking Algorithm.....	56
	<b>Chapter 3 Results.....</b>	<b>57</b>
3.1	Introduction .....	58
3.2	HPLC-based PrAO assay monitoring benzaldehyde formation .....	59
3.3	Polyphenol Screening of PrAO Modulation.....	64
3.3.1	Green Tea Catechins.....	64
3.3.2	Computational Modelling of ECG, EGCG, and Epicatechin binding to PrAO.....	74
3.3.3	Octopamine Inhibition of PrAO .....	79
3.3.4	Quercetin .....	83
3.3.5	Umbelliferone.....	87
3.4	Methylxanthines and related compounds as PrAO inhibitors.....	88
3.4.2	Modelling of Caffeine, Theobromine and Theophylline interactions with PrAO .....	95
3.5	Amino Acids.....	101
3.5.1	L-cysteine .....	102
3.5.2	D-norvaline.....	103
3.5.3	Ornithine.....	104
3.5.4	D-ethionine .....	104
3.5.5	L-arginine .....	105
3.5.6	D-serine .....	106
3.6	Vitamins as PrAO modulators.....	107
3.6.1	Thiamine.....	108
3.6.2	Pyridoxine.....	111
3.7	Summary.....	120
	<b>Chapter 4 Discussion .....</b>	<b>121</b>
4.0	General Introduction.....	122
4.1	Methylxanthines in PrAO Inhibition .....	122

4.2	Computational Docking of Methylxanthines to PrAO .....	129
4.2.1	Docking Interactions with Theobromine, Caffeine and Theophylline .....	129
4.2.2	Model of PrAO Inhibition by Theobromine, Caffeine and Theophylline .....	130
4.2.3	Methylxanthines Summary .....	131
4.3	Inhibition of PrAO by polyphenols .....	132
4.3.1	Green Tea .....	133
4.3.2	HPLC Method Development .....	135
4.3.3	Deamination of Benzylamine by Catechins.....	136
4.3.4	Subtraction of the non-enzymatic Deamination Reaction by Catechins .....	137
4.3.5	PrAO Substrates that may deaminate .....	138
4.3.6	Gallated Polyphenol Inhibition of PrAO .....	138
4.4	Molecular docking of Selected Catechins with PrAO .....	139
4.4.1	Residue Binding Interaction and Location of ECG, EGCG, Epicatechin on PrAO	139
4.4.2	Comparison of Computational Docking Results and Experimental Results .....	141
4.5	Octopamine Inhibition of PrAO .....	141
4.5.1	Inhibition of PrAO by Quercetin .....	142
4.5.2	Additional Phenolic Compounds Screened for PrAO Inhibition.....	143
4.6	Amino Acids.....	143
4.6.1	L-lysine inhibition of PrAO and Testing of Similar Amino Acids.....	144
4.6.2	Cysteine inhibition of PrAO and Testing of Similar Amino Acids .....	144
4.7	Modulation of PrAO by selected Vitamins.....	145
4.7.1	Pyridoxine Inhibition of PrAO .....	145
4.7.2	Inhibition of PrAO by Thiamine (Vitamin B1) .....	145
4.7.3	Other Vitamins Assayed .....	146
4.8	Selection of Non-Dietary Compounds Chosen for PrAO Inhibition testing .....	146
4.8.1	Inhibition of PrAO by Benzylhydrazine.....	146
4.8.2	Testing of Sulphanilamide for PrAO Inhibition .....	147
4.8.3	Testing of Acrylamide for PrAO Inhibition .....	147
4.9	Conclusion/Future work .....	147
<b>5</b>	<b>Bibliography.....</b>	<b>149</b>



## List of Abbreviations

5-HT	5-hydroxytryptamine 5-HT
AA	Amino acids
Ab	$\beta$ -amyloid
AD	Alzheimer's disease
ADME	Absorption, distribution, metabolism, and excretion
AGE	Advanced Glycation End Products
AOs	Amine Oxidases
Arg	Arginine
Asn	Asparagine
Asp	Aspartic Acid
CAA	Cerebral Amyloid Angiopathy
CNS	Central Nervous System
CRAO	Chlorgyline resistant amine oxidase
Cu	Copper
CuAOs	Copper containing amine oxidases
DAO	Diamine Oxidase
DHFR	Dihydrofolate Reductase
DNA	Deoxyribonucleic acid
EC	Enzyme classification
ECG	Epicatechin Gallate
EGCG	Epigallocatechin Gallate
FAD	Flavin adenine dinucleotide
GA	Genetic Algorithm
GABA	Gamma-aminobutyric Acid
GLUT 4	Glucose Transporter Type 4
GTPs	Green Tea Polyphenols
H <sub>2</sub> O <sub>2</sub>	Hydrogen peroxide
HPAO	Human Placental Amine Oxidase
HPLC	High Performance Liquid Chromatography
HRP	Horseradish peroxidase
IC <sub>50</sub>	Half maximal inhibitory concentration
Ile	Isoleucine
IUBMB	International Union of Biochemistry and Molecular Biology

K <sub>i</sub>	Inhibitory Constant
K <sub>m</sub>	Michaelis constant
LB	Lineweaver Burk
LBDD	Ligand Based Drug Design
LD50	Median Lethal Dose (50%)
Leu	Leucine
LOX	Lysyl Oxidase
MAO	Monoamine Oxidase
Met	Methionine
NMR	Nuclear Magnetic Resonance
NT-KB	Nuclear factor K <sub>B</sub>
O <sub>2</sub>	Oxygen
PAO	Polyamine Oxidase
PDB	Protein Data Bank
Phe	Phenylalanine
PI3K	Phosphatidylinositol 3-Kinase
PrAO	Primary Amine Oxidase
Pro	Proline
SARs	Structure-activity Relationships
SBDD	Structure Based Drug Design
Siglec-10	Sialic Acid-binding Immunoglobulin-like Lectin-10
SSAO	Semicarbazide Sensitive Amine Oxidase
Thr	Threonine
TPQ	2,4,5-trihydroxyphenylalanine quinone
Tyr	Tyrosine
VAP-1	Vascular Adhesion Protein-1
V <sub>max</sub>	Maximum Rate

## List of Figures

Fig. 1.1. Structures of selected catechins .....	4
Fig. 1.2. Amine Oxidase-catalysed deamination reaction .....	5
Fig. 1.3. PrAO stick model of TPQ and the active site location on both monomers.	9
Fig. 1.4. VAP-1 (PrAO) mediated leukocyte extravasation to a site of insult.....	14
Fig. 1.5. Reaction of oxidative deamination of primary amine catalysed by PrAO	17
Fig. 1.6 TPQ represented in an equilibrium state.....	18
Fig. 1.7. Range of PrAO Substrates .....	20
Fig. 1.8. The relationship between PrAO and disease (e.g. kidney fibrosis).....	21
Fig. 1.9. Selection of methylxanthine structures.....	29
Fig. 1.10. An overview of Green Tea Polyphenol health benefits in diseases.....	32
Fig. 1.11. Chemical structures of the most abundant polyphenols in green tea.....	33
Fig. 3.1. HPLC chromatogram of a benzaldehyde standard at 254 nm .....	59
Fig. 3.2. HPLC chromatogram of PrAO produced benzaldehyde .....	60
Fig. 3.3. HPLC chromatogram of PrAO inhibition by semicarbazide.....	61
Fig. 3.4. HPLC Standard curve for pure benzaldehyde standards.....	62
Fig. 3.5. Progress curve of PrAO-catalysed benzaldehyde formation over 3 hr.....	63
Fig. 3.6. Structures of selected catechins screened for PrAO inhibition.....	65
Fig. 3.7. 1:100 dilution of crude green tea extract inhibition of PrAO.....	66
Fig. 3.8. Inhibition of PrAO by epicatechin.....	67
Fig. 3.9. Inhibition of PrAO by epigallocatechin gallate .....	68
Fig. 3.10. Inhibition of PrAO by epicatechin gallate .....	69
Fig. 3.11. EGCG inhibition of PrAO .....	70
Fig. 3.12. Epicatechin gallate inhibition of PrAO.....	70
Fig. 3.13. A non-enzymatic reaction between a polyphenol and a primary amine..	71
Fig. 3.14. Structure of caffeic acid.....	72
Fig. 3.15. Caffeic acid inhibition of PrAO.....	72
Fig. 3.16. Oxidation scan of a 100 $\mu$ M concentration of EGCG .....	73
Fig. 3.17. A molecular surface representation of Epicatechin gallate .....	74
Fig. 3.18. A computational stick model representation of Epicatechin gallate.....	75
Fig. 3.19. Epigallocatechin gallate molecular surface representation .....	76
Fig. 3.20. A stick model of Epigallocatechin gallate .....	76
Fig. 3.21. Epicatechin molecular surface representation .....	77

Fig. 3.22. A stick model of Epicatechin.....	78
Fig. 3.23. Overview diagram of Green tea experimental methods .....	78
Fig. 3.24. Structure of octopamine.....	79
Fig. 3.25. Octopamine inhibition of PrAO .....	80
Fig. 3.26. Octopamine IC <sub>50</sub> inhibition plot for PrAO .....	81
Fig. 3.27. Substrate (benzylamine) pattern of inhibition of PrAO by octopamine ..	82
Fig. 3.28. Chemical structure of quercetin.....	83
Fig. 3.29. Quercetin inhibition of PrAO .....	84
Fig. 3.30. Quercetin IC <sub>50</sub> inhibition plot for PrAO .....	85
Fig. 3.31. Pattern of inhibition of PrAO by quercetin.....	86
Fig. 3.32. Chemical structure of umbelliferone .....	87
Fig. 3.33. Umbelliferone inhibition of PrAO.....	87
Fig. 3.34. Structures of the caffeine-related methylxanthines .....	88
Fig. 3.35. Effect of selected methylxanthines on PrAO activity.....	89
Fig. 3.36. Effect of xanthines and related compounds on PrAO activity.....	90
Fig. 3.37. Compounds related to caffeine screened for PrAO inhibition.....	90
Fig. 3.38. Effect of selected diazoles at 500 $\mu$ M and 1 mM, on PrAO.....	91
Fig. 3.39. Structures of diazole compounds selected for PrAO inhibition .....	91
Fig. 3.40. Theobromine IC <sub>50</sub> inhibition plot .....	92
Fig. 3.41. Pattern of inhibition of PrAO by theobromine .....	93
Fig. 3.42. Lisofylline inhibition of PrAO at 1mM and 0.5 mM concentrations .....	94
Fig. 3.43. Structure of Lisofylline screened for PrAO inhibition .....	95
Fig. 3.44. Molecular surface docking interaction of Theobromine and PrAO .....	97
Fig. 3.45. A stick model of the interaction of Theobromine and PrAO.....	97
Fig. 3.46. Caffeine molecular surface representation .....	98
Fig. 3.47. A stick model representation of caffeine .....	98
Fig. 3.48. Theophylline molecular surface representation .....	99
Fig. 3.49. A stick model of Theophylline .....	99
Fig. 3.50. Overview of methods of Methylxanthine inhibition of PrAO.....	100
Fig. 3.51. Chemical structures of selected amino acids .....	101
Fig. 3.52. L-cysteine inhibition of PrAO .....	102
Fig. 3.53. D-norvaline inhibition of PrAO .....	103
Fig. 3.54. Ornithine inhibition of PrAO .....	104

Fig. 3.55. D-ethionine inhibition of PrAO .....	104
Fig. 3.56. L-arginine inhibition of PrAO .....	105
Fig. 3.57. D-serine inhibition of PrAO .....	106
Fig. 3.58. Chemical structure of thiamine and pyridoxine.....	107
Fig. 3.59. Thiamine inhibition of PrAO .....	108
Fig. 3.60. Thiamine IC <sub>50</sub> inhibition plot for PrAO.....	109
Fig. 3.61. Pattern of inhibition of PrAO by thiamine .....	110
Fig. 3.62. Pyridoxine inhibition of PrAO .....	111
Fig. 3.63. Pyridoxine IC <sub>50</sub> inhibition plot .....	112
Fig. 3.64. Pattern of inhibition of PrAO by pyridoxine .....	113
Fig. 3.65. Chemical structure of benzylhydrazine .....	114
Fig. 3.66. Benzylhydrazine inhibition of PrAO .....	115
Fig. 3.67. Benzylhydrazine IC <sub>50</sub> inhibition plot for PrAO.....	115
Fig. 3.68. Patterns of inhibition of PrAO by benzylhydrazine .....	116
Fig. 4.1. Caffeine structure of N-methyl groups around the xanthine nucleus .....	124
Fig. 4.2. The metabolites of caffeine <i>in vivo</i> .....	125
Fig. 4.3. Mechanism of noncompetitive inhibition.....	126
Fig. 4.4. The structure of Lisofylline compared to caffeine.....	128

### List of Tables

Table 1.0. The five classes of Amine Oxidases subdivided by cofactor type.....	6
Table 1.1. An overview of residue variations between bovine and human PrAO ...	12
Table 1.2. Common substrates between members of the amine oxidase family .....	19
Table 1.3. Inhibitors of PrAO .....	25
Table 1.4. Hydroxamic based inhibitors of PrAO .....	26
Table 1.5. The dry chemical composition of green tea .....	31
Table 1.6. Selection of vitamins modulating lactoperoxidase .....	35
Table 1.7. Docking tools and their respective algorithms.....	40
Table 3.1. Binding interactions for catechins with PrAO by AutoDock .....	79
Table 3.2. Binding interactions for Methylxanthines with PrAO by AutoDock ...	100
Table 3.3. Summary of various compounds tested for inhibition of PrAO .....	117
Table 3.4. Summary table of various inhibitors tested as PrAO inhibitors .....	119

# CHAPTER 1

## *Introduction*

## **1.0 Diet and health benefits**

Diet analysis is an area of increasing interest in terms of health benefits and disease prevention. Diets, such as the Mediterranean diet, that are rich in fruits, vegetables, legumes and cereals accompanied by high olive oil consumption, have been shown to be clinically relevant in the amelioration of mortality from diseases, including Type II diabetes, cancer, cardiovascular disease as well as Parkinson's and Alzheimer's disease (Lourida *et al.*, 2013; Singh *et al.*, 2014).

The residents of the Japanese island of Okinawa are known for their longevity, having a high number of centenarians and a markedly low incidence of age-related disease (Suzuki *et al.*, 2016). Their longevity is thought to be mainly due to the avoidance, or delay, of the onset of major age-related illnesses such as cancer, heart disease, stroke and diabetes. These health benefits are attributed to a diet rich in vegetable and fruit intake suggesting an important role for phytonutrients, minerals, vitamins and antioxidant-containing foods in the maintenance of good health (Willcox *et al.*, 2014). Particular dietary habits, such as the daily consumption of various teas and coffee have been extensively studied and are associated with numerous health benefits and the amelioration of various diseases (da Silva Pinto, 2013; Ferrucci *et al.*, 2014; George *et al.*, 2008). For instance, a study by O'Keefe *et al.* in the United States, where over 400 million cups of coffee are consumed daily has shown, in both human and animal trials, that regular coffee consumption is associated with reduced vascular disease, type II diabetes and obesity (O'Keefe *et al.*, 2013). A recent study of the relationship between coffee consumption and mortality in diverse European populations showed that coffee drinking was associated with reduced risk of death from various causes such as cardiovascular disease and cerebrovascular disease (Gunter *et al.*, 2017).

The principal bioactive present in coffee, caffeine, is the subject of particular interest in disease prevention. A large-scale study by (Furman *et al.*, 2017) showed that moderate caffeine consumption suppressed systemic inflammation, caused by inflammasome activation, which could account for its correlation with decreased mortality. Arendash and Cao (2010) in a study linking the reduction of Alzheimer's disease and caffeine consumption found a direct correlation between the reduction of amyloid plaque formation and caffeine consumption in mice. Moreover, Chen *et al.* (2010) have shown that caffeine has a protective effect against the onset of Alzheimer's and Parkinson's disease: although the underlying mechanisms are not fully understood, it was postulated that caffeine aids in keeping the blood-brain barrier intact. Thus, caffeine may act to prevent blood-brain barrier leakage a possible contributor to the progression of both Alzheimer's and Parkinson's pathogenesis. Although there are many positive health benefits associated with moderate intake of caffeine, excessive consumption (considered as being over 5 cups of coffee or excess of 400 mg of caffeine a day (see Nehlig, 2015)) can have negative effects. Mood alteration such as increased anxiety or motor control impairment has been reported (Smith, 2002) as has sleep deprivation with some users experiencing withdrawal symptoms (Rogers *et al.*, 2005).

Green tea is a commonly consumed beverage, particularly in Asia, but is growing in popularity in the West due to increasing reports of health benefits (Mak, 2012). Notable health benefits associated with green tea consumption include the prevention of cancer, cardiovascular disease, type II diabetes and obesity. Many of these reported benefits are ascribed to the high polyphenol content of green tea. Catechins are the



principal polyphenol components of Green Tea (Chacko *et al.*, 2010). Catechins are Flavan-3-ols, derived from flavans, that contain the 2-phenyl-3,4-dihydro-2H-chromen-3-ol skeleton as part of their structure (see Fig. 1.1).

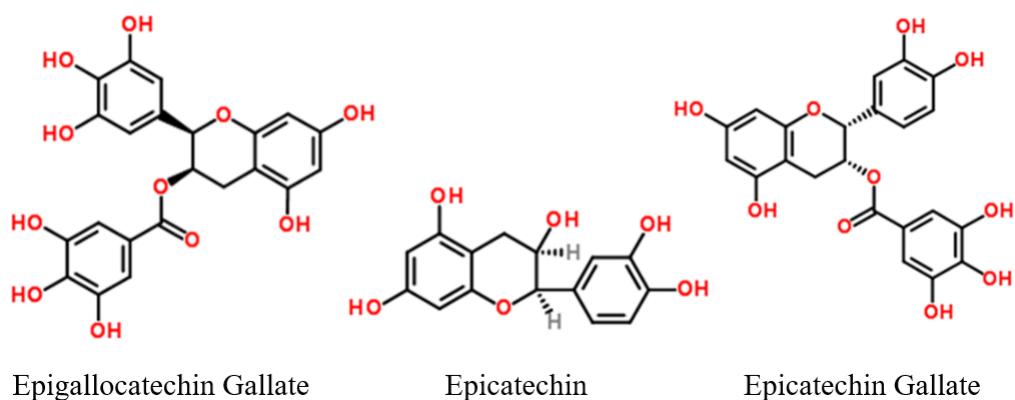


**Fig. 1.1.** Structures of some Green Tea catechins considered in this study.  
<http://www.chemspider.com/Chemical-Structure>

The mechanistic link between ingestion of specific dietary components and health is not well understood (Kozłowska and Szostak-Wegierek, 2014). Thus, while a diet rich in fruits and vegetables can be linked to good health, the specific components of the diet that confer a health advantage are not known. In recent years, attention has focused on phytochemicals such as polyphenols, catechins and methylxanthines. However, our understanding of the molecular mechanisms underlying such effects are still at an early stage (Franco *et al.*, 2013; Kozłowska and Szostak-Wegierek, 2014; Sarriá *et al.*, 2015). It has been shown that methylxanthines such as caffeine are able to bind to adenosine receptors and much of their health benefits are attributed to this property. Catechins, the main polyphenols in green tea are known to have antioxidant properties (Rashidinejad *et al.*, 2015) and to regulate gene expression and prevent DNA methylation and damage (Fujiki *et al.*, 2015). These observations may account for some of the health benefits associated with these compounds and raise the

possibility that there may be other important physiological targets yet to be explored. (Franco *et al.*, 2013; Fukushima *et al.*, 2009; Kozłowska and Szostak-Wegierek, 2014; Rashidinejad *et al.*, 2015; Sarriá *et al.*, 2015).

## 1.1 Amine Oxidases

Amine oxidases (AOs) are ubiquitous enzymes among living species and are responsible for the breakdown of mono and poly-amines from the diet and the environment (Gong and Boor, 2006). AOs are involved in a wide range of physiological functions such as the removal of toxic amines; neurotransmitter breakdown, leukocyte recruitment and collagen stabilisation (Baker *et al.*, 2007). AOs catalyse amine catabolism by their oxidation into an aldehyde, ammonia and hydrogen peroxide products (Fig. 1.2; Agostinelli *et al.*, 2010).

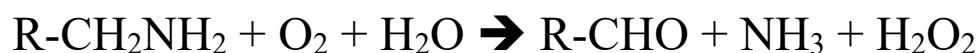


**Fig. 1.2:** Amine Oxidase-catalysed deamination reaction. On the left, a primary amine, oxygen and water are transformed to (on the right) the corresponding aldehyde, ammonia and hydrogen peroxide as products.

There are five main classes of amine oxidases, namely; diamine oxidases (DAO) E.C. 1.4.3.22, monoamine oxidases (MAO) E.C 1.4.3.4, lysyl oxidase (LOX) E.C 1.4.3.13, polyamine oxidases (PAO) E.C 1.5.3.13 and primary amine oxidases (PrAO) E.C 1.4.3.21 (BRENDA, 2015). These five AOs can be further divided into two main groups based upon their cofactor preferences (see Table 1.0).

**Table 1.0** The five Classes of Amine Oxidases subdivided by Cofactor type (see Yraola et al., 2009; Black and Whetstine, 2012; Binda et al., 2013; Tomitori et al., 2012; Agostinelli et al., 2010)

	Flavin adenine dinucleotide (FAD) used as cofactor		2,4,5-trihydroxyphenylalanine quinone (TPQ) used as cofactor		
	MAO E.C 1.4.3.4	PAO E.C 1.5.3.13	PrAO E.C 1.4.3.21	DAO E.C. 1.4.3.22	LOX E.C 1.4.3.13
<b>Substrates</b>	Noradrenaline Dopamine Spermidine Benzylamine	Spermine Spermidine	Benzylamine Methylamine Aminoacetone	Histamine Cadaverine Putrescine	Amino Groups in lysine residues in collagen and elastin
<b>Inhibitors</b>	Chlorgyline	MDL. 72,527	Semicarbazide	Semicarbazide	Semicarbazide
<b>Location</b>	Mitochondria	Intracellular	Cell Surface/Plasma	Intracellular	Extracellular
<b>Function</b>	Breakdown of Neurotransmitters	Cell Growth	Leukocyte Adhesion, Breakdown of Primary Amines	Breakdown of Histamine	Formation of Extracellular Matrix

MAO and PAO belong to a group that uses flavin adenine dinucleotide (FAD) as cofactor while LOX, PrAO and DAO belong to a group that uses 2,4,5-trihydroxyphenylalanine quinone (TPQ) as cofactor (Yraola *et al.*, 2009). MAOs are mitochondrial enzymes responsible for the breakdown of neurotransmitters. MAO exists in two forms designated MAO-A and MAO-B that differ in terms of substrate specificity and inhibitor sensitivity. MAOs are targeted extensively in the treatment of mental health diseases such as depression, neurological diseases and Alzheimer's disease (Binda *et al.*, 2013). PAOs, on the other hand, are known to break down secondary amines including, spermidine and spermine which are involved in cell growth (Tomitori *et al.*, 2012).

Of the TPQ-containing group: LOX is responsible for the crosslinking of an amino group of lysine with residues of other peptide strands which acts to stabilise the extracellular matrices of collagen and elastin (Black and Whetstone, 2012). DAO is primarily responsible for the breakdown of amines, such as, putrescine, spermidine and cadaverine (Armenta and Blanco, 2012). PrAO is known to oxidise primary amines and has received a lot of attention due to its multiplicity of functions (see O'Sullivan *et al.*, 2004). Studies have shown a correlation between disease and abnormal or elevated PrAO levels in the body (Wong *et al.*, 2013). Further details of the structure and function of PrAO are given below.

## 1.2 PrAO: An Introduction

PrAO (EC 1.4.3.21) is an enzyme that can be found either membrane bound or free-floating in plasma (Wong *et al.*, 2014). PrAO belongs to the oxidoreductase (deaminating) family of enzymes. The International Union of Biochemistry and Molecular Biology (IUBMB) classify such enzymes as follows:

*“a group of enzymes that oxidize primary monoamines but have little or no activity towards diamines, such as histamine, or towards secondary and tertiary amines. They are copper quinoproteins (2,4,5-trihydroxyphenylalanine quinone) and, unlike EC 1.4.3.4, monoamine oxidase, are sensitive to inhibition by carbonyl-group reagents, such as semicarbazide. In some mammalian tissues the enzyme also functions as a vascular-adhesion protein (VAP-1)”* (BRENDA, 2015) (see section 1.3).

PrAO has been given different names over the years being variously known as benzylamine oxidase and chlorgyline resistant oxidase (CRAO; Buffoni and Blaschko, 1964; Clarke *et al.*, 1982). In recent years PrAO was often commonly named as Semicarbazide Sensitive Amine Oxidase (SSAO) since it is potently inhibited by this compound. At present, the recommended nomenclature is to refer to this enzyme as Primary Amine Oxidase (PrAO) (O'Sullivan *et al.*, 2004).

When it is membrane bound, PrAO is found in high quantities in vascular, kidney, lung and adipose tissues and is known to increase in activity when associated diseases are present. For example, high PrAO activity in diabetic patients with vascular disease was reported at first clinical diagnosis indicating that high PrAO activity precedes the appearance of vascular complications (Göktürk *et al.*, 2003). The involvement of PrAO in diseases such as diabetes, vascular diseases, neurological disease, inflammation and obesity is not well understood (see Section 1.6 for further details).

PrAO has been shown to be involved in the pathogenesis of inflammatory diseases by mediating the migration of leukocytes into tissue and promoting an inflammatory response. Since the action of PrAO, either in the oxidative deamination of endogenous amines or in its role as a vascular adhesion protein (see section 1.3), requires its catalytic activity to be intact, PrAO inhibition appears to be a logical strategy to limit inflammation in various diseases.

Some of the deleterious effects attributed to elevated PrAO levels are thought to be due to the toxic products formed during the oxidation of endogenous substrates such as aminoacetone (a product from adrenaline and creatinine metabolism) and methylamine (a product of amino acid catabolism). These endogenous substrates are

oxidised into highly reactive formaldehyde and methylglyoxal which are cytotoxic and genotoxic compounds (Hernandez *et al.*, 2006a; Ullah *et al.*, 2013; Wong *et al.*, 2014).

### 1.2.1 PrAO Molecular Structure

PrAO is a dimeric enzyme that is 180 kDa in size (Fig. 1.3); each 90kDa monomer has a TPQ moiety as cofactor in the active site along with a copper atom in close proximity to the metal (Peet *et al.*, 2011).

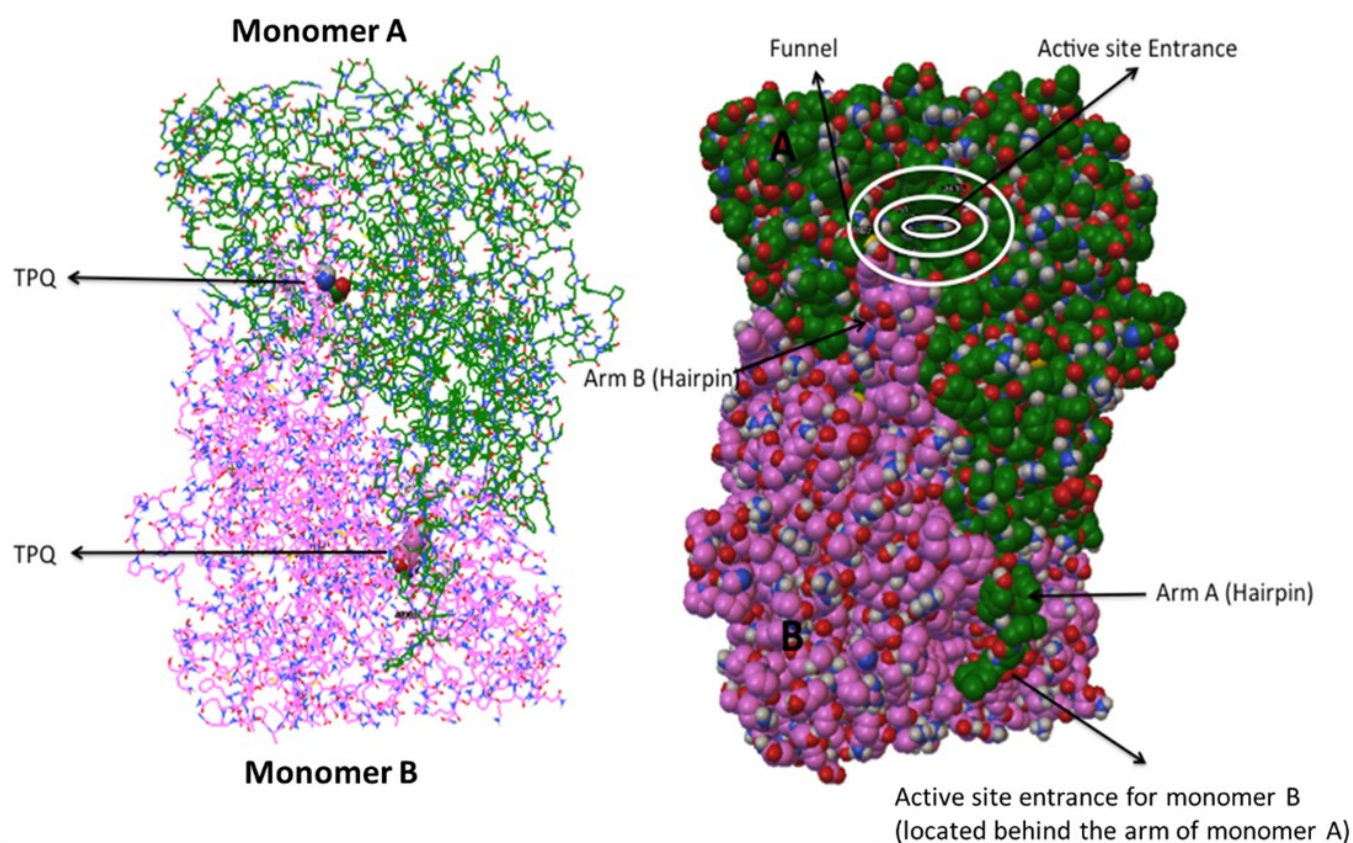


**Fig. 1.3:** Structure of dimeric PrAO (PDB-2PNC). On the left PrAO is shown as a stick model highlighting TPQ at the active site. The two monomers are shown as “A” green and “B” pink. The right-hand image depicts PrAO as a space filling model highlighting the funnel (concentric circles) leading to the active site entrance. It also shows the junction of the two monomers and the location of the joining hairpin “arms” of the dimer structure. (Sanner, 1999).

The structures of some copper containing amine oxidases (CuAOs) have been resolved by X-ray crystallography and they show a highly conserved active site across all species i.e. human, bovine, and murine. The active site is deeply buried within the structure and is accessed by a “funnel” formed by the D3 and D4 domains. TPQ, the quinone cofactor, is formed post-translationally by a non-enzymatic oxidation reaction of the amino acid tyrosine (Tyr471 in humans) in the presence of molecular oxygen and Cu<sup>II</sup> (Shepard and Dooley, 2015). The copper atom in PrAO has a penta-coordinate state and is bonded to three histidines and to a pair of water molecules that stabilize the copper ion in the ‘off’ state (discussed in greater detail in Section 1.5). There are four domains present in PrAO designated D1, D2, D3 and D4, where D4 is known to contain the active site (Shepard and Dooley, 2015).

### **1.2.2 Inter species variation in PrAO active site ligand access.**

The crystal structures solved for PrAO indicate it has a wide-mouthed funnel leading to the active site entrance (Fig. 1.3). Variations in structure between PrAO species, such as between human and bovine enzymes, are found within the funnel and at the active site entrance which leads to widening, or narrowing, of the funnel at the active site entrance thereby giving rise to variations in ligand access (see Table 1.1)

Two long hairpins or “arms” join the two PrAO monomers forming the dimer unit. One of these arms stretches along the surface of the enzyme to the funnel entrance and may play a role in determining substrate/inhibitor specificity. The residues at the end of the arm differ between human and bovine forms (Yraola *et al.*, 2006). PrAO is known to be glycosylated at several sites. It is possible that carbohydrates attached to

PrAO may also serve to regulate ligand access. Finally, the funnel wall leading to the active site is lined with hydrophobic and aromatic amino side chains which potentially form bonds to an incoming ligand which can further influence active site access and substrate specificity (Holt *et al.*, 2008a; Jakobsson *et al.*, 2005).

Bovine PrAO has a somewhat more open active site entrance than the human enzyme with the funnel being less obstructed thus permitting greater ligand access to the active site. (Jakobsson *et al.*, 2005). A specific leucine residue acts as an active site “gate” (Leu469 in human and Leu468 in bovine) to control ligand access at the active site entrance (Yraola *et al.*, 2006). Notwithstanding these observations the active site of both human and bovine enzymes can accommodate substrates as large as benzylamine and phenethylamine and they show similar inhibitor sensitivities.



**Table 1.1:** A selection of residue variations between bovine and human PrAO and conserved active site residues. These residues are located in the vicinity of the funnel entrance leading to the active site. (Holt *et al.*, 2008a; Jakobsson *et al.*, 2005; Yraola *et al.*, 2006).

<b>Location</b>	<b>Bovine Residue</b>	<b>Human Residue</b>	<b>Comparison</b>
<b>Funnel brim</b>	Leu172	Phe173	Both hydrophobic  Phe larger due to phenyl group
<b>Funnel</b>	Tyr392	Arg393	Tyr Hydrophobic  Arg Positive Charge, larger residue
	Phe393	Tyr394	Both hydrophobic  Tyr having an additional hydroxyl group
	Asn211	Thr212	Both polar  Asn being larger
<b>Funnel base</b>	Pro237	Phe238	Both hydrophobic  Pro is a cyclic amide  Phe larger due to phenyl group
	Tyr238	Phe239	Both hydrophobic  Tyr has an additional hydroxyl group
<b>Hairpin (arm) tip, near active site entrance</b>	Phe 446	Leu 447	Both hydrophobic  Phe larger due to phenyl group
	Leu 447	Tyr 448	Both hydrophobic  Tyr larger due to phenyl group
Active site entrance	Leu468	Leu469	Leu468 acting as a "gate"  Leu469 acting as a "gate"
<b>Conserved Active Site Residues Between Both Species</b>	TPQ, His520, His522, His684, Asp386, Tyr372, Tyr384, Phe389, Tyr394 and Leu468		

### 1.3 Physiological role of PrAO

The physiological role of PrAO is confusing since its best substrate, benzylamine, is a non-physiological compound. Indeed, identifying physiological substrates for this enzyme has proven difficult. The main catalytic function of PrAO is thought to be the breakdown and removal of primary amines in the body. However, in view of the observation that the aldehydes derived from amines such as aminoacetone and methylamine (the best physiological substrates) may be more toxic than their parent amines this role is unclear (Hernandez *et al.*, 2006b). In its role as a vascular adhesion protein PrAO binds human sialic acid-binding immunoglobulin-like lectin-10 (Siglec-10) which acts as a substrate. The amino group on siglec-10 that gives rise to this activity has not been identified (Elovaara *et al.*, 2016).

In previous studies, it has been shown that PrAO is expressed in high concentrations in smooth muscle, endothelial and adipose cells, suggesting its involvement in important functions at these locations (Enzsoly *et al.*, 2013). Hydrogen peroxide (H<sub>2</sub>O<sub>2</sub>), when produced by PrAO, is known to act as an insulin mimetic having the ability to stimulate the uptake of glucose from blood plasma by recruiting glucose transporter type 4 (GLUT 4) and GLUT 1 transporters extracellularly (McDonald *et al.*, 2007).

Another highly important physiological function of PrAO is its ability to act as a vascular adhesion protein (Fig. 1.4). This function was discovered in 1998, when a Finnish group cloned a gene coding for the protein they called: vascular adhesion protein 1 (VAP-1) (Smith *et al.*, 1998). They were surprised when they found that their protein had already been cloned under the name human placental amine oxidase

(HPAO) (Zhang and McIntire, 1996). This important finding greatly stimulated interest in PrAO (Luo *et al.*, 2013).

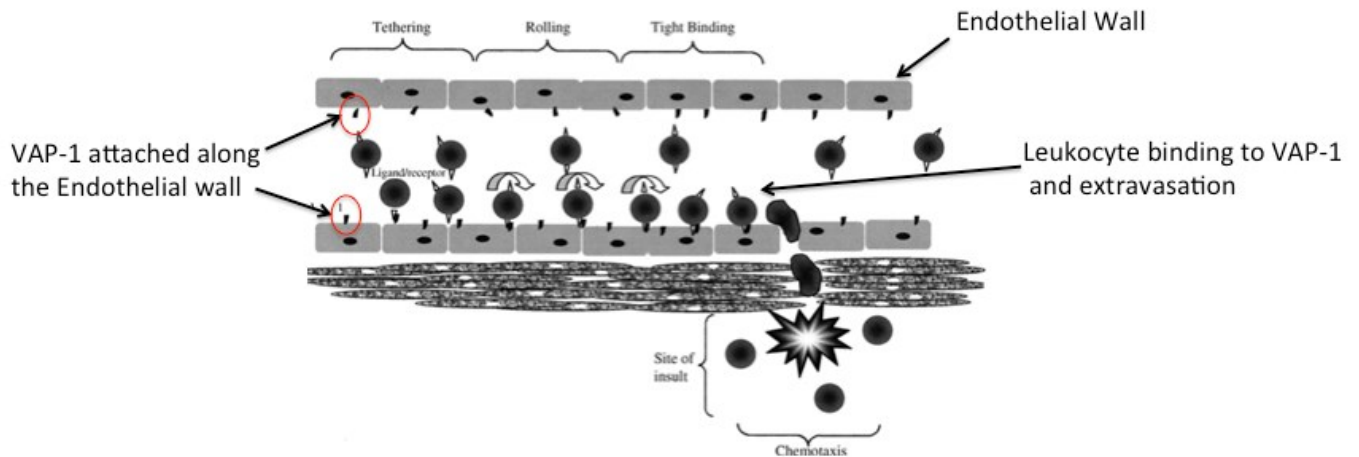


**Fig. 1.4:** Image depicting VAP-1 (PrAO) mediated leukocyte extravasation. Extravasation refers to the crossing of the endothelial cell wall to a site of insult via tethering, rolling and tight binding to VAP-1. Leukocytes with their attached ligand or receptor are shown binding or “tethering” to VAP-1 on the vascular endothelium. After the leukocytes bind to VAP1 they roll along the endothelium before establishing a tight binding complex. The formation of the complex allows the extravasation of leukocytes to a site of injury in a tissue (O’Sullivan *et al.*, 2004).

PrAO is known to be involved in vascular smooth muscle cell differentiation, influencing extracellular matrix composition and the regulation of vascular tone (Olivieri *et al.*, 2011). The cellular matrix composition and maturation of collagen and elastin was disrupted in rat models when PrAO was inhibited with semicarbazide. This effect was probably due to PrAO-derived formaldehyde protein cross-linking (Mercader *et al.*, 2011). Elastin structure maturation tests performed on rat aorta revealed that PrAO inhibition reduced mature elastin levels and compromised collagen elastin matrices, suggesting PrAO involvement in these physiological processes. PrAO is found at high amounts on fat cell surfaces and has been shown to be directly involved in adipose cell maturation and differentiation (Mercier *et al.*,

2003). Murine studies demonstrated a decrease in fat cell size and weight gain in mice when PrAO was inhibited with semicarbazide (Mercader *et al.*, 2011).

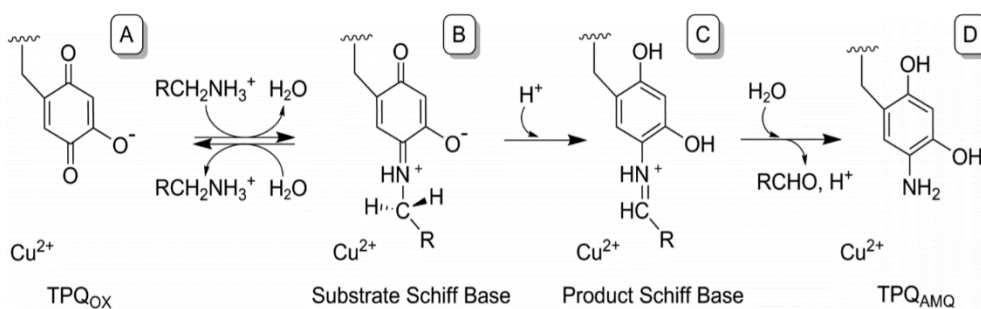
While PrAO is predominantly found either membrane-bound or free floating in plasma it can also be found intra-cellularly in GLUT4-containing intracellular vesicles in adipocytes. Amine oxidase substrates such as benzylamine and methylamine have been shown to stimulate glucose uptake in rat adipocytes by increasing the recruitment of the glucose transporter GLUT4 from vesicles within the cell to the cell surface via the phosphatidylinositol 3-kinase (PI3K) pathway. It is thought that PrAO can mimic the adipogenic effect of insulin in cultured pre-adipocytes through the production of H<sub>2</sub>O<sub>2</sub> during amine oxidation. Furthermore, it has been suggested that PrAO not only represents a novel late marker of adipogenesis, but could also be directly involved in the triggering of terminal adipocyte differentiation (Enrique-Tarancon *et al.*, 1998; Göktürk *et al.*, 2003; McDonald *et al.*, 2007).

#### 1.4 PrAO catalysed Oxidation of Amines

The oxidation reaction that converts primary amines into their respective aldehyde, ammonia and hydrogen peroxide products by PrAO is carried out at the active site involving the TPQ cofactor and Cu<sup>II</sup> (Autio *et al.*, 2013). A ping-pong kinetic mechanism was proposed for this reaction (Fig. 1.5). Catalysis proceeds by, firstly, a reduction of TPQ to release an aldehyde product and secondly, an oxidative cycle releasing H<sub>2</sub>O<sub>2</sub> and ammonia (Largeron, 2011). In brief, this reaction occurs when TPQ in its oxidised state reacts with a primary amine substrate producing a Schiff base. Subsequently, a quinolaldimine “product schiff base” is formed whose formation is facilitated by an  $\alpha$ -carbon extraction from a conserved aspartate. The aldehyde product is then released via hydrolysis simultaneously forming the reduced aminoquinol (Fig. 1.5, Scheme 1) thus completing the first half of the reaction.

In the second part of the reaction TPQ is re-oxidised by O<sub>2</sub>. There is some controversy over the mechanistic details of the oxidative half reactions and Figure 1.5 shows two possibilities.

**Scheme 1.** Proposed reductive half-reaction mechanism



**Scheme 2.** Alternative pathways for the oxidative half-reaction.

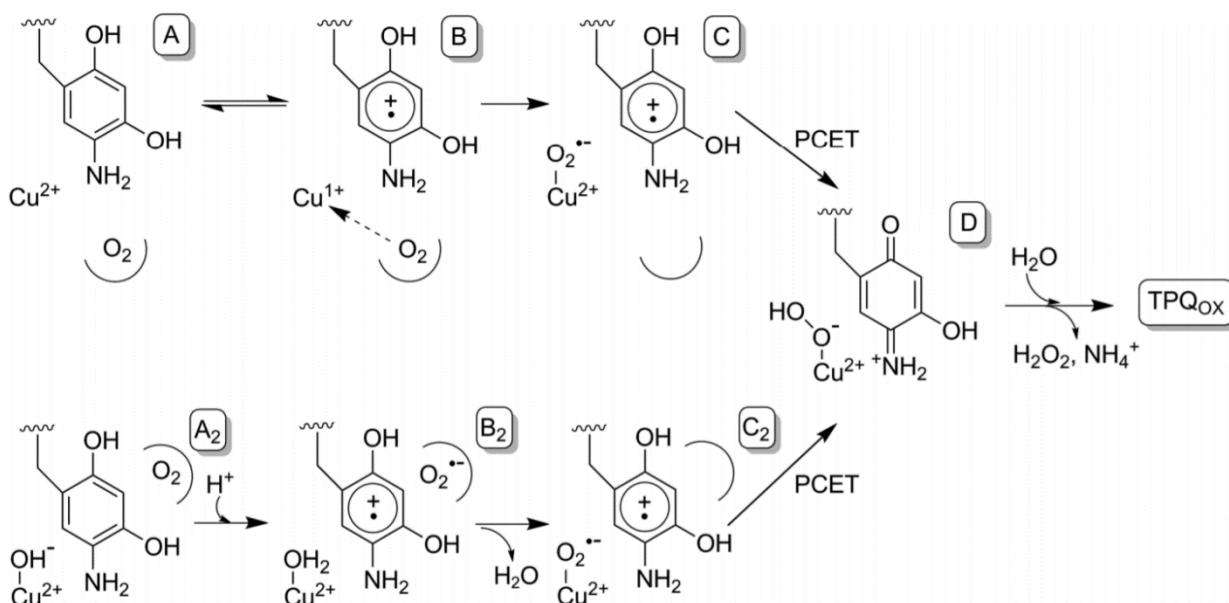


**Fig. 1.5:** Reaction mechanism for the oxidative deamination of a primary amine catalysed by PrAO. In this scheme TPQ<sub>ox</sub> is the oxidised form of the cofactor and TPQ<sub>AMQ</sub> is the reduced amino quinol form. **Scheme 1** shows the reductive half reaction where the primary amine forms a Schiff base with the cofactor. After protonation a product Schiff base is formed which is hydrolysed to release the aldehyde product. The cofactor at this stage is in the aminoquinol form which is oxidised in the second oxidative half reaction. **Scheme 2** shows two alternative pathways proposed for the oxidative half reaction. Both pathways lead to the formation of an iminoquinone intermediate which is hydrolysed to produce ammonia and H<sub>2</sub>O<sub>2</sub> (Shepard and Dooley, 2015).

Despite mechanistic uncertainties both possibilities lead to formation of a Copper (Cu<sup>II</sup>)–hydroperoxide, iminoquinone intermediate. Finally, this intermediate is hydrolysed to release ammonia and hydrogen peroxide regenerating the TPQ cofactor (TPQ<sub>ox</sub> in Fig. 1.5; Scheme 2) (Shepard and Dooley, 2015).

An equilibrium state occurs between copper and TPQ in the active site where the copper atom transitions between an ‘on’ and ‘off’ position (Fig. 1.6). A reaction with an amine substrate occurs only when the Cu is in the ‘off’ (meaning not attached to TPQ) position whereby it is bonded to three histidines and two water molecules. In the ‘on’ position, the Cu is bound directly to a hydroxyl group of the TPQ cofactor preventing a nucleophilic attack on TPQ (Klema and Wilmot, 2012).

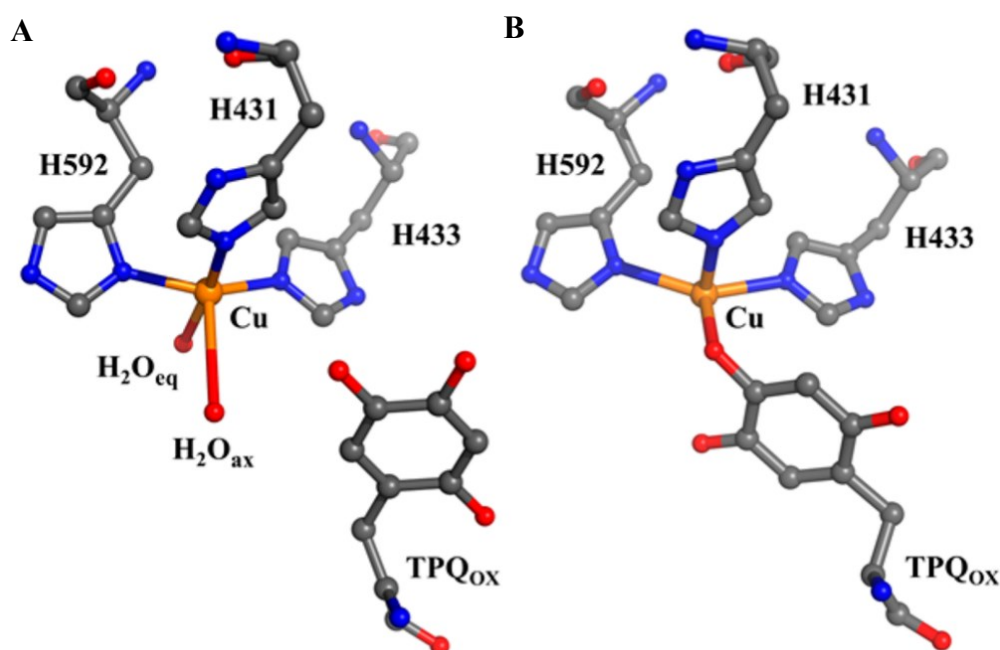


**Fig. 1.6:** TPQ represented in an equilibrium state in both the ‘off’ positions. The off position is depicted in A and the ‘on’ position in B where the ‘off’ state involves Cu bound to three histidines and two water molecules. The ‘on’ state involves TPQ replacing the water molecules and binding to Cu (Shepard and Dooley, 2015). Only the ‘off’ position can catalyse amine oxidation.

## 1.5 PrAO Substrates

PrAO substrates can include long or short aliphatic and arylalkylamines (Kinemuchi *et al.*, 2004b). Aminoacetone, methylamine and allyamine are well-characterised aliphatic substrates. Benzylamine, tyramine and spermidine (see Figure 1.7) are some of the more well-known substrates. The main physiological substrates are thought to be methylamine and aminoacetone (Hernandez *et al.*, 2006a).

Substrate specificity can overlap between Cu/TPQ and flavin-containing amine oxidase species (see Table 1.2). For example, both PrAO and MAO can use substrates such as dopamine, tyramine and benzylamine. While there is no clear physiological reason for these overlaps, studies have shown that if MAO is suppressed, PrAO can provide an alternative pathway for metabolism of these amines (Yraola *et al.*, 2009).

**Table 1.2:** Common substrates between members of the amine oxidase family. The members are: diamine oxidase (DAO), monoamine oxidase (MAO), lysyl oxidase (LOX), polyamine oxidase (PAO) and primary amine oxidase (PrAO) (Floris and Mondovi, 2009; Hernandez *et al.*, 2006a; Yraola *et al.*, 2009).

Substrates	PrAO	DAO	LOX	MAO	PAO
	Copper containing			Flavin containing	
Allylamine	Yes	-	-	No	No
Aminoacetone	Yes	-	-	No	No
Benzylamine	Yes	Yes/low	Yes	Yes	No
Cadaverine	+/-	Yes	Yes	No	No
Dopamine	Yes	Yes	-	Yes	No
Histamine	+/-	Yes	+/-	No	No
L-lysine	+/-	No	+/-	No	No
Noradrenaline	+/-	+/-	-	Yes	No
Methylamine	Yes	No	-	No	No
Putrescine	+/-	Yes	-	No	No
Spermidine	Yes	Yes	-	No	No
Tryptamine	+/-	No	-	Yes	No
Tyramine	Yes	-	-	Yes	No

Notes: +/- some studies show catalysis and some not. The dash,-, indicates no data available.

### 1.5.1 Sources of Amines

PrAO substrates can be ingested directly through the diet; for example, dopamine from fruit, histamine from fish and cheese and 2-phenylethylamine from chocolate and meat



(Olivieri *et al.*, 2011). In addition, amine substrates such as allylamine, a compound used in the manufacture of vulcanized rubber, can enter the body through the environment. Certain aromatic amines can be absorbed via tobacco smoke (Olivieri *et al.*, 2011). Although PrAO breaks down potentially toxic amines, sometimes the products formed can be more toxic than the amine substrate itself, i.e. methylamine is deaminated to the more toxic and reactive species formaldehyde (Section 1.8; Sun *et al.*, 2014).

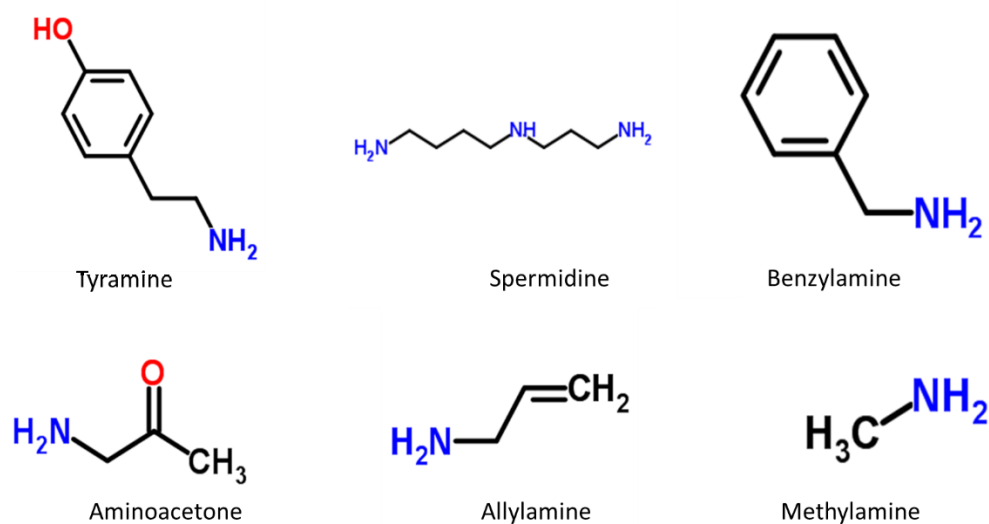


**Fig. 1.7.** Range of known PrAO substrates Images taken from ChemSpider (<http://www.chemspider.com/Chemical-Structure>).

## 1.6 PrAO and Disease

High PrAO catalytic activity is associated with the progression of a variety of disease states from obesity and vascular disease to kidney disease (Wong *et al.*, 2013; Mátyus *et al.*, 2013). PrAO substrates such as methylamine, aminoacetone and allyamine can be oxidised into even more reactive and toxic products, such as formaldehyde, methylglyoxal and acroelin, respectively. These highly reactive species can cause protein crosslinking, oxidative stress and the formation of Advanced Glycation End (AGE) products (Fig. 1.7). The reaction product accompanying amine oxidation, hydrogen peroxide, can also be transformed to a reactive hydroxyl radical, further increasing cell damage (Mercier, 2009; Wong *et al.*, 2013).

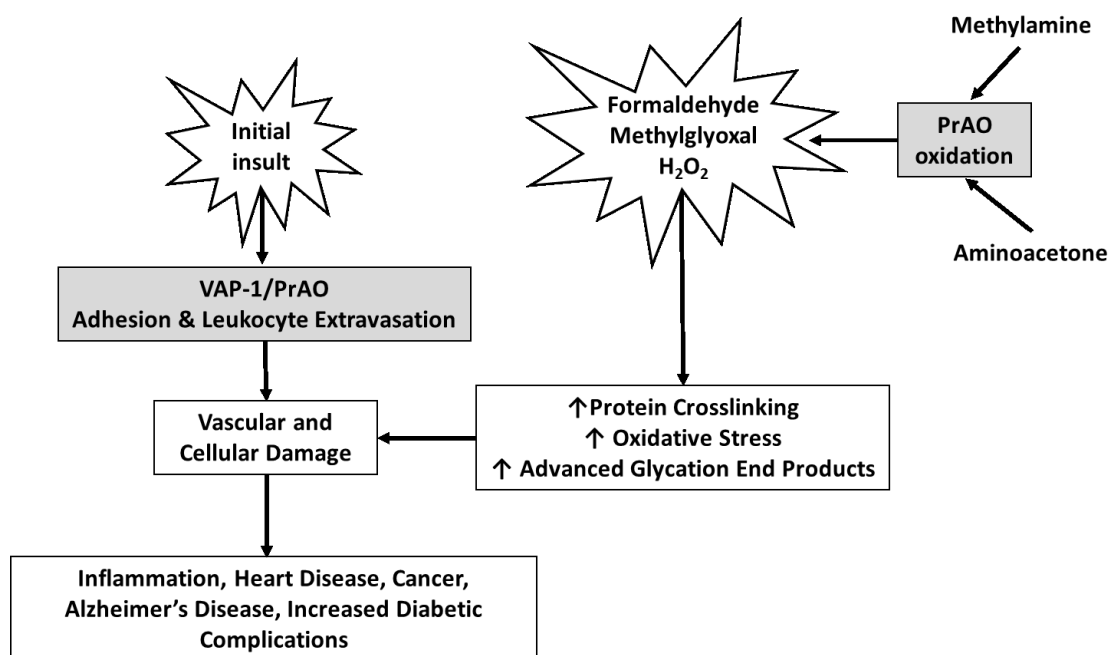


**Fig. 1.8:** Diagram illustrating the relationship between PrAO and disease. PrAO is associated with disease (e.g. kidney fibrosis). Repeated initial insult (hyperglycemia, inflammation, toxins, endothelial stress, uremia, etc.) leads to increased production of PrAO substrates. It also stimulates leucocyte transmigration which leads to further inflammatory response. The aldehydes produced by PrAO - catalysed amine oxidation cause vascular damage directly by cytotoxic insult and indirectly by formation of advanced glycosylation end products (AGE's). This damage causes the upregulation of pro-inflammatory and pro-fibrinogenic cytokines in addition to promoting local tissue hypoxia, all of which contribute to tissue damage (Wong *et al.*, 2013).

### 1.6.1 Elevated PrAO Activity and Disease

For some conditions the state of disease advancement is often correlated with an increase in PrAO activity as evidenced by diabetes (Januszewski *et al.*, 2014). A higher concentration of PrAO in turn leads to a higher turnover of reactive products, for example formaldehyde, methylglyoxal and acrolein, which may directly increase Advanced Glycation End product formation and exacerbate diabetic complications of vascular injury and capillary cell damage (Nunes *et al.*, 2010) as well as heart disease (Marinho *et al.*, 2010).

Alzheimer's disease, stroke and multiple sclerosis are also associated with elevated levels of PrAO causing the formation of reactive species and the associated inflammation mediated by VAP-1 (Alferova *et al.*, 2010; Salter-Cid *et al.*, 2012; Valente *et al.*, 2012). Alzheimer's disease (AD) is a progressive neurological disorder of the central nervous system (CNS), which leads to dementia and cognitive impairment (Dubois *et al.*, 2014). One of the major pathological features in the progression of AD is cerebral amyloid angiopathy (CAA), which is caused by the deposition of  $\beta$ -amyloid (Ab) plaques. Overexpression of PrAO has been found in areas of  $\beta$ -amyloid plaque deposits (Chen *et al.*, 2007b; Unzeta *et al.*, 2007). Indeed, elevated levels of aldehydes are associated with Alzheimer's disease and might play a role in  $\beta$ -amyloid aggregation. Chen *et al* investigated the link between elevated endogenous aldehydes, either from lipid peroxidation or from amine deamination, and the formation of  $\beta$ -amyloid plaques. Their findings support the involvement of endogenous aldehydes in amyloid deposition related to Alzheimer's Disease. When PrAO was inhibited in the presence of methylamine, it led to a marked decrease of  $\beta$ -amyloid plaque aggregation by up to 80% (Chen *et al.*, 2007a)

Type I and type II diabetes have been associated with high levels of PrAO in blood plasma (Boomsma *et al.*, 2005; Göktürk *et al.*, 2003). Studies have shown PrAO oxidation products, formaldehyde and methylglyoxal, can form AGEs. These aldehydes along with H<sub>2</sub>O<sub>2</sub> produced by PrAO cause crosslinking of proteins and exacerbate diabetic complications such as retinopathy, neuropathy, nephropathy and atherosclerosis (Li *et al.*, 2016). *In vivo* studies comparing patients with a known history of diabetes and vascular complications with a control group of similar age and gender revealed a correlation with high PrAO levels and the state of progression of this disease. Those with diabetic conditions had above average PrAO blood plasma levels when compared to healthy individuals (Januszewski *et al.*, 2014).

### **1.6.2 VAP-1 and Inflammation**

As previously discussed, the membrane bound form of PrAO (VAP-1) has been shown to have an important role in the adhesion and recruitment of leukocytes to sites of inflammation. This function has shown to be problematic when overexpressed at sites where VAP-1 is predominately found such as vascular and adipose tissue (Göktürk *et al.*, 2003). Silvola *et al.*, 2016 showed that VAP-1 was expressed on endothelial cells, where inflamed atherosclerotic lesions were present. Furthermore, they demonstrated that the inhibition of VAP-1 activity decreased the density of macrophages in inflamed atherosclerotic plaques in mice. Their findings led these workers to suggest VAP-1 inhibition as a therapeutic approach in the treatment of atherosclerosis.

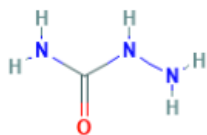
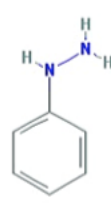
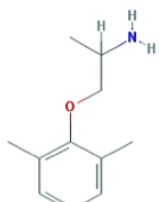
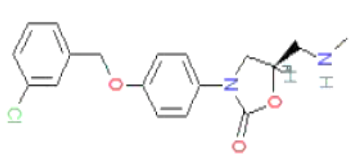
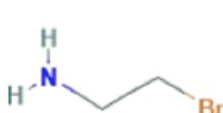
Studies indicated that VAP-1 could mediate inflammation leading to tumor initiation and progression in a mouse model (Ferjančič *et al.*, 2013; Salmi and Jalkanen, 2011).

Their studies showed that VAP-1 deficient mice had less efficient leukocyte-endothelial cell contacts resulting in reduced leukocyte recruitment and inflammation. In addition, Salmi and Jalkanen found that, in VAP-1-deficient mice, cancers such as melanoma spread more slowly than in wild type. This clearly points to a role for VAP-1 (PrAO) in regulating the spread of cancer. Similar findings were obtained with wild type mice where small molecule inhibitors of VAP-1 were employed showing a strong link between VAP-1 and cancer progression (Salmi and Jalkanen, 2011).

### **1.7 Inhibitors of PrAO**

A number of attempts have been made to develop specific, potent inhibitors of PrAO as therapeutics. It has proven challenging to find an inhibitor with the required specificity and potency due to similarities in active site structure to other AOs (see Section 1.5, Table 1.2). It is important that an inhibitor of PrAO does not overlap in specificity and inhibit other amine oxidases and is nontoxic and readily absorbed. Enzyme inhibitors can be chemically and structurally similar to their substrate counterparts (see section 1.6) when bound within the active site such as with the substrate benzylamine and the inhibitor Phenylhydrazine. PrAO inhibitors can be classified by structure or functional groups into a few categories: hydrazines, arylalkylamines, propenyl- and propargylamines, oxazolidinones, and haloalkylamine derivatives. A selection of known inhibitors of PrAO include hydrazine compounds, i.e. semicarbazide and aminoguanidine, arylalkylamine compounds, i.e. phenylhydrazine, and mexiletine and haloalkylamines such as 2-bromoethylamine are shown in Table 1.3, (Foot *et al.*, 2013).

**Table 1.3:** Inhibitors of PrAO. Images taken from PubChem (<https://www.ncbi.nlm.nih.gov/pccompound>).

Inhibitor Class	Example	Structure
Hydrazine	Semicarbazide	
Arylalkylamine	Phenylhydrazine	
Propenyl-propargylamines	Mexiletine	
Oxazolidinone	Almoxatone	
Haloalkylamine	2-bromoethylamine	

For PrAO, inhibition can be achieved in the active site via reaction with TPQ or by steric blockage of the active site entrance or funnel (see Jakobsson *et al.*, 2005).



Since PrAO has been reported to oxidize peptides containing lysine the possibility that cell-surface lysyl residues might be the PrAO/VAP-1 recognition sites was considered. Olivieri *et al.* (2010) reported that the free amino acid L-lysine acted as an H<sub>2</sub>O<sub>2</sub>-dependent inhibitor of beef plasma PrAO.

## **1.8 Dietary components in Health and disease**

Previous work in these laboratories explored the role of dietary components in health and disease. The protective effect of plant food sources against chronic diseases are often attributed to bioactive non-nutrients called phytochemicals (Vayalil, 2012). Phytochemicals are secondary plant metabolites that are not essential nutrients but known to have protective or disease preventive properties. In plants they can play a substantial role in the prevention of microbial, insecticidal or herbivorous attack (Naz *et al.*, 2013).

Interest in phytochemicals is growing in the research community (Monteiro *et al.*, 2016). One such family of phytochemicals, methylxanthines, have been the subject of much research over the years for their ability to block A<sub>2A</sub> adenosine receptors thereby acting as psychoactive stimulants and potential therapeutics for neurodegenerative diseases (Daly, 2007). The effect of methylxanthines on neurodegenerative diseases (Oñatibia-Astibia *et al.*, 2017), cardiovascular disease (Khan *et al.*, 2012), inflammation, (Frost-Meyer and Logomarsino, 2012) and cancer (Sang *et al.*, 2013) are active areas of current research.

Another family of phytochemicals, polyphenols, are also being studied for their health benefits associated with cancer, diabetes, inflammation, heart disease, Parkinson's



disease and obesity (Chang *et al.*, 2015; González-Castejón and Rodríguez-Casado, 2011).

Organic nutrients such as amino acids (AAs) and vitamins are also being studied for their health benefits. AAs are being studied for their potential in prevention and treatment of obesity, diabetes, and cardiovascular disorders, intestinal and neurological dysfunction, and infectious disease (including viral infections) (Wu, 2013; Wu, 2014).

Micronutrients like vitamins are known to be of interest in the prevention of a number of diseases such as migraine, anaemia, cancer, hyperglycemia, hypertension, diabetes mellitus, and oxidative stress. (Eitenmiller *et al.*, 2016; Takata *et al.*, 2013; Thakur *et al.*, 2017). The following sections will consider some of the more prominent phytochemicals in greater detail.

### **1.8.1 Caffeine and Related Methylxanthines**

Methylxanthines are secondary plant metabolites formed from purine nucleotides. They are classed as purine alkaloids and are ubiquitously found in plants. High concentrations of methylxanthines are found in *Coffea arabica* (coffee), *Camellia sinensis* (tea) and *Theobroma cacao* (cacao). The two most common and well-studied methylxanthines are caffeine and theobromine (Fig. 1.8). Other types of methylxanthine's commonly found in food include theophylline, paraxanthine and 7, methylxanthine (Ashihara and Crozier, 1999).

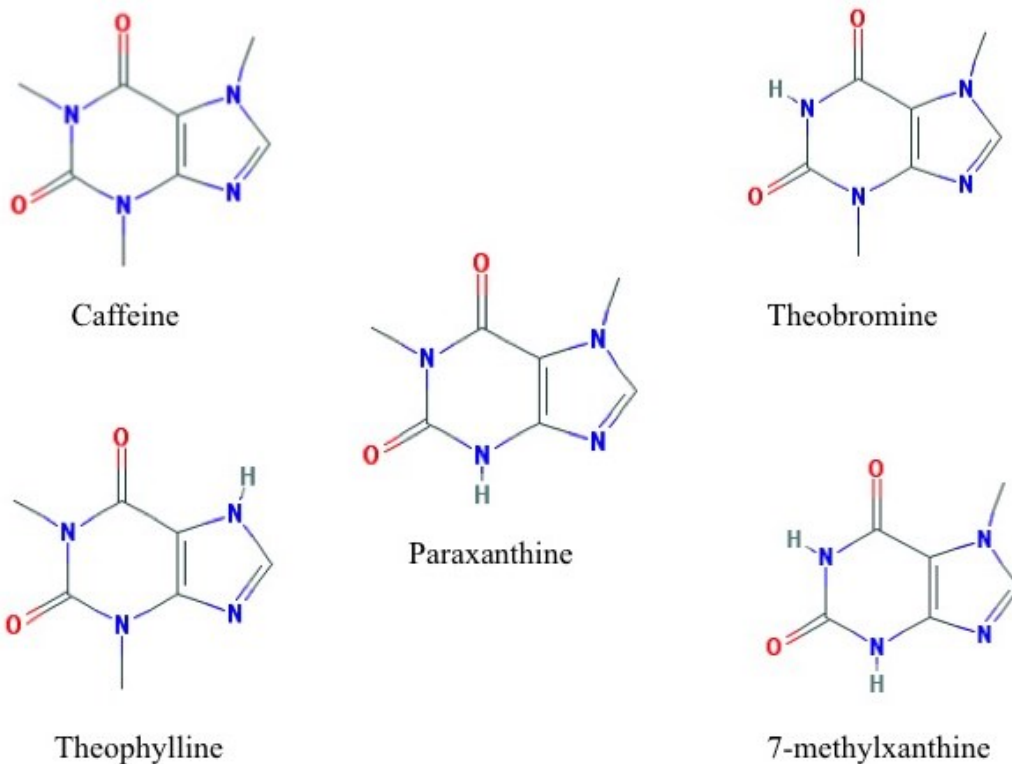


**Fig. 1.9:** Selection of methylxanthine structures. Images taken from PubChem (<https://www.ncbi.nlm.nih.gov/pccompound>).

Caffeine (1,3,7-trimethylxanthine) is a white crystalline alkaloid, which is found in the beans, fruits and leaves of over 60 plant varieties. However, the primary dietary sources are roasted coffee beans and tea leaves (Barone and Roberts, 1996). Caffeine and related xanthine analogues are known to have physiological effects on adenosine receptors, phosphodiesterases and calcium release channels and are thought to be potential therapeutics for Alzheimer's disease, diabetes and cancer (Daly, 2007). Olivieri and Tipton (2011) noted caffeine to non-competitively inhibit Bovine PrAO with a  $K_i$  value of 1.0 mM. (Olivieri and Tipton, 2011). Other methylxanthines closely related to caffeine are theophylline, paraxanthine, 7,methylxanthine and theobromine, These molecules differ from caffeine by one, or more, methyl groups at either position

1, 2 or 3 around the xanthine structure (Fig. 1.8) and are also found naturally in the diet.

Theobromine is most abundant in cocoa beans with a dry weight composition of 2.7% (Ashihara and Crozier, 1999). The reported health benefits of theobromine include anticancer, anti-inflammatory and cardiovascular protection without the unwanted stimulatory side effects such as insomnia, high heart rate and nervousness that can be associated with high caffeine intake (Martínez-Pinilla *et al.*, 2015; Sugimoto *et al.*, 2014).

Theobromine although structurally similar to caffeine has a number of chemical and physiological differences. For instance, theobromine has a calming sleep inducing effect on the body while caffeine is known for its stimulant properties (Khan *et al.*, 2017). Interestingly, a study with human molars showed remarkable protection of the enamel surface upon application of 200 mg/L of theobromine solution. The effect was not observed with other methylxanthines (Kargul *et al.*, 2012).

The half-life of theobromine in humans is much higher than for caffeine. Caffeine is highly water soluble, peaks in the blood 30–40 min after ingestion, and has a half-life of 2.5–5 h, while theobromine is less water soluble, attains peak blood concentrations 2–3 h after ingestion and has an estimated half-life of 7–12 h (Baggott *et al.*, 2013). Theobromine consumption is generally safe for humans but for dogs it is highly toxic. The half-life of theobromine in dogs is 17.5 h. Theobromine median lethal dose (LD<sub>50</sub>) is about 1000 mg/kg in humans and in dogs 300 mg/kg (Ahlawat *et al.*, 2014). The three main metabolites of caffeine are paraxanthine (84%) theophylline (4%) and theobromine (12%) (Santos *et al.*, 2015). The positive health benefits associated with

caffeine could be partly due to the products of its metabolism such as theobromine and theophylline (Martínez-Pinilla *et al.*, 2015).

### 1.8.2 Green Tea

Tea from the *Camellia sinensis* plant is a popular drink that is consumed worldwide and is specifically noted for its beneficial health effects. These health benefits are attributed to the leaf polyphenols. These flavonoids account for the majority of green tea polyphenols (GTPs) (Steinmann *et al.*, 2013; Table 1.5).

**Table 1.5:** The chemical dry composition of green tea (Sinija and Mishra, 2008)

<b>Polyphenols</b>	30%
<b>Proteins</b>	15 - 20%
<b>Fibre</b>	26%
<b>Carbohydrates</b>	5 - 7%
<b>Lipids</b>	7%
<b>Minerals and trace elements</b>	5%
<b>Amino acids</b>	1 - 4%
<b>Pigments</b>	2%

The steaming of tea leaves during processing inactivates the enzyme (Polyphenol Oxidase, EC. 1.14.18.1). This enzyme is responsible for the breakdown of polyphenols and colour pigments and its inactivation gives the tea its green colour - in contrast to enzymatically fermented black tea (Cabrera *et al.*, 2010). Many health benefits have been associated with green tea and numerous studies carried out to investigate these claims. Health benefits are thought to include the prevention of cancer, diabetes, inflammation, heart disease, Parkinson's disease and obesity (Chacko *et al.*, 2010; Hara, 2001; Schneider and Segre, 2009; Sinija and Mishra, 2008). See Fig. 1.10.

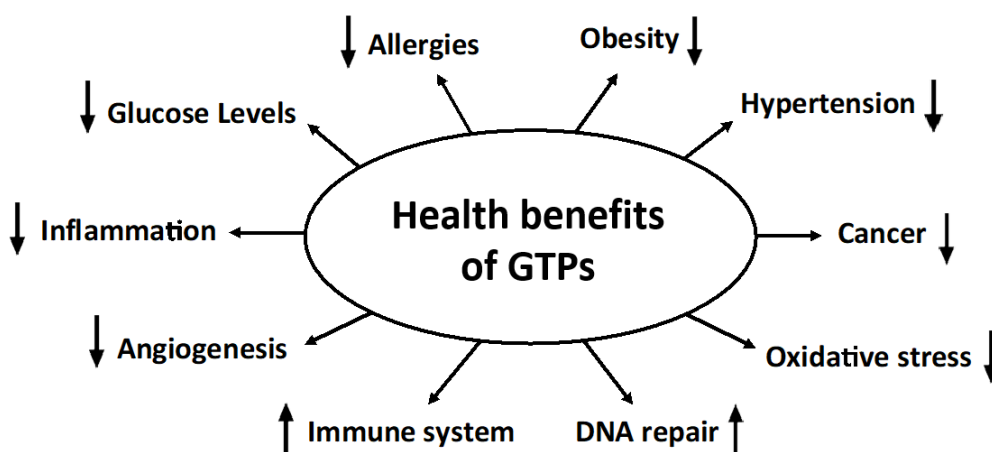


**Fig. 1.10.** An overview of Green Tea Polyphenols health benefits in a range of diseases. Arrows indicate an increase or decrease in effect.

### 1.8.2.1 Polyphenols

Polyphenols are secondary metabolites found in plants that have been reported to act as antioxidants, anti-allergic, anti-inflammatory, anticancer, antihypertensive, and antimicrobial agents in human health (Daglia, 2012). Polyphenols can be broken into subclasses such as phenolic acids, lignans, stilbenes, isoflavones and flavonoids. Flavonoids can be further subdivided into flavanols, flavonols, anthocyanins, flavones, flavanones and flavanonols. For instance, flavonols include quercetin and kaempferol while flavanols include the catechins; Epigallocatechin gallate (EGCG) and Epicatechin gallate (ECG) (González-Castejón and Rodríguez-Casado, 2011).

The most abundant type of polyphenols found in green tea are flavonoids of which catechins are the most abundant (Fig. 1.10). The four most significant catechins are epigallocatechin gallate (59%), epigallocatechin (19%), epicatechin gallate (13.6%) and epicatechin (6.4%) (Steinmann *et al.*, 2013).

Polyphenols may be useful in ameliorating the deleterious effects associated with obesity. Cellular studies demonstrated that dietary polyphenols reduce viability of adipocytes and proliferation of pre-adipocytes, they suppress adipocyte differentiation and triglyceride accumulation, stimulate lipolysis and fatty acid  $\beta$ -oxidation and reduce inflammation. Animal studies strongly suggest that commonly consumed polyphenols have a pronounced effect on obesity. Their administration gives rise to lower body weight, fat mass, and triglycerides. They seem to act through enhancing energy expenditure and fat utilization, and by modulating glucose hemostasis. (Wang *et al.*, 2014a). Epigallocatechin gallate (EGCG) has been the compound most widely explored (Chen *et al.*, 2011; Wang *et al.*, 2014a).

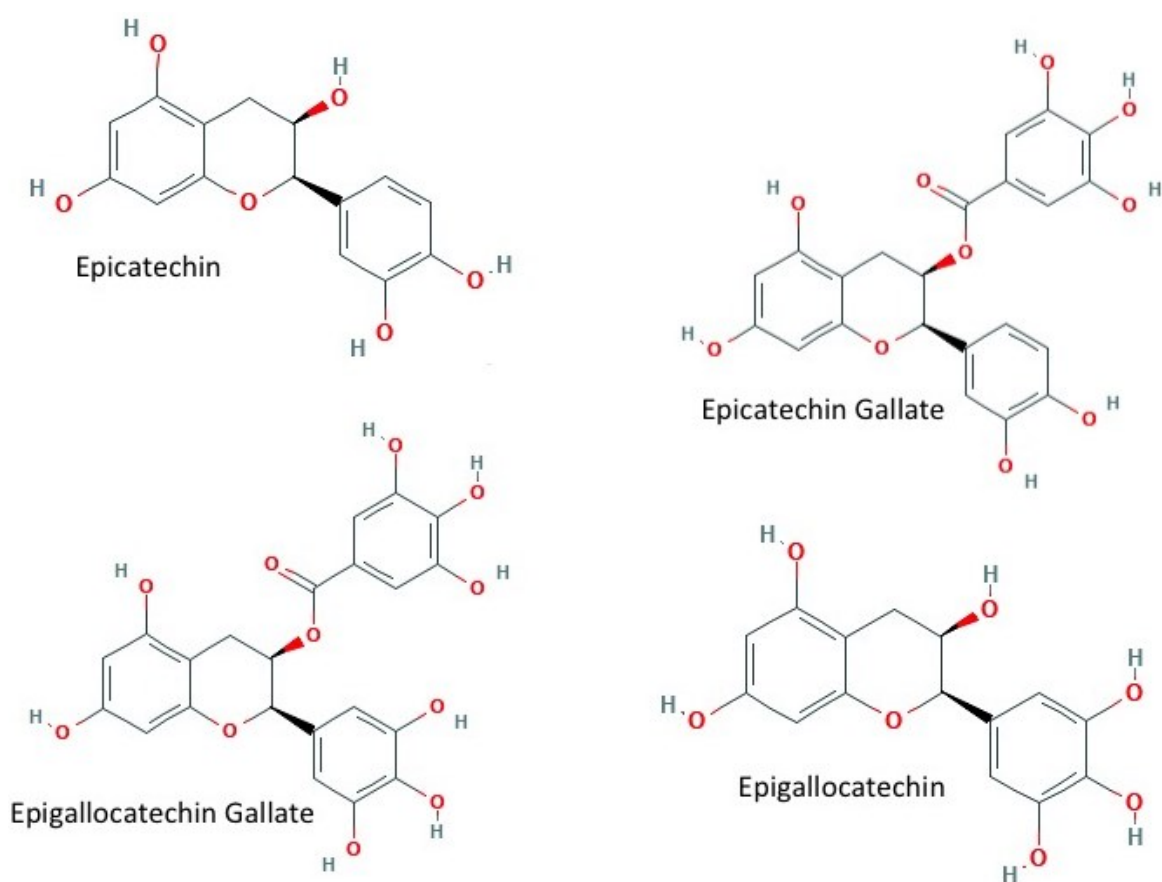


**Fig. 1.11.** Chemical structures of the four most abundant polyphenols found in green tea. Images acquired from (<https://www.ncbi.nlm.nih.gov/pccompound>).

### **1.8.2.2 Green Tea Polyphenols in Health**

Studies have shown that GTPs, particularly EGCG, contribute to the prevention of cancer. (Chen *et al.*, 2011) have shown that EGCG protects DNA from methylation and mutation which can be a first step in the formation of cancer. GTPs can prevent oncogene expression of cancer-causing genes, promoting expression of p53 and p27 thus inducing apoptosis. Furthermore, GTPs inhibit proteasome activity, which can prevent the degradation of regulatory cell proteins that can also lead to cancer. *In vivo* studies by Chacko and colleagues (2010), demonstrated that the administration of GTPs lowered plasma glucose levels in diabetic rat models at a dose of GTPs at 100 mg kg<sup>-1</sup> and that EGCG exhibited an insulin mimic effect, lowering glucose levels by 44% whilst concomitantly increasing tyrosine phosphorylation of the insulin receptor (Chacko *et al.*, 2010).

Inflammation studies with EGCG, the principal polyphenol of Green Tea, at 100 mmol/L showed 50% inhibition of TNF $\alpha$  production in a dose-dependent fashion in a macrophage cell line. EGCG also showed 30–40% inhibition at 100 mmol/L of TNF $\alpha$  mRNA expression and nuclear NF-KB-binding activity (Guo *et al.*, 2009; Yang *et al.*, 1998) which could be a factor for GTPs and associated decrease in inflammation.

### **1.8.3 Amino Acids**

Amino Acids are involved in protein formation and cell signaling and are regulators of gene expression and are also precursors of many hormones (Wu, 2009). Free AAs are readily available through the diet, have primary amine groups and can therefore serve as potential modulators of PrAO.

In the present study, research interest in AAs and PrAO modulation was spurred by previous findings in these laboratories (Olivieri *et al.*, 2007) which showed *L*-lysine binding to PrAO. *L*-lysine, showed inhibition of VAP-1/PrAO and gave an apparent  $K_i$  value  $166 \pm 48 \mu\text{M}$ . *L*-lysine could not inhibit directly, but required the presence of  $\text{H}_2\text{O}_2$  to have an inhibitory effect (Olivieri *et al.*, 2007).

#### 1.8.4 Vitamins and Health Benefits

Vitamins A, C, D, K and E have all been examined as agents in cancer prevention (Block, 1991; Klein *et al.*, 2003; Lotan, 1980; Ness *et al.*, 2015). Many of the exact mechanisms of actions with regards to these health benefits have not been fully characterised. For example, studies with vitamin B supplements demonstrated a positive effect with Alzheimer's patients (Dangour *et al.*, 2010), although the exact mechanism was not fully elucidated.

An area of research where vitamins have been shown to inhibit enzymes was reported with the inhibition of lactoperoxidase, an enzyme that functions as a bactericide and uses hydrogen peroxide as an oxidising agent (see Table 1.6). Vitamins reported to have an inhibitory effect on this enzyme include vitamin C, K3 and folic acid. Reported inhibition mechanism for all three vitamins showed a competitive type of inhibition mechanism, Sisecioglu *et al.* (2010).

**Table 1.6:** Selection of vitamins that have a modulating effect on lactoperoxidase, (Sisecioglu *et al.* 2010).

Inhibitor	IC <sub>50</sub> Values	K <sub>i</sub> Values
<b>Folic Acid</b>	0.0925 mM	$0.0218 \pm 0.0019 \text{ mM}$
<b>Vitamin K3</b>	0.025 mM	$0.0107 \pm 0.0044 \text{ mM}$
<b>Vitamin C</b>	2.03 $\mu\text{M}$	$0.508 \pm 0.257 \mu\text{M}$



Fernando and Soysa (2015) examined the oxidant scavenging activity of Vitamin C and related compounds. The test method employed 4-aminoantipyrine, in the presence of horseradish peroxidase (HRP), to produce a pink coloured quinoneimine dye. This is the same method used to detect activity rates of PrAO in the visible region through conjugation of H<sub>2</sub>O<sub>2</sub> to produce the quinoneimine dye (see Section 2.5.1). False inhibition results can be observed if compounds that have antioxidant properties are being screened as potential inhibitors, as happened with the reported inhibition by Sisecioglu *et al.* (2010), using vitamin C, K3 and folic acid. These compounds are all antioxidants that caused interference where the assay detection method involves hydrogen peroxide as the oxidising agent. Careful controls must be set in place for ligands screened with PrAO, to account for such antioxidant interactions.

## 1.9 Computational Modelling

Traditionally, laboratory-based methods were used to discover novel leads in drug discovery via strategies such as high-throughput screening. Some disadvantages of this approach include high cost, the use of significant resources and frequent low hit rates (Williams *et al.*, 2015). The completion of the human genome project has permitted drug targets to be identified and studied via computational approaches. This, coupled with recent advances in biological structure analysis, such as X-ray crystallography and nuclear magnetic resonance (NMR) structure determination has opened new avenues for analysing and predicting ligand-target binding interactions (Voet *et al.*, 2014). Moreover, advances in computing power and software have resulted in faster and cheaper *in-silico* methods becoming available in early-stage drug discovery. Such *in-silico* methods are growing in popularity (Cosconati *et al.*, 2010) and can be used to predict the interactions of a ligand with a protein binding site as

well as estimating their binding strengths or relative affinity (Yuriev and Ramsland, 2013).

There are two main approaches to computational modelling: ligand based drug design (LBDD) and structure based drug design (SBDD) modelling. Ligand based modelling is applied when the molecular target is not known or fully understood but experimental binding/functional data is available for given ligands with a certain protein or molecular target. A “*training set*” of ligands that are known to bind or interact with a molecular target are employed where similar features among these ligands such as size, charge and functional groups, aid in describing the structure-activity relationships (SARs) (Kaserer *et al.*, 2015). In the structure-based approach the macromolecule structure or target complexes are known and are obtained either from computational homology modelling, experimental nuclear magnetic resonance (NMR) data or X-ray crystallography. The main purpose of SBDD techniques such as molecular docking is to design or analyse ligands with specific electrostatic and stereochemical attributes to achieve high receptor binding affinity. These compounds can then be used for developing potential therapeutics (Ferreira *et al.*, 2015).

### **1.9.1 Molecular Docking**

Molecular docking, which is an SBDD approach, is a computational method that predicts the binding of a small a molecule or ligand to a known macromolecule receptor-binding site. There are many docking tools in use today such as *Autodock*, *GOLD*, *FlexX* or *ICM* (see Table 1.7), which can generate various poses of a ligand and receptor and employ mathematical algorithms such as Monte Carlo, genetic algorithms or fragment-based algorithms to select the best interacting binding poses

(see Table. 1.7) (Azam and Abbasi, 2013). Autodock and GOLD employ a genetic algorithm based on an iterative process. They begin by docking the ligand into various conformational spaces allowing the optimum binding conformations to go forward to another round of modelling. In the first round the software eliminates energetically unfavorable conformations. DOCK and FlexX employ an incremental reconstruction algorithm where fragments are identified, docked into a receptor until the completed ligand is added step by step: only the highest scoring fragments progress to subsequent rounds of modelling (Agarwal and Mehrotra, 2016).

To achieve virtual docking of a ligand to a binding site a target structure is computationally modelled or experimentally solved, for example, by X-ray crystallography. The ligand and target structures are prepared by assigning tautomeric, stereoisomeric and protonation states. Docking generally gives rise to two main interrelated outcomes where:

- i. A series of binding conformations or interactions of a given ligand (with tautomer/stereoisomers/protonation states enumerated) with a protein are generated
- ii. Docking poses are ranked in order of predicted binding affinity via an algorithm scoring function.

The scoring function can be either empirical, knowledge based or employ force field computation (Liu and Wang, 2015). Empirical scoring functions have been developed to reproduce experimental binding affinity data, knowledge-based functions have been developed based on the statistical analysis of interacting atom pairs from known

protein–ligand complexes with available three-dimensional structures (Cheng *et al.*, 2012).

Force field, which is the scoring function used in this study, utilises a probe atom, typically carbon, to estimate the free binding energy of a target macromolecule at a certain grid point location. The force field calculation accounts for the bonded (bond, angle and dihedral) and non-bonded (Van der Waals and electrostatic forces) interactions. A ranked list is then provided of the lowest predicted binding energy scores (Hill and Reilly, 2015).

Attempts at computationally docking small ligands to PrAO have been reported. A library of 48 potential compounds that could potentially bind to PrAO were reduced to the most favorable 20, based on the best scores achieved for each compound. Of those 20 lead compounds 3 newly discovered hits or substrates were found. These hits resulted in a good correlation between docking calculations and experimental data when these substrates were tested for activity with PrAO (Yraola *et al.*, 2006).

Another study used Glide docking software where PrAO and MAO were both computationally docked and subsequently assayed with a range of phenolic compounds (quercetin, resveratrol, pterostilbene and caffeic acid). Experimental data showed that none of the phenolic compounds inhibited PrAO and only quercetin and resveratrol had any effect on MAO (Carpéné *et al.*, 2016).

**Table 1.7:** A selection of docking tools and their respective algorithms. The table highlights the pros and cons of each type (Chaudhary and Mishra, 2015; Morris *et al.*, 2009).

Docking Tool	Algorithm	Scoring Function	Pros	Cons
AutoDock	Genetic algorithm, Lamarckian genetic algorithm, Simulated annealing	Auto Dock (force-field methods)	Targeted flexible docking	Target protein too flexible, Flexible ligands
Gold	Genetic algorithm	Gold score, Chem score, User defined,	Small binding sites, Opened cavities, Small hydrophobic ligand	Flexible ligands, Highly polar ligands, Very flexible ligands
FlexX	Incremental construction	FlexX score, PLP	Small binding sites, Opened cavities, Small hydrophobic ligands, Small binding sites	Highly polar ligands, Flexible ligands
Glide	Monte Carlo	Glide Score, Glide Comp	Flexible ligands, Small hydrophobic ligands	Ranking very polar ligands, Slow speeds

### 1.9.2 Molecular Docking with AutoDock Tools

For this study, AutoDock Tools V1.5.6 was used to simulate bindings of ligands to PrAO. AutoDock has been in use since 1990 (Hsieh *et al.*, 2016) and over the years has been an effective tool in predicting bound conformations as well as binding energies for ligands with a chosen molecular target (Jung *et al.*, 2016; Morris *et al.*, 2009; Wang *et al.*, 2014b).

The AMBER force field scoring function is used by AutoDock tools (<http://autodock.scripps.edu>) and the calculation used to predict the list of binding affinity scores is as follows:

$$\Delta G_{\text{Binding}} = \Delta G_{\text{vdW}} + \Delta G_{\text{elec}} + \Delta G_{\text{hbond}} + \Delta G_{\text{desolv}} + \Delta G_{\text{tors}}$$

Where  $\Delta G_{\text{vdW}}$  accounts for the Van der Waals energy and calculates the “fitting” of the molecule thereby defining the pocket or space where a ligand may dock to a macromolecule.  $\Delta G_{\text{elec}}$  calculates the ionic or polar interactions between charged atoms,  $\Delta G_{\text{hbond}}$  calculates hydrogen bonding between, for example, bases and carboxyl groups,  $\Delta G_{\text{desolv}}$  accounts for water molecules that surround the ligand and binding site that need to be displaced for binding to occur,  $\Delta G_{\text{tors}}$  calculates the entropy or degrees of freedom of the ligand and macromolecule. (Santos-Martins *et al.*, 2014).

One major limitation of many docking simulations is setting the ligand and/or macromolecule to be too rigid where rotatable bonds are set in a fixed position. Although this may be considered a disadvantage it greatly reduces the computational time needed to perform docking simulation. Rigidity of the macromolecule does not allow for ligand-induced fit that is a critical factor when looking at enzyme ligand interaction. This “rigidity” disadvantage can be overcome with Autodock whereby side chains that are known to be important in binding interactions may be allowed to be flexible. This creates a more computationally intensive but more accurate simulation with a better docking fit and score (Morris *et al.*, 2009).

Previous studies have shown Autodock’s ability to screen binding interactions of small ligands with PrAO. In one study a PrAO physiological substrate methylamine was

successfully docked with PrAO. The lowest computational score showed methylamine to be bound in the active site and the amine of methylamine to be hydrogen bonded to TPQ and Asp336 as expected (Bonaiuto *et al.*, 2010). A computational docking simulation was employed to design a multi-target inhibitor to simultaneously inhibit two enzymes, PrAO and acetyl-cholinesterase. AutoDock software was used to compare a crystallised bound ligand / PrAO complex with the *in-silico* bound equivalent to validate the method. Binding of a known ligand, galantamine, with the co-factor TPQ in an X-ray structure was compared to a computationally docked galantamine equivalent with PrAO. Thereinafter, known inhibitors from each target were deconstructed into small fragments that were modelled into the *in-silico* model. In all, this study produced four potential molecules that were designed *in-silico* for experimental testing (Gharaghani *et al.*, 2013).

These examples show Autodock to be effective in predicting probable binding interactions between a ligand and macromolecule target, effectively scoring these ligands in order of optimum interaction.

### **1.10 Proposed Research and Aims**

The proposed research involves the exploration of the interaction between PrAO and selected phytochemicals. Several compounds will be chosen as possible inhibitors of PrAO. Compounds such as polyphenols and methylxathines are of particular interest. These compounds are known to be associated with health benefits that offset the negative effects associated with overly expressed PrAO. At the outset, we employed a plate reader assay that monitored H<sub>2</sub>O<sub>2</sub> produced from PrAO-catalyzed oxidation of benzylamine. A direct spectrophotometric assay was employed to monitor the product

benzaldehyde produced by benzylamine oxidation by PrAO at a wavelength of 254 nm. Enzyme kinetic studies were used to estimate  $IC_{50}$  and  $K_i$  for significant inhibitors. Finally, computational docking software was used to predict binding interactions and active site binding locations of some inhibitors of interest.

The aims of this research were to explore selected phytochemicals with known health benefits for activity as PrAO inhibitors. The study focused on establishing the mode of inhibition and identifying the structural features necessary to be a useful PrAO inhibitor. We aimed to support our observations using computational modelling in an attempt to identify inhibitor binding sites on the enzyme surface.



# **CHAPTER 2**

## *Materials & Methods*

## 2.1 List of Reagents

Reagent	Supplier
Acetonitrile	Sigma
Acrylamide	Sigma
Adenine	Sigma
Adenosine	Sigma
4-Aminoantipyrine	Sigma
4-amino-phenol	Sigma
L-Alanine	Sigma
L-Arginine	Sigma
Ascorbic Acid	Sigma
Benzaldehyde	Sigma
Benzylamine	Sigma
Benzylhydrazine Dihydrochloride	Sigma
8-Bromocaffeine	Sigma
Caffeic Acid	Sigma
Caffeine	Sigma
Catechol	Sigma
2 Chloromethyl benzimidazole	Sigma
L-Cysteine	Sigma
Cystic Acid	Sigma
EGTA	Sigma
Epicatechin	Sigma
Epicatechin Gallate	Sigma
Epigallocatechin Gallate	Sigma
D-Ethionine	Sigma
GABA	Sigma
Green Tea	Twinings
Horseradish Peroxidase	Sigma
Hypoxanthine	Sigma
Isatin	Sigma
D-Iso-Leucine	Sigma
Methyl Gallate	Sigma
1-Methyl-L-histidine	Sigma
1-Methylimidazole	Sigma

1,7-Dimethylxanthine	Sigma
7-Methylxanthine	Sigma
Monoamine Oxidase	In house
N-alpha-methylhistamine Dihydrochloride	Sigma
D-Norvaline	Sigma
Octopamine	Sigma
Lisofylline	Sigma
L-Ornithine	Sigma
Phenylalanine	Sigma
Phloroglucinol	Sigma
Potassium Phosphate Dibasic	Sigma
Pyridoxine	Sigma
Quercetin	Sigma
Riboflavin	Sigma
Rutin	Sigma
Saponin	Sigma
Semicarbazide	Sigma
Primary Amine Oxidase	Langanbach Services
D-Serine	Sigma
Spermidine	Sigma
Spermine	Sigma
Sucrose	Sigma
Sulphanilamide	Sigma
Theobromine	Sigma
Theophylline	Sigma
Trigonelline	Sigma
TRIS	VWR
Tryptamine	Sigma
Umbelliferone	Sigma
Uric Acid	Sigma
Vitamin B1	Sigma
Vitamin B12	Sigma
Vanillic Acid	Sigma
Xanthine	Sigma

## 2.2 List of Instrumentation & Equipment

<b>Instrument/Equipment</b>	<b>Manufacturer &amp; Type</b>
Balance Weigh Scales	Mettler – college 150
6-Cell Automated Cuvette Changer	Shimadzu CPS-240A
Centrifuge	Eppendorf – 5415 R
Filter Paper	Whatman™ 0.45 µM Polyamide
Hand Held Homogeniser	Thomas
Heating Bath	Julabo - 5
Heating Block and Stirrer	IKA RH – KT/C
HPLC	Waters 2690
HPLC Acquisition Software	Empower 2
HPLC Detector	Waters 2487 Dual Absorbance
Visible Kinetics Software	Softmax Pro – 6.2.1
UV Kinetics Software	UV Probe – 2.42
UV-Vis Spectrophotometer	Shimadzu - UV-2600
pH Meter	Corning - 240
UV-Vis Spectrophotometer Plate Reader	Molecular Devices – Spectra Max M3
Vortex mixer	Wisemix – VM-10
Water Purification Unit	Millipore Milli-U10
Sample Vials	VWR Glass 2 mL
Separation Column	Nucleosil C18 (3.9 x 150 mm)
Spectrophotometer Plate Reader UV-Vis	Molecular Devices – Spectra Max M3
Vacuum Pump	WELCH - MPC090E
96 Well Plates	Greiner – Flat Bottom Crystal Clear Plate

### **2.3 Preparation of PrAO for Storage and Use**

Lyophilised bovine plasma PrAO was purchased from Langanbach Services. PrAO was reconstituted to a final concentration of 10 mg.mL<sup>-1</sup> from a pure lyophilised state with 50 mM phosphate buffer (pH 7.2) which was gently inverted to mix and aliquoted into 0.5 mL aliquots into 1.5 mL eppendorfs. The enzyme solution was retained in long-term storage at -20°C. From these aliquots working stock concentrations of PrAO were made up to approximately 0.3 mg.mL<sup>-1</sup> by adding 30 µl to a final volume of 1000 µl of buffer. This was then brought to a final working activity concentration of 1.2 U.µl<sup>-1</sup> by adding 50 µl of working stock solution to 200 µl of a final assay volume.

All working stock solutions were stored on ice during use. For short-term storage, the working concentration of enzyme was refrigerated at 4°C due to an observed decrease in enzyme activity beyond three freeze thaw cycles. The enzyme was placed on ice at all times while assays were being carried out.

### **2.4 Preparation of Substrates, Controls and Inhibitor Solutions**

All solutions were prepared with deionised water from a Millipore Milli-U10 water purification system and compounds were weighed using a 4 decimal place balance (Mettler – College 150 weigh scales). Volumes were measured either with 0.5 µL – 5000 µL pipettes (Gilson) or by use of appropriate volumetric glassware. Where solutions were required at a certain pH, a Corning – 240 pH meter was used to monitor pH during buffer preparation, with adjustments made using an appropriate acid/base. The pH probe was calibrated when first used each day with pH 4, 5 and 10 standard buffer solutions as per manufacturer's recommendations. Any poorly soluble compounds tested were either solubilized in DMSO or ethanol,

as advised by the supplier's chemical data sheet, at a minimal percentage to solubilise to a maximum of 5% (v/v) concentration. A control using this percentage of solvent solution was examined in the presence of the enzyme under normal experimental conditions to identify any inhibitory effects on catalysis, if any.

## **2.5 Standard U.V. Spectrophotometric assay of PrAO; Monitoring Benzaldehyde Production at 254 nm**

The oxidative deamination reaction of PrAO was recorded by monitoring benzaldehyde aldehyde production from benzylamine at 254 nm. This was a continuous spectrophotometric assay. The substrate used was benzylamine (final concentration: 5.0 mM), which PrAO converts to benzaldehyde, ammonia and H<sub>2</sub>O<sub>2</sub>. The reaction mixture contained 1.2U of PrAO, 50 mM potassium phosphate buffer (pH 7.2) and benzylamine (5 mM). When required, a selected inhibitor or semicarbazide (1 mM) were added to provide a control, to a total final volume of 1 mL in a Quartz cuvette. Reaction rates were monitored in a Shimadzu UV-2600 UV-Vis Spectrophotometer with a 6-cell cuvette automated changer, employing the UV Probe-2.42 software. All components of the reaction mixture were screened for absorbance interference in the 254 nm or 498 nm range via a spectral scan between 200 nm – 500 nm or 350 nm – 700 nm depending on assay method in question. Each compound tested was examined in the buffer being used for the assay, before and after each assay, to verify that no unusual spectral readings that might offset, or interfere with, the data were obtained. Quartz cuvettes were used and cleaned after each use by soaking cuvettes in 50% (v/v) sulfuric acid 2.0M and 50% (v/v) de-ionised water to remove any residues that may occur over time.

Positive controls for PrAO, without inhibitor, and negative controls using 1 mM semicarbazide, a well-established inhibitor of PrAO (O'Sullivan *et al.*, 2004) at this concentration, were employed. All assays were performed in triplicate at 37°C.

### **2.5.1 Holt Coupled-Assay of PrAO Monitoring Hydrogen Peroxide Production at 498 nm.**

In addition to the continuous spectrophotometric assay we also employed a colourimetric assay (the method of Holt and Palcic (2006)). This assay was easily automated as a plate reader assay and was used for initial screening of possible inhibitors. It monitors H<sub>2</sub>O<sub>2</sub> production via a coupled reaction and formation of a quinoneimine dye (see below section 2.5.2) and can therefore use a wider range of substrates than the spectrophotometric assay (section 2.5). However, as detailed below, we found certain substrates or inhibitors, could react with the redox dye used in this assay to provide anomalous readings.

The activity of PrAO was determined by following the production of H<sub>2</sub>O<sub>2</sub> at 498 nm, by the method of Holt and Palcic (2006). The enzyme was typically assayed in the presence of 5.0 mM benzylamine and 1.2U PrAO. Triplicate assays were carried out in a total reaction volume of 200 µL in 96-well microtitre plates, at 37°C, using a SpectraMax 340PC plate reader (Molecular Devices, Inc. Sunnyvale, CA 94089-1136, USA). Control assays for the coupling system, in the presence of 0.1M H<sub>2</sub>O<sub>2</sub>, 1mU/mL HRP but in the absence of PrAO were employed. Each compound was assayed both in intra and inter triplicates, at a final concentration of 1 mM at 37°C, before adding substrate.

GraphPad Prism (Version 5.0) was used for all curve fitting procedures. Double-reciprocal plots were created for illustrative purposes only. Mean standard errors were determined from at least 3 separate experiments.

### **2.5.2 Preparation of Chromogenic Solution for H<sub>2</sub>O<sub>2</sub> Detection and Initial Rate Determination.**

The chromogenic solution for the detection of H<sub>2</sub>O<sub>2</sub> produced by oxidation of amines by PrAO contained 1 mM vanillic acid, 0.5 mM 4-aminoantipyrine and horseradish peroxidase (4U/mL) in a 'physiological' buffer (200 mM potassium phosphate buffer, pH 7.6). The pH of the buffer was adjusted to 7.6 with 0.1M NaOH. The solution was then stored at 4°C in a universal tube and covered in tinfoil, since the solution is light sensitive. The peroxidase produces a coupled reaction via H<sub>2</sub>O<sub>2</sub> production, resulting the formation of a quinoneimine dye, which absorbs strongly at 498 nm.

### **2.5.3 HPLC Assay for Monitoring Inhibition of Benzaldehyde at 254 nm**

Benzaldehyde formation from benzylamine by PrAO was monitored at 254 nm using a Waters 2487 dual absorbance detector and a Waters 2690 separations module. A Nucleosil C18 (3.9 x 150 mm) separation column was used with a flow rate of 0.8 mL/min and at a working pressure of approx 800 psi. This HPLC assay method was performed using isocratic elution with an optimum mobile phase blend of Acetonitrile and deionised water (50:50), which was filtered and degassed. Chromographic data was acquired and processed using an Empower<sup>TM</sup> 2, chromatography data software package.



Benzaldehyde standards were first prepared as controls and peaks eluting were monitored at 254 nm to measure retention times and peak areas. Standards were prepared from pure Benzaldehyde (99.9%; Sigma) dissolved in a 50 mM potassium phosphate buffer pH7.4. The standard curve was produced with seven concentrations ranging from 10  $\mu$ M – 120  $\mu$ M to determine PrAO product (i.e. benzaldehyde) concentrations.

Inhibition assays were carried out in triplicate in a 50 mM phosphate buffer (pH 7.2) containing 1.2 U of PrAO, 5 mM benzylamine and variable concentrations of selected inhibitor in a final volume of 1 mL. All inhibition reactions and controls were thoroughly mixed, allowed to incubate for 3hrs at room temperature (22 °C) and then simultaneously quenched by heating at 85°C for ten minutes. The samples were centrifuged at 20,800 g for 20 minutes. 10  $\mu$ L of each sample was injected with an acquisition time of 6 minutes for each sample. Positive and negative controls were included as standard U.V. spectral analysis method (see Section 2.5).

## **2.6 Green Tea Extraction**

A crude extract of green tea (*Twinings*) was prepared from dried tealeaves in distilled water. In brief, this entailed boiling 2.5 g tealeaves in 100 mL of dH<sub>2</sub>O (prepared by passage through a Millipore Milli-U10 purification unit) for 5 minutes. The extract was then sieved and initially filtered through standard grade Whatman filter paper, then filtered using a 0.45  $\mu$ M cartridge filter and stored at 4°C. The inhibition range was obtained by serial dilution with assay buffer until an inhibiting rate was achieved (noted as 1:100 dilution of the original extract).

## 2.7 IC<sub>50</sub> Inhibition Plots

IC<sub>50</sub> plots utilizing *GraphPad Prism* were carried out to ascertain 50% inhibition concentrations for each compound showing significant inhibition (Version 5.0). Assays were carried out with PrAO saturated with substrate (5 mM Benzylamine) in the presence of the chromogenic coupled reaction solution and inhibitor as previously (see Section 2.5.2). Rates were recorded in units of mAbs.min<sup>-1</sup>. Kinetic assays were performed under steady state conditions, as defined by a linear reaction progress curve. All kinetic parameters were calculated using the Michaelis-Menten equation function within *GraphPad Prism*. All assays were carried out in triplicate. IC<sub>50</sub> sigmoidal curve plots were produced by plotting initial rate against the logarithmic concentration of inhibitor using *GraphPad Prism*.

## 2.8 Lineweaver Burk Plots and K<sub>i</sub> Estimation

Lineweaver Burk plots at different inhibitor concentrations were employed to identify the pattern of PrAO inhibition as determined by the observable effects on K<sub>m</sub> and/or V<sub>max</sub> parameters. K<sub>i</sub> values were estimated from resulting slope values replots. In brief, this approach provided a simple screening mechanism to examine compounds that demonstrated significant inhibition. Assays were carried out using 1 mM to 5 mM substrate concentrations for each inhibitor concentration. As per Section 2.8, kinetics analyses were performed employing the Michaelis-Menten equation to estimate kinetic parameters. All assays were carried out in triplicate. Plots were then graphed using *GraphPad Prism* (Version 5.0) and employed the embedded Lineweaver Burk equation function which subsequent non-linear regression analysis. The slopes from the individual reciprocal plots, were used to determine corresponding K<sub>i</sub> values.

## 2.9 PrAO Computational Docking Studies

AutoDock tools 4.0 (ADT; <http://autodock.scripps.edu>) was the computational docking software used to examine binding interactions between PrAO and various ligands. The software and hardware resources of the DJEI/DES/SFI/HEA Irish Centre for High-End Computing (ICHEC) were utilized. Ligand files were sourced in the ChEMBL section of the European Bioinformatics Institute (EMBL-EBI) website (<https://www.ebi.ac.uk/chembl/>) and saved in a *mol2* format. Ligand tautomers and stereoisomers were enumerated using Biovia Discovery Studio (Version 4.0). Ligand files were then converted to a Protein Data Bank, Partial Charge (Q), & Atom Type (T) format (PDBQT) using ADT and rotatable bonds were identified and set for flexible ligand docking.

The enzyme structure of bovine PrAO was taken from the protein data bank (PDB; <http://www.rcsb.org/pdb/home/home.do>) under the PDB ID 2PNC (Holt *et al.* 2008). Structurally relevant hydrogen atoms were added to heavy atoms such as carbon, oxygen and nitrogen to fulfill valency requirements. The structure was checked for any additional water molecules that could be added from the original x-ray-crystallography structure and saved. A separate, flexible, file was created that permitted certain side chains of the macromolecule to be flexible. Flexible residue side chains were chosen based on prior research as noted in the literature and were: Arg173, Asp177, Ile232, TPQ470, Asn469, Leu468, Thr466, Thr381 and Met384. These amino acids and or location were noted in the literature to be involved in inhibitor interactions (Jakobsson *et al.*, 2005; Bligt-Lindén *et al.*, 2013; Gharaghani *et al.*, 2013).

### 2.9.1 Grid File Generation

The parameter file for each atom type found on the structure of bovine PrAO was created from the known energy values for each atom hosted within the internal AutoDock valuation file. A grid file was generated from this validation file. AutoDock's parameter atom file may not have all atom parameters available and some were added manually (<http://autodock.scripps.edu/faqs-help/how-to/adding-new-atom-parameters-to-autodock>). In this study, the value for a copper atom was not found in this file and was manually inserted ([http://bioinf.modares.ac.ir/Courses/Docking/AD4\\_parameters.dat](http://bioinf.modares.ac.ir/Courses/Docking/AD4_parameters.dat)).

### 2.9.2 Grid Size Determination

A rectangular grid size of  $38\text{\AA} \times 40\text{\AA} \times 70\text{\AA}$  with a spacing of  $0.375\text{\AA}$  was selected as the default grid size. A grid center location of  $41.807 \times -10.752 \times 27.939$  was placed on the bovine PrAO structure covering the active site entrance, the active site and active site funnel. The grid point and the interaction energies between the probe and the target point are computed from the parameter atom file. Grid points spacing typically ranged from  $0.2\text{\AA}$  to  $1.0\text{\AA}$ , where the default was  $0.375\text{\AA}$ . This completed the entire grid value of energies for each atom type selected in the grid box and was subsequently used as a reference during the docking simulation, thereby speeding up the calculation process (Morris *et al.*, 2009).

### **2.9.3 Docking Algorithm**

The docking algorithm chosen was a Genetic Algorithm (GA) with 50 GA runs with a maximum number of evaluations of 2,500,000 and a set value of the number of GA generations of 27,000. All other algorithm variables were set to the default parameters.

Docking results were analysed using the ADT software. The resulting output file provided a ranked list in order of the top hit (this being the lowest binding energy) of each pose, along with a lowest mean bind. Resulting images, or poses, were generated with Biovia Discovery Studio (Version 4), in combination with Python Molecular Viewer (PMV) (<http://mgltools.scripps.edu/documentation/tutorial/python-molecular-viewer>). In this research the poses are represented in stick model or atomic fill display, visually indicating the predicted hydrogen bonding, electrostatic charges, pi-pi interactions and Van der Waals forces of the docked ligand interaction with side chains of the enzyme.

# CHAPTER 3

## *Results*

### 3.1 Introduction

A wide range of molecules found in foods and beverages have been associated with health benefits (Chapter 1, Section 1.0). In this Chapter the effect of a range of polyphenols, methylxanthines, selected amino acids and vitamins on PrAO activity are investigated. The aim was to examine whether these compounds might influence PrAO activity and provide a link between the health benefits ascribed to specific food components and a known therapeutic target. This approach was prompted by previous studies in these laboratories establishing that caffeine was an inhibitor of PrAO (Olivieri and Tipton, 2011) and the suggestion that caffeine might be used therapeutically to treat a range of conditions (Che *et al.*, 2012). Despite the interest in caffeine as a potential PrAO inhibitor, little is known about the effect of related methylxanthines on its activity, or indeed, the effects of a broader class of phytochemicals on the enzyme. In the course of this study a range of phytochemicals were examined as well as some structurally related xenobiotics.

The research herein is separated into sections that focus on green tea catechins, methylxanthines, selected amino acids and vitamins as well as specific endogenous and xenobiotic compounds. Data are primarily represented in bar graph form with associated tables indicating statistical significance throughout the chapter. Furthermore, a synoptic table of results can be found at the end of the chapter (see Tables 3.3 and 3.4). Where compounds were of particular interest,  $IC_{50}$  and  $K_i$  estimations were performed. Where compounds showed significant inhibition, molecular modeling software was utilized in an attempt to identify their binding sites on PrAO.

Colorimetric and UV-Vis spectrophotometric assays were initially employed to study the effect of polyphenols on PrAO activity. However, the assay results were anomalous with some polyphenols inhibiting PrAO at low concentrations whilst giving *increased* activity at higher concentrations. This necessitated the development of an alternative HPLC assay that was not subject to interference and provided a direct readout of product formation. Our initial screening studies relied on a colorimetric assay or the spectrophotometric assay described in Chapter 2 while the HPLC assay was adopted for all later studies involving polyphenols.

### 3.2 HPLC-based PrAO assay monitoring benzaldehyde formation

A simple HPLC based assay to monitor Benzaldehyde formation from Benzylamine was devised. Figure 3.1 shows a pure benzaldehyde standard chromatogram using the HPLC method.

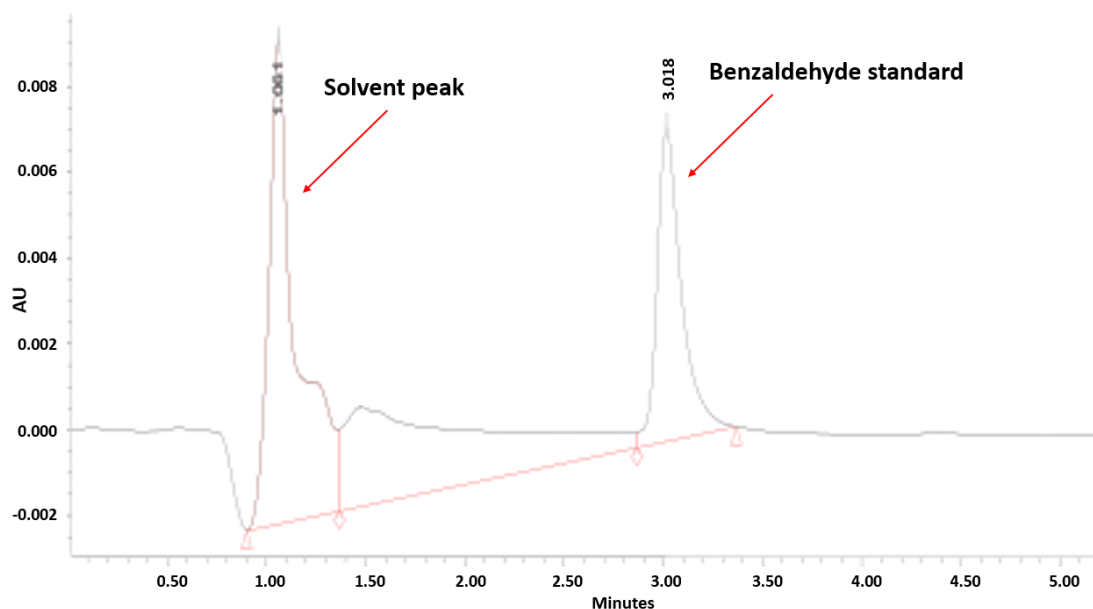


**Fig. 3.1.** HPLC chromatogram of a 40  $\mu$ M pure benzaldehyde standard. The HPLC eluate was monitored at 254 nm as described in Section 2.5.3. A retention time for Benzaldehyde of approximately 3.0 minutes was observed. AU represents Absorbance Units.



Benzaldehyde formation from the substrate benzylamine (Fig.3.2), produces a similar chromatogram showing a peak with a comparable retention time (approx. 3 minutes) thereby verifying the HPLC method's ability to monitor benzaldehyde formation. This assay was kept as standard for inhibition studies as described in section 2.5.3 for all further studies.

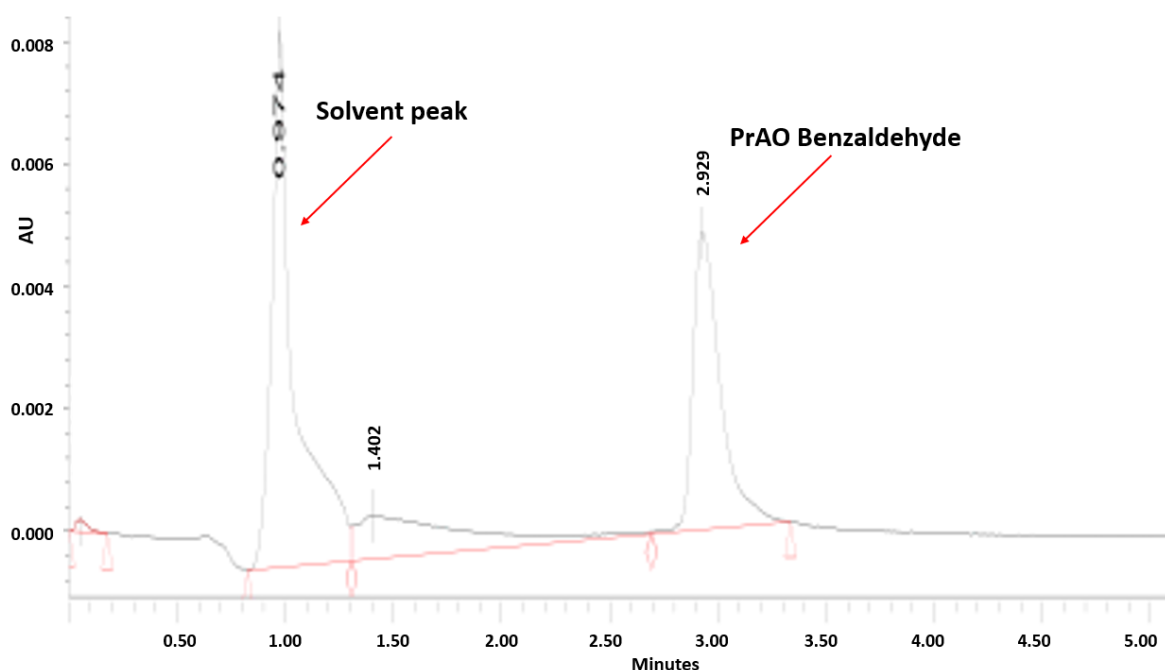


**Fig. 3.2.** HPLC chromatogram of benzaldehyde produced from PrAO-catalyzed oxidation of Benzylamine. Benzylamine was converted to the product Benzaldehyde as described in section 2.5.3 (i.e. 1.2 units of enzyme, 5 mM benzylamine in 1 mL of phosphate buffer pH.7.2). The assay duration was 3.0 hrs. Enzyme activity was quenched by heating to 85 °C and protein removed by centrifugation before HPLC injection.

A chromatogram showing the effect of PrAO inhibition by the potent and specific inhibitor semicarbazide is shown in Fig. 3.3. Semicarbazide addition caused the disappearance of the benzaldehyde peak as expected. This clearly showed that the benzaldehyde formed was as a result of enzyme activity. This experiment established that the HPLC method could be used to measure PrAO activity.

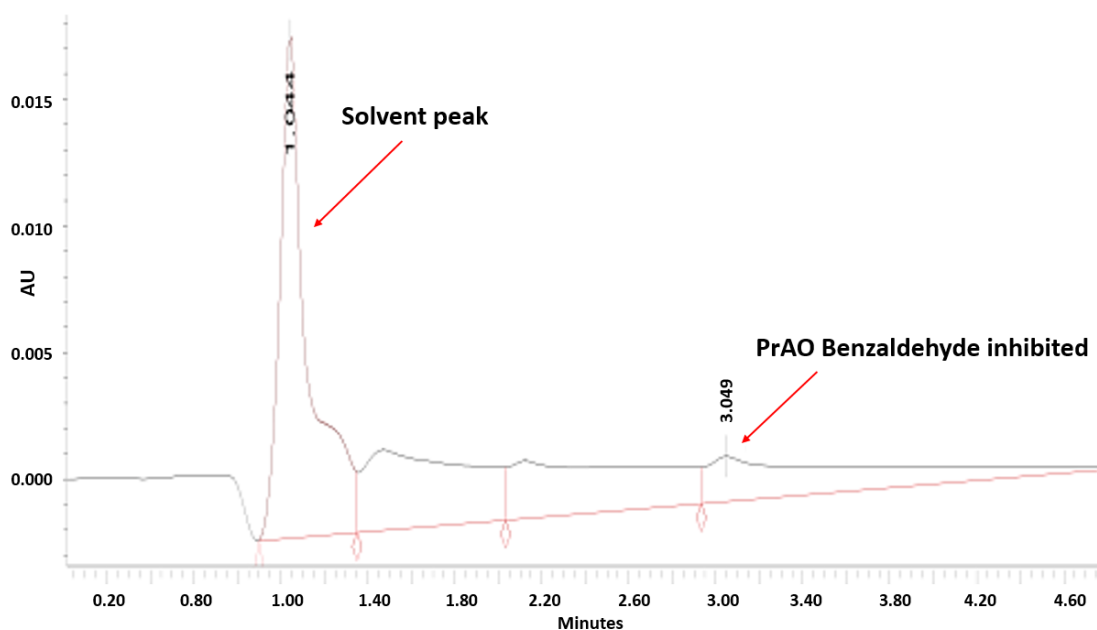


**Fig. 3.3.** HPLC chromatogram showing PrAO inhibition using 1 mM semicarbazide. The assay was performed by monitoring benzaldehyde production at 254 nm as described in section 2.5.3. Assay time was 3hrs. Enzyme activity was quenched by heating to 85 °C and protein removed by centrifugation before HPLC injection.

An HPLC assay standard curve using pure benzaldehyde standards was linear over the working range (Fig. 3.4), indicating that the HPLC method is appropriate for detecting benzaldehyde over the range of concentrations used in this study.

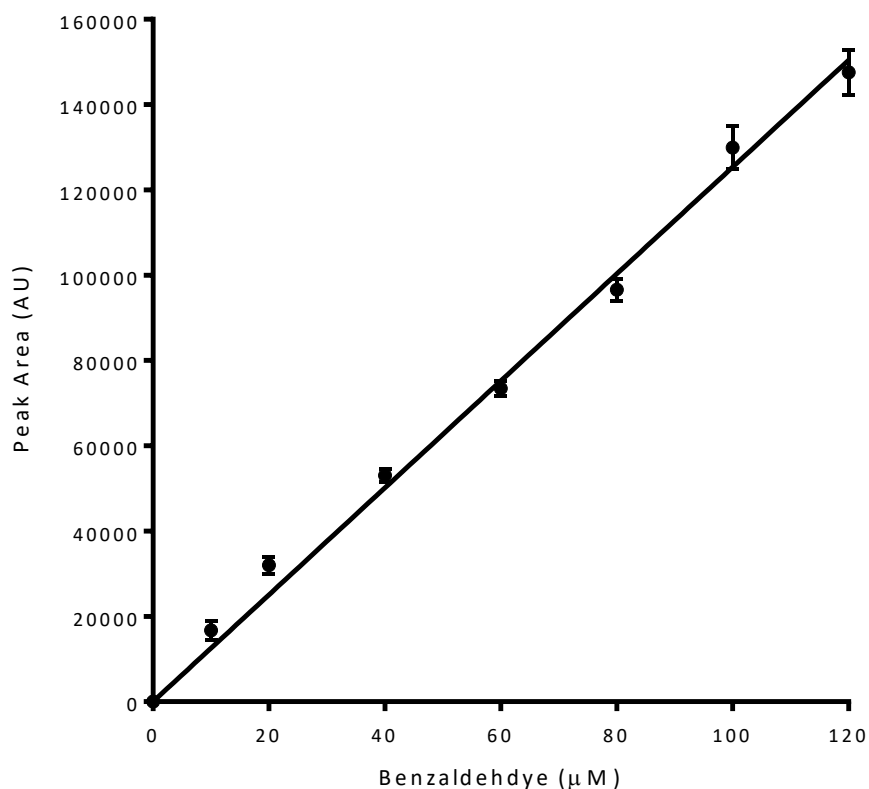


**Fig. 3.4.** HPLC assay standard curve pure benzaldehyde (99.9%). Standard concentrations of Benzaldehyde were injected ranging from 10  $\mu\text{M}$  to 120  $\mu\text{M}$ . The measuring of peak area at 254 nm was as described in section 2.5.3. linear regression  $R^2 = 0.9976$ .

Fig 3.5 shows a 3.0hr PrAO assay progress curve monitoring benzaldehyde production monitored at 254 nm using the UV spectrophotometric assay. The production of Benzaldehyde product over the three-hour incubation time was linear. Assay conditions for this plot are the same as for the standard assays used in all HPLC screening of PrAO as described in the methods section 2.5.3.

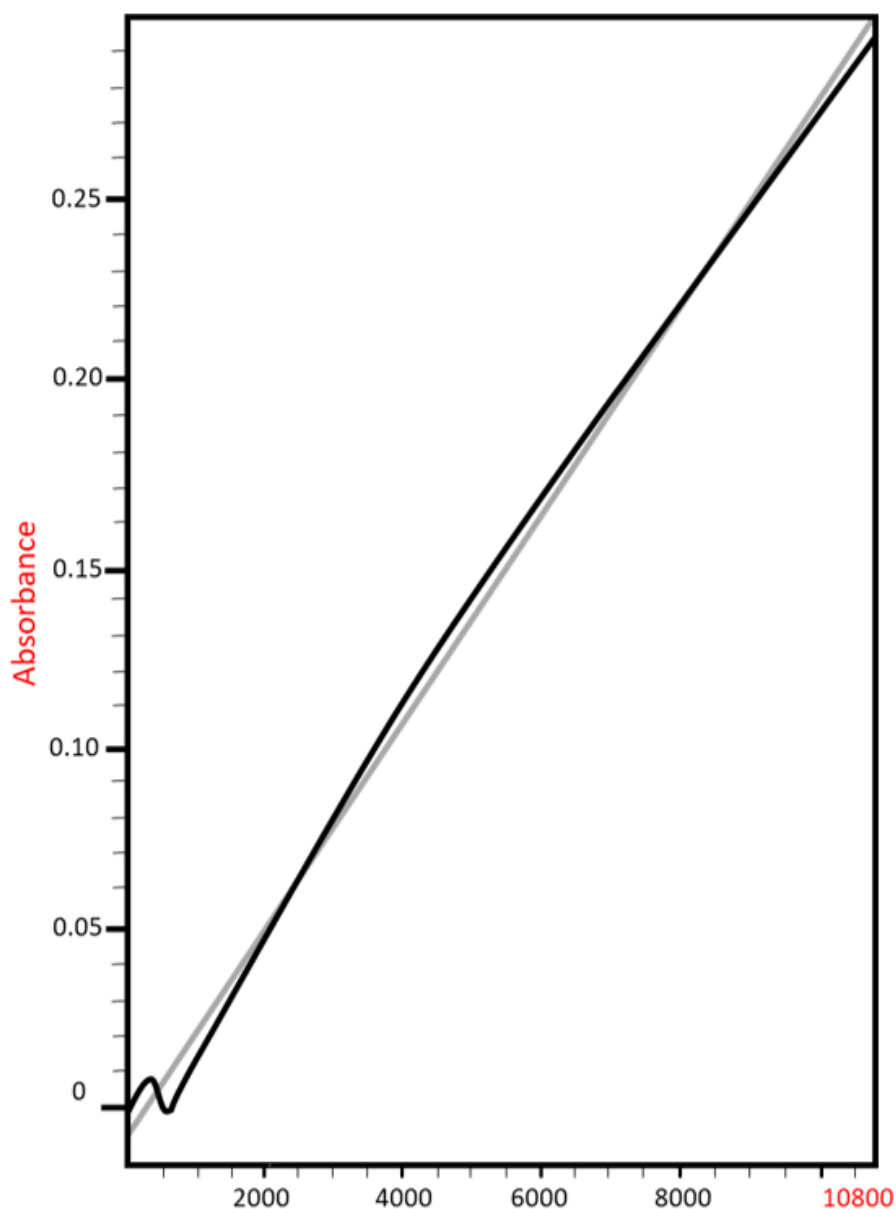


**Fig. 3.5.** Progress curve of PrAO benzaldehyde formation over a 3hr period. Absorbance readings were monitored continuously at 254 nm. Assays were carried out using the standard conditions as described in section 2.5.3. The horizontal axis units are in seconds.

The HPLC assay was clearly a convenient method to monitor PrAO activity and was not subject to the interference we had observed in our initial studies with the colorimetric assay. This assay was used to examine the effect of a range of bioactive compounds on PrAO activity.

### **3.3 Polyphenol Screening of PrAO Modulation**

#### **3.3.1 Green Tea Catechins**

Green Tea catechins have long been associated with a wide variety of health benefits (see Chapter 1 Section 1.8.2). It was of interest to examine the interaction of these compounds with PrAO. In this section, Green Tea extracts along with pure green tea catechins; epigallocatechin gallate, epicatechin gallate and epicatechin (Fig 3.6) were examined for inhibition of PrAO.

As indicated above (section 3.2), the colorimetric assay used for PrAO inhibition studies was found to give problems in our hands. That prompted us to devise an HPLC based assay method to monitor PrAO activity. In the following section we describe the issues that arose with the colourimetric assay and how reliance on this assay can give rise to misleading conclusions.

##### **3.3.1.1 Crude Green Tea extracts**

Initial screening of green tea extracts used a colorimetric microtiter plate reader assay (see Chapter 2, section 2.5.1) since it was convenient and allowed for screening of a large number of compounds simultaneously.

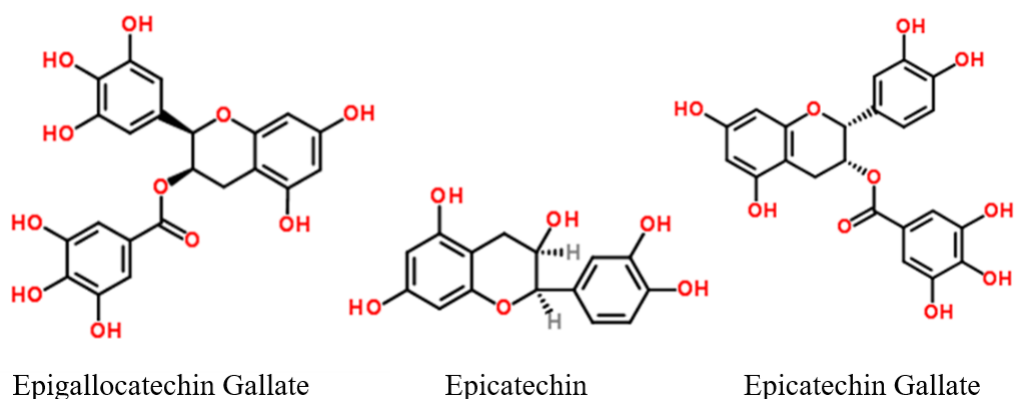


**Fig. 3.6.** Structures of selected catechins screened for PrAO inhibition.  
<http://www.chemspider.com/Chemical-Structure>

The first experiments examining the effect of Green Tea on PrAO activity were performed with a crude extract that was prepared as described in Section 2.6. Fig. 3.7 shows a 1:100 dilution of crude green tea extract tested for inhibition of PrAO at various concentrations. These results show an apparent inhibition at low concentrations and, surprisingly, an apparent *increase* in PrAO activity at higher concentrations. These findings pointed to inhibition by Green Tea components followed by subsequent activation. GABA, a primary amine present in Green Tea, was first tested as it was a likely compound to be a substrate or inhibitor of PrAO, but no modulation was found upon testing (see Table 3.3). Since it was not possible to envisage a mechanism whereby an inhibitor would become an activator at higher concentrations, we were prompted to explore this phenomenon further using pure components of Green Tea. It is well known that the major bioactive properties of Green Tea are ascribed to the catechins. The dominant catechins found in Green Tea are epigallocatechin gallate (EGCG), epicatechin (EC) and epicatechin gallate (ECG).

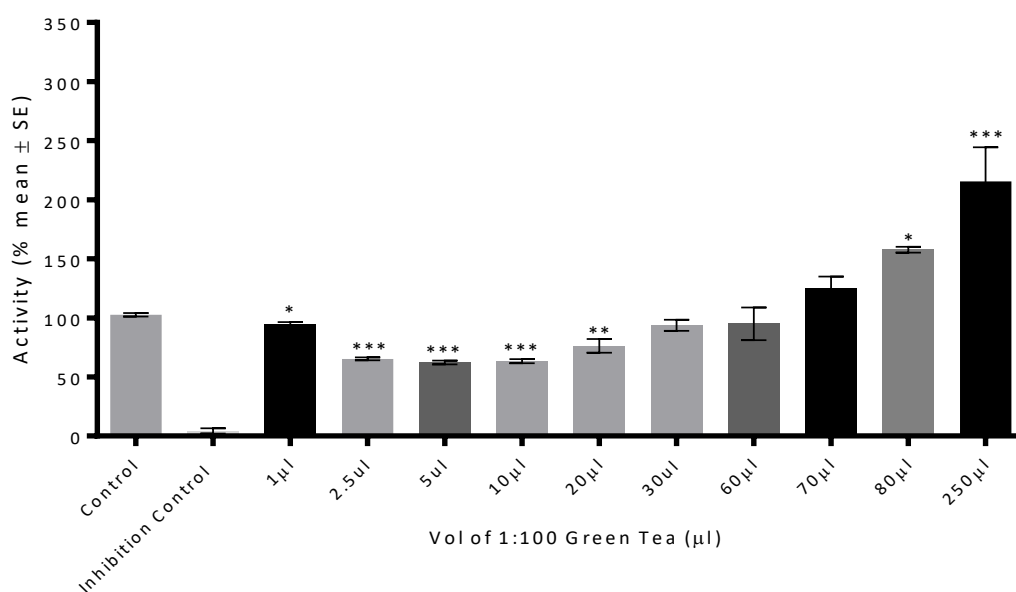


**Fig. 3.7.** 1:100 dilution of crude green tea extract was examined in an inhibition assay ranging from 1 µl to 250 µl of extract added to a final volume of 1000 µl. The data show inhibition by the Green Tea extract at low concentrations and an apparent rise in PrAO activity as concentration of green tea extract increases. Assays were performed using the colorimetric plate reader assay at 250 nM, as described in chapter 2, Section 2.5, monitoring dye reduction. All assays were performed in triplicate. Positive and negative controls were employed. Data were analyzed using ANOVA, Significant differences are denoted by an asterisk (\* $P \leq 0.05$ ; \*\* $P \leq 0.01$ ; \*\*\* $P \leq 0.001$ ) using ANOVA and Dunnett's test.

### 3.3.1.2 Catechins as PrAO inhibitors

It was possible that inhibition studies using a crude Green Tea extract might be complicated due to the large number of compounds in the crude extract. Accordingly, we decided to examine components of Green Tea individually. Firstly, epicatechin testing of PrAO showed no significant inhibition across the range of concentrations tested (Fig. 3.8).

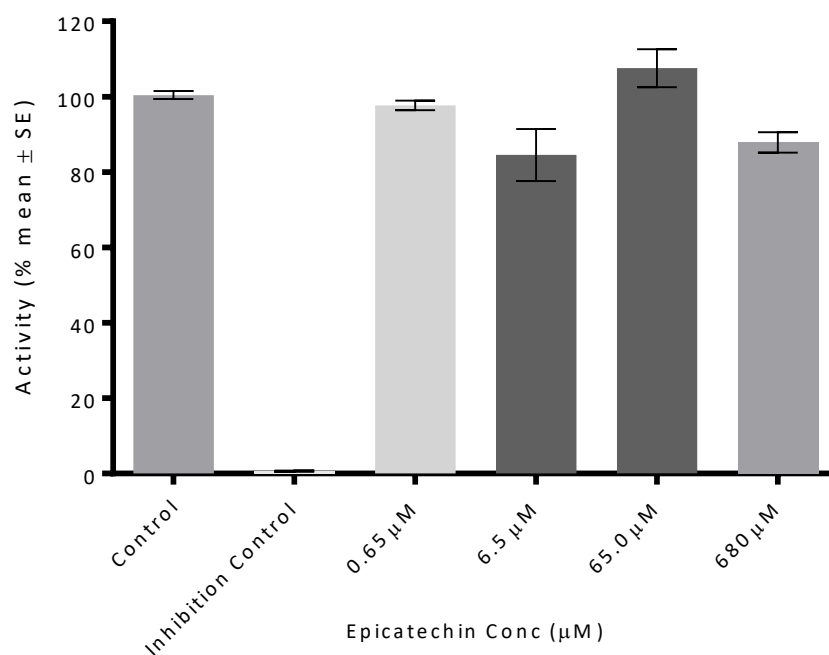


**Fig. 3.8.** Epicatechin inhibition of PrAO with concentrations of epicatechin from 0.65µM to 680µM. The data show no significant decrease in rate (% activity) as concentration increases compared to control. Assays were performed at 250nM using the spectrophotometric U.V assay monitoring aldehyde production in intra and inter triplicates as described in section 2.5. Positive controls with PrAO and substrate and negative inhibition controls with PrAO, substrate and 1 mM semicarbazide were included.

Surprisingly, micromolar concentrations of EGCG, when tested as an inhibitor of PrAO, showed inhibition at lower concentrations and a rise in activity as concentration increased (Fig. 3.9). Since this was broadly the same pattern of inhibition/activation observed with a crude extract we concluded that EGCG was responsible for this puzzling behavior.



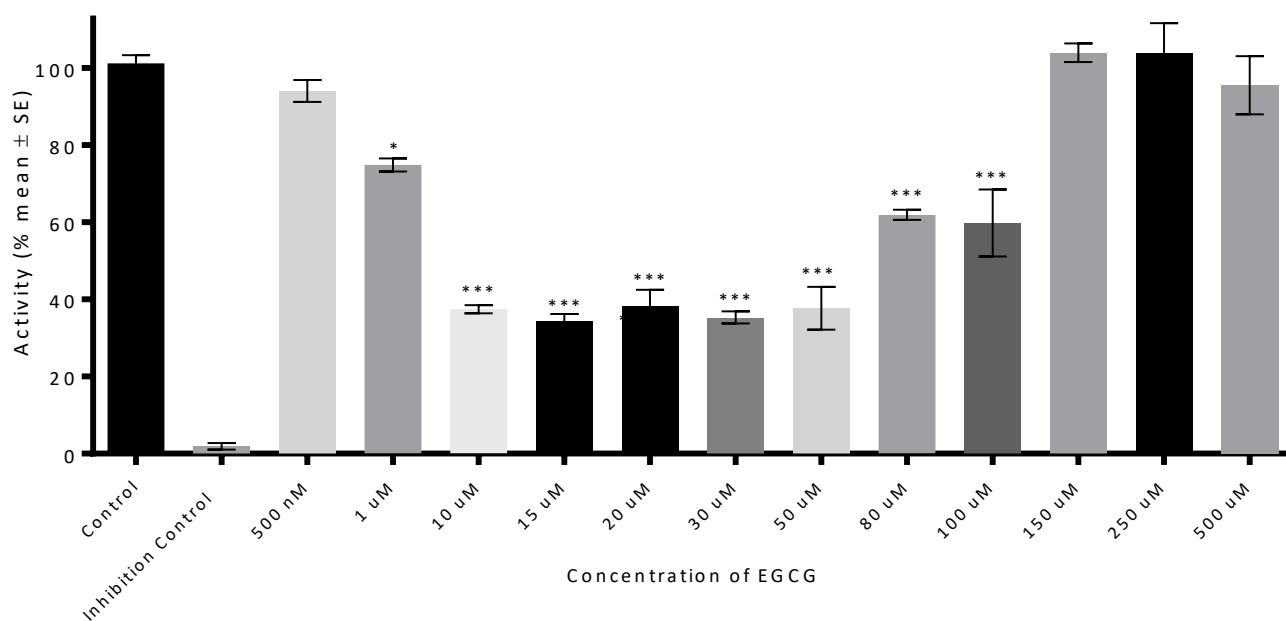


**Fig. 3.9.** Epigallocatechin gallate inhibition of PrAO at concentrations ranging from 500nM to 500µM. Data show an initial decrease in activity at low concentrations followed by an increase in rate (% activity) as concentrations increase when compared to the control. Assays were performed at 250nM using the colorimetric plate reader assay as described previously, see chapter 2 section 2.5, monitoring aldehyde production in triplicate. Positive controls with PrAO and substrate and negative inhibition controls with PrAO, substrate and 1 mM semicarbazide were included. An asterisk denotes a significant difference between treatments and the control (\*\*P ≤ 0.05; \*\*\*P ≤ 0.001) using ANOVA and Dunnett's test.

It was even more surprising when the same pattern of inhibition followed by activation was found with epicatechin gallate (Fig 3.10), i.e. inhibition at low concentrations with an increase in rates at a higher concentration of the inhibitor; although the increase in rates at high concentrations was much less than observed with epigallocatechin gallate

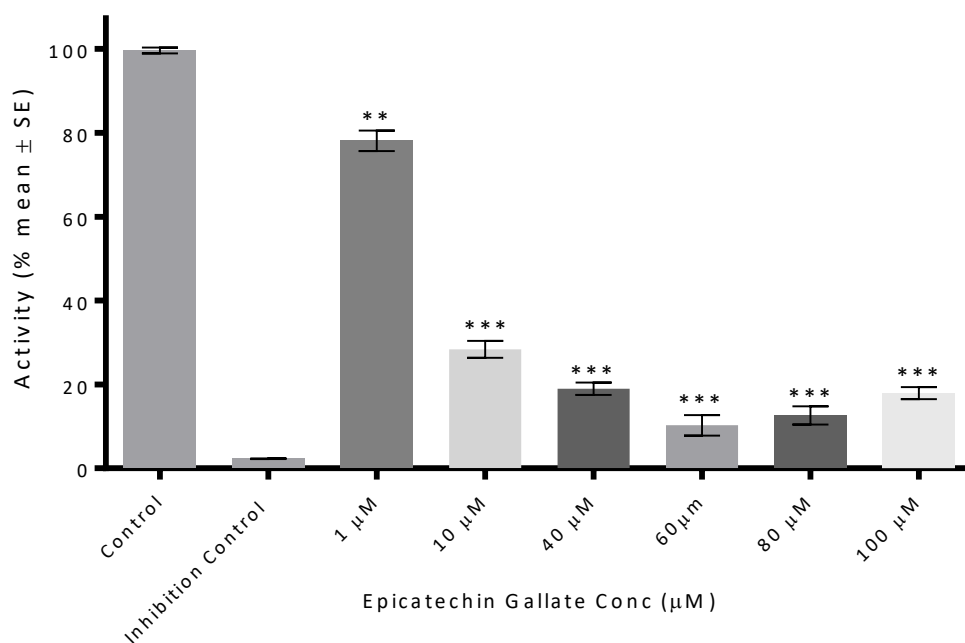


**Fig. 3.10.** ECG Inhibition of PrAO. with concentrations from 1μM to 100μM. Assays were performed at 250nM using the colorimetric plate reader assay monitoring aldehyde production in intra and inter triplicates as described in chapter 2 section 2.5. Positive controls with PrAO and substrate and negative inhibition controls with PrAO, substrate and 1 mM semicarbazide were included. An asterisk denotes a significant difference between treatments and the control (\*\*\*)  $P \leq 0.001$  using ANOVA and Dunnett's test.

Since there was a possibility that the colourimetric assay might be interfering with the findings we decided to make use of the HPLC based assay method that could directly monitor benzaldehyde formation. This assay was free of the redox dye which might react with catechins and cause anomalous findings. The HPLC assay revealed a startling reaction: we observed the formation of benzaldehyde in the *absence* of enzyme. In fact, when the non-enzymatic formation of benzaldehyde (deamination) was subtracted from the rate due to enzyme catalysis it was seen that continuous inhibition of PrAO was occurring as EGCG and ECG concentrations were increased (Fig 3.11 and 3.12).

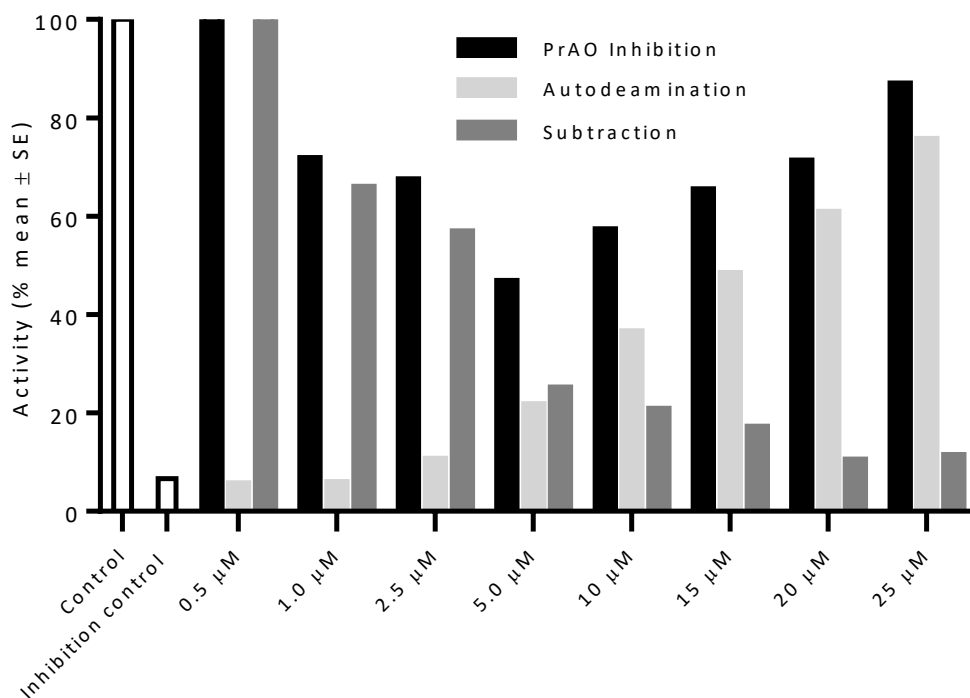


**Fig. 3.11.** EGCG inhibition of PrAO subtracting the non-enzymatic deamination reaction of EGCG with benzylamine (autodeamination). PrAO activity was measured by HPLC at 254nm for benzaldehyde detection. Assays used the HPLC assay described in Chapter 2, section 2.5.3.

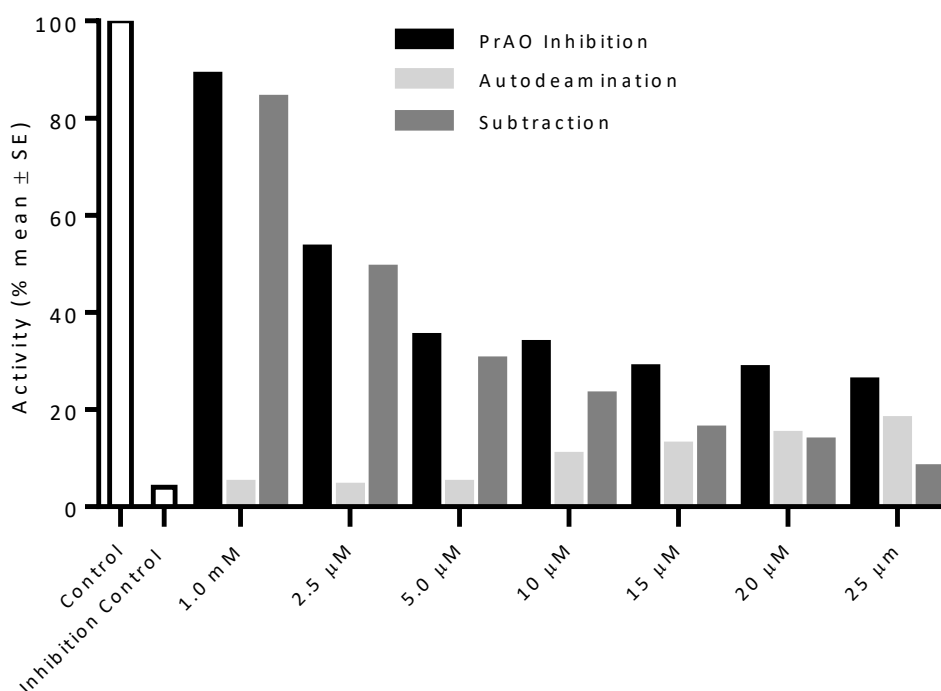


**Fig. 3.12.** Epicatechin gallate inhibition of PrAO subtracting absorbance values due to the non-enzymatic deamination reaction between epicatechin gallate and benzylamine. PrAO activity was monitored by HPLC at 254nm for benzaldehyde detection. Assays were performed as single data points using the HPLC assay described in materials and methods section 2.5.3. These findings show that micromolar levels of catechin can inhibit PrAO but that such inhibition may be masked by a non-enzymic reaction between Benzylamine and catechins.

Upon further investigation of the literature it was discovered that a research team (Akagawa *et al.*, 2005) had previously documented this reaction and provided a proposed mechanism (Fig 3.13). Thus, a non-enzymatic reaction between polyphenols and certain amines can give rise to deamination that mimics Amine Oxidase activity.

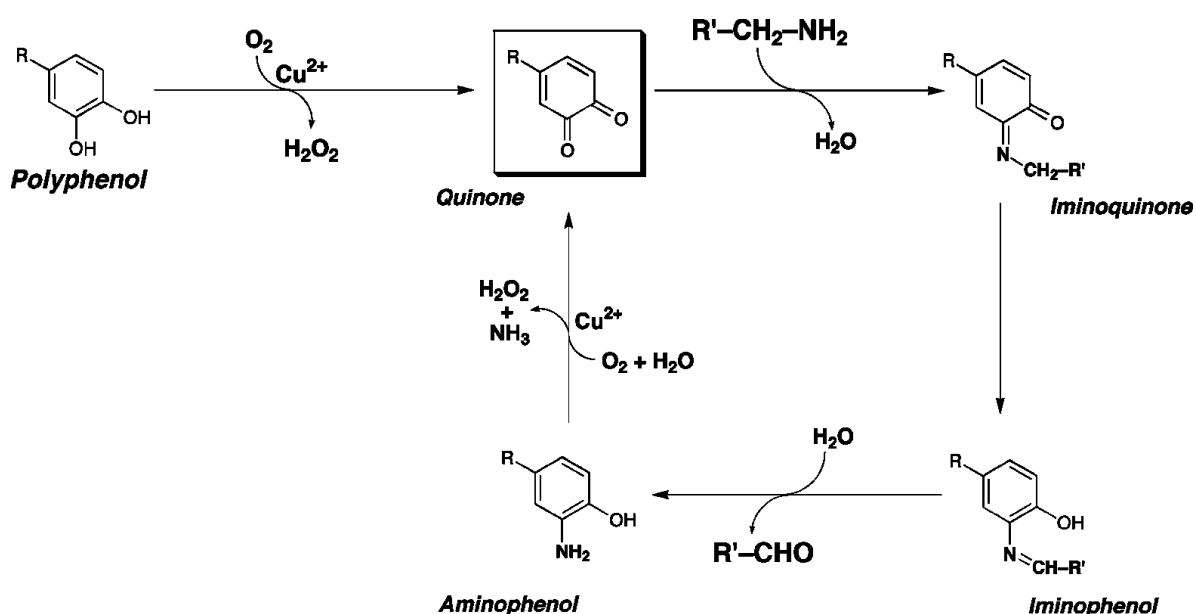


**Fig. 3.13.** Schematic showing the proposed deamination reaction between a polyphenol and a primary amine forming the products H<sub>2</sub>O<sub>2</sub>, benzaldehyde and ammonia. This is similar to the PrAO oxidation reaction mechanism with a primary amine forming the same end products (Akagawa *et al.*, 2005).

### 3.3.1.3 Caffeic Acid as an inhibitor of PrAO

Caffeic acid is a minor polyphenol component of coffee. It is known to react non-enzymatically with polyphenols as previously reported by Akagawa and co-workers (2005; Fig. 3.13). Caffeic acid (Fig. 3.14) was screened as an inhibitor of PrAO using the HPLC method. The previously reported non enzymic reaction with benzylamine was observed. Unlike the reaction with catechins no residual PrAO inhibition was observed (Fig 3.15).

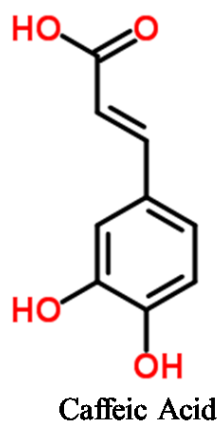


**Fig. 3.14.** Structure of caffeic acid. <http://www.chemspider.com/Chemical-Structure>

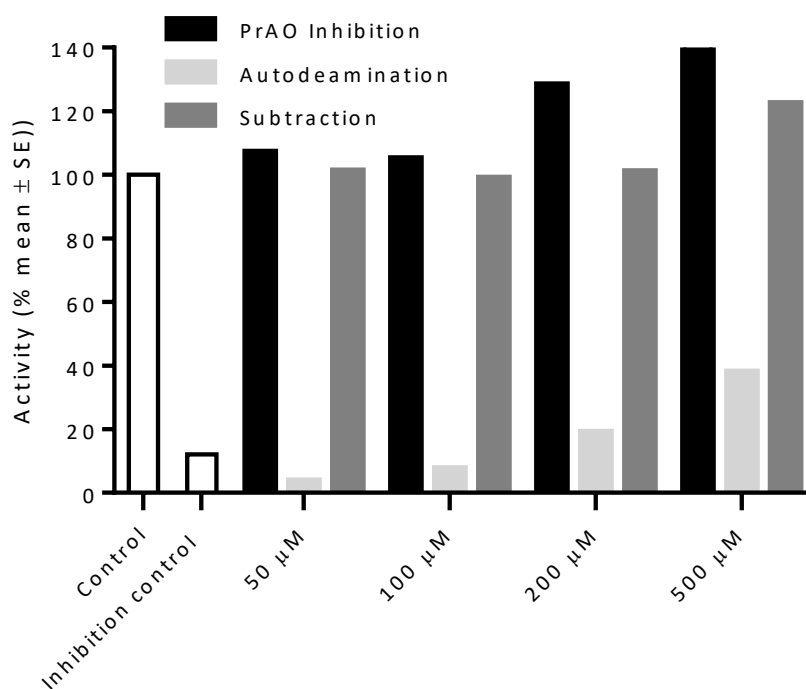


**Fig. 3.15.** Caffeic acid inhibition of PrAO. By subtracting the observed non-enzymatic deamination reaction between caffeic acid and benzylamine. PrAO activity was measured by HPLC at 254nm for benzaldehyde detection. Assays were carried as single data points out using the HPLC assay described in materials and methods section 2.5.3.

### 3.3.1.4 Catechin stability test

There was a possibility that under the conditions of the assay being used in these studies that catechins might be unstable leading to the formation of new species. EGCG was examined for stability over a 4hr period- the time taken to carry out the inhibition assays with PrAO (Fig. 3.16).

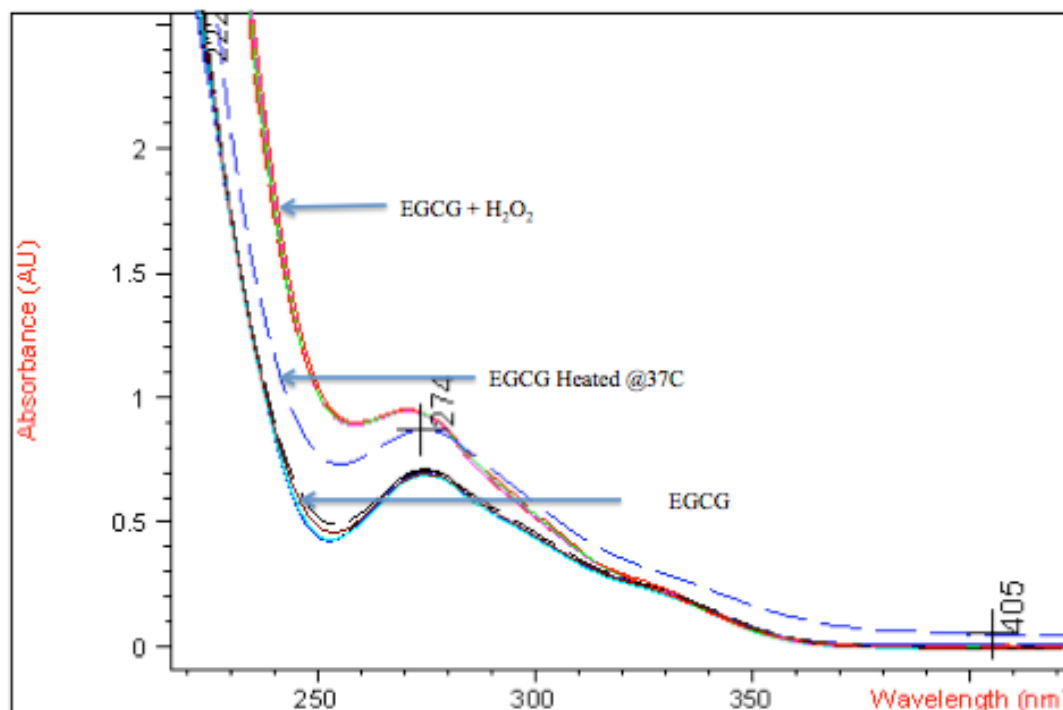


**Fig. 3.16.** A 4hr time dependent scan of a 100 $\mu$ M concentration of EGCG to monitor the stability of EGCG over time. EGCG control, EGCG with hydrogen peroxide and EGCG heated to 37°C were scanned. Lambda max for EGCG is approx. 279nm and spectral scans were taken spanning this wavelength.

These data clearly show that the non-enzymic formation of benzaldehyde is causing apparent activation at high concentrations of ECG or ECGC. Such a reaction is expected to increase as the concentration of catechin rises. The subtraction of this rate from the overall rate of benzaldehyde formation shows that a residual inhibition of PrAO observed. This finding shows that the observed effect of EC and ECGC on PrAO has two components: a non-enzymic rate that is

more pronounced at high catechin concentrations and an apparent direct effect on PrAO catalysed benzaldehyde formation. The experiment with caffeic acid showed that this type of interaction was not found for all polyphenols and appears to be unique to catechins containing the gallate moiety.

### 3.3.2 Computational Modelling of the binding of ECG, EGCG, and Epicatechin to PrAO

Computational modelling of ECG, EGCG and EC was carried out to examine binding interactions with PrAO. A computational model for Bovine PrAO was constructed as described in Section 2.9. The top ranking scores (the more negative the ranking value the more energetically favorable the binding) and binding interactions between inhibitor and PrAO residue side chains are detailed. Figure 3.17 shows a molecular surface representation of epicatechin gallate binding to PrAO.

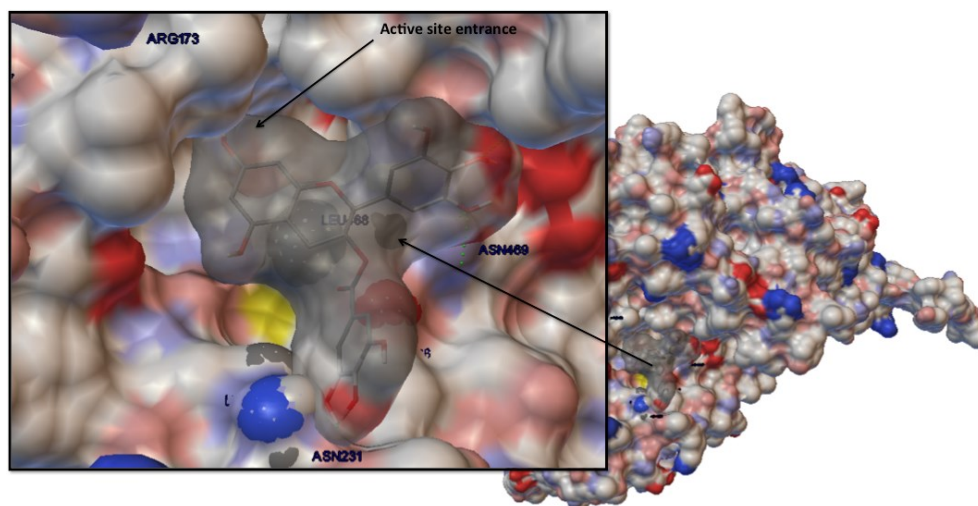


**Fig. 3.17.** Modelling Epicatechin gallate binding to PrAO. This interaction had a top rank docking score of  $-5.76$  ( $\Delta G_{\text{bind}}$ ) as calculated by AutoDock Tools 1.5.6 when bound to PrAO. A molecular surface representation with polarity shading is depicted for the docking interaction of ECG and PrAO, indicating the active site entrance of PrAO and binding location of epicatechin gallate. Residues labeled are Asn469, Asn231 and Arg173, which are at or near the active site entrance. Polarity regions are indicated by grey hydrophobic, blue positively charged and red negatively charged.

Figure 3.18 depicts a computational stick model of the same binding depicted in Figure 3.17 giving a more detailed image of the bindings and residues involved.

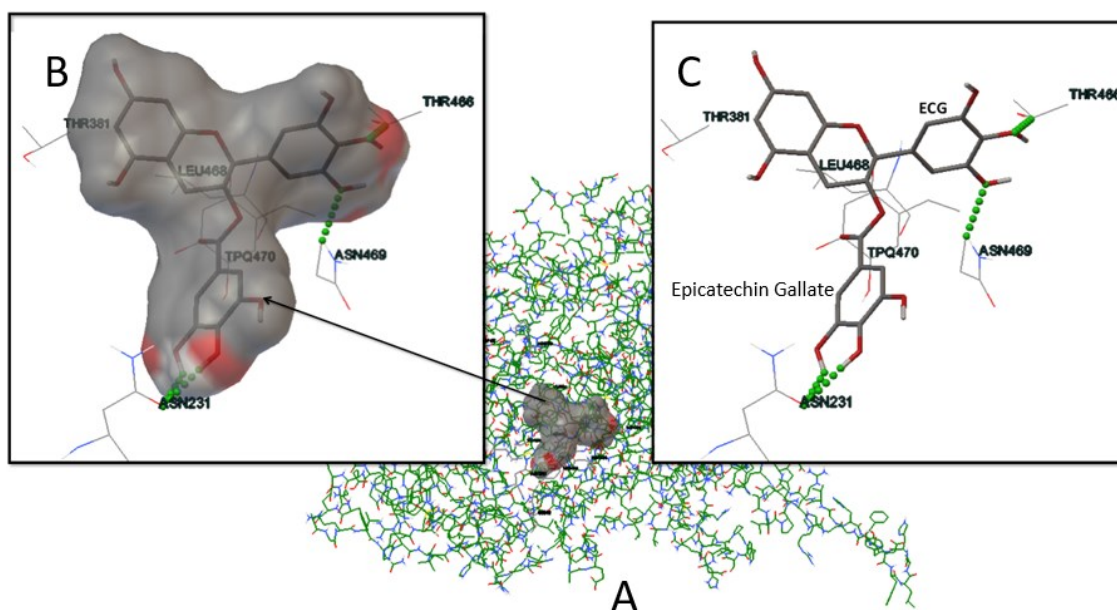


**Fig. 3.18.** A computational stick model representation of Figure 3.17. Image A shows epicatechin gallate, shown in grey, to be externally bound to the enzyme in close proximity to the active site entrance. Image B is a magnification of the binding interaction of image A, depicting polarity regions such as blue for positively charged and red for negatively charged binding interactions. The grey shading indicates hydrophobic regions. Image C shows the removal of the surface representation, which depicts the hydrogen binding interactions via the gallated phenol group binding to the amine group of Asn231 and also binding via other phenol groups to the amine group of Asn469 and the hydroxyl group of Thr466, while giving a better visual of the ligand and interacting side chains involved.

It is clear that binding of ECG at the active site covers a wide area and could block substrate entry. Figure 3.19 and Figure 3.20 show similar molecular docking for epigallocatechin gallate.



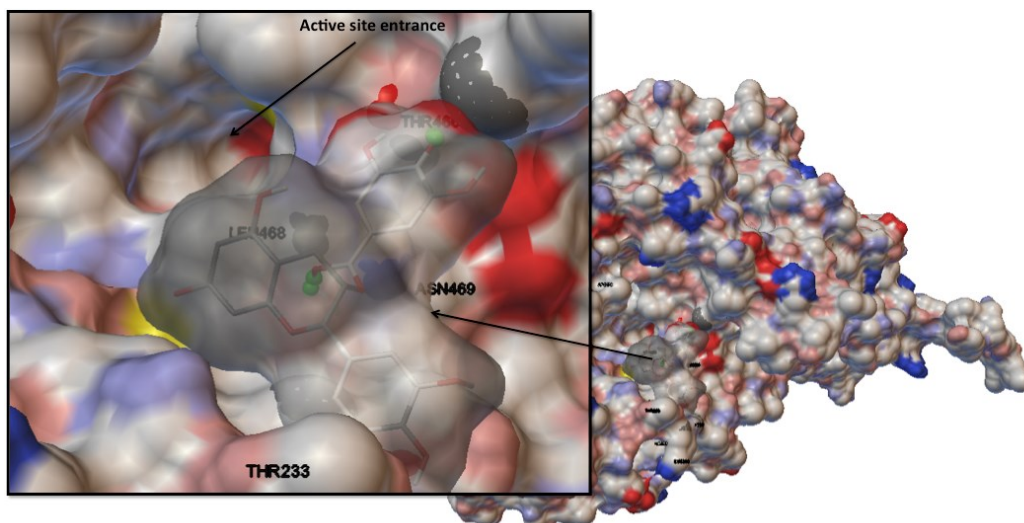


**Fig. 3.19.** Epigallocatechin gallate had a top rank docking score of  $-6.91$  ( $\Delta G_{\text{bind}}$ ) as calculated by AutoDock Tools 1.5.6 when bound to PrAO. A molecular surface representation with polarity shading is depicted for the docking interaction of ligand and macromolecule, indicating the active site entrance of PrAO and binding location of epigallocatechin gallate. Asn469 and Thr233 are highlighted at or near the active site entrance. Polarity regions are indicated by blue, positively charged and red, negatively charged, indicating potential charged binding interactions. The grey shading depicts hydrophobic interactions.

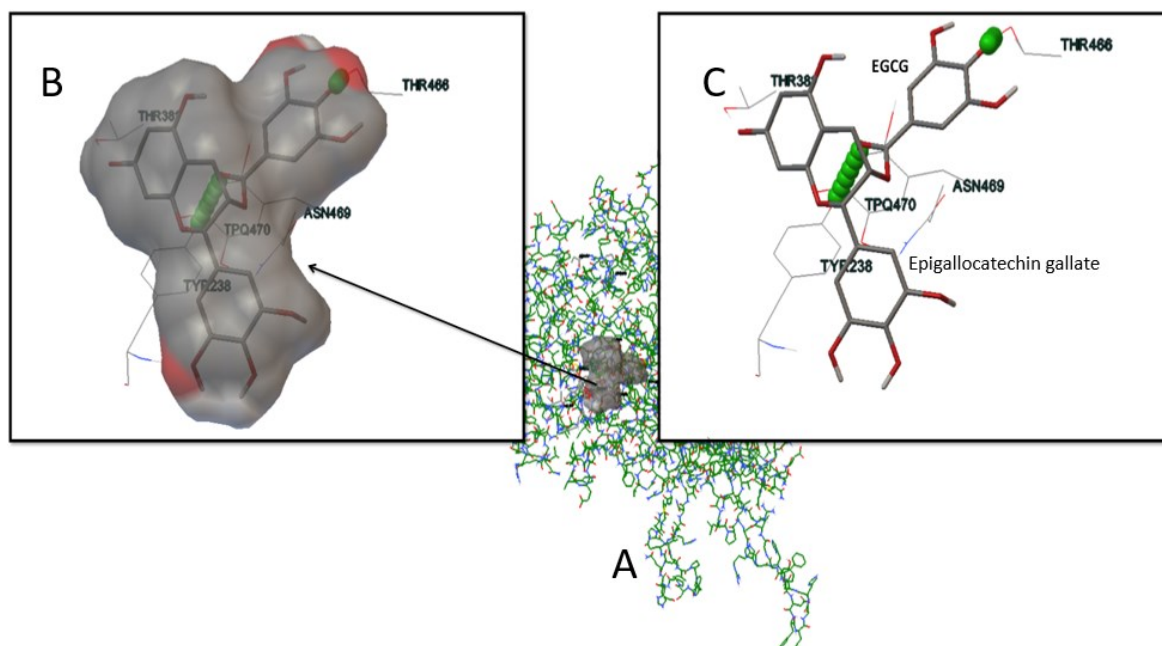


**Fig. 3.20.** A computational stick model of Figure 3.19. Image A shows epigallocatechin gallate, shown in grey, to be externally bound to the enzyme in close proximity to the active site entrance. Image B is a magnification of the binding interaction of image A, depicting polarity regions such as blue for positively charged and red for negatively charged, indicating potential charged binding interactions. The grey shading indicates hydrophobic regions. Image C is the removal of the surface representation, which depicts hydrogen bonding via the phenol groups of the gallate binding to hydroxyl groups of both Thr466 and Tyr238, while giving a better visual of the ligand and interacting side chains involved.

Epicatechin gallate and epigallocatechin gallate were computationally modelled as they significantly inhibited PrAO. Modelling of Epicatechin (EC), Figures 3.21 and 3.22, which did not significantly inhibit PrAO was performed to compare with the other catechins.

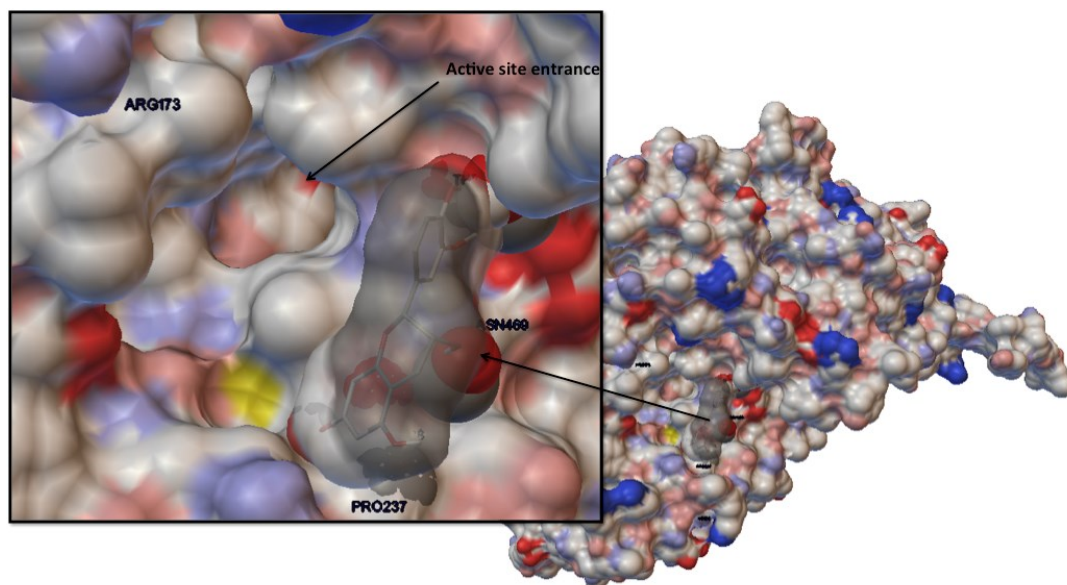


**Fig. 3.21.** Epicatechin had a top rank docking score of -5.30 ( $\Delta G_{\text{bind}}$ ) as calculated by AutoDock Tools 1.5.6 when bound to PrAO. A molecular surface representation with polarity shading is depicted for the docking interaction of ligand and macromolecule, indicating the active site entrance of PrAO and binding location of epicatechin. Asn469, Pro237 and Arg173 are highlighted at or near the active site entrance. Polarity regions are indicated by grey hydrophobic, blue positively charged and red negatively charged, indicating potential binding interactions.

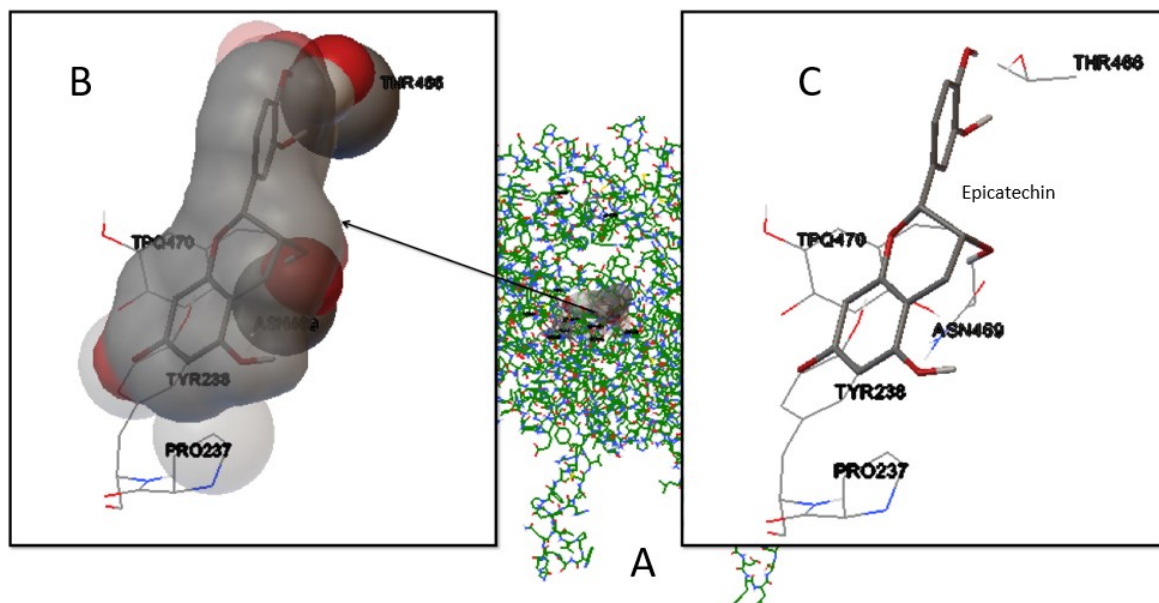


**Fig. 3.22.** A computational stick model of Figure 3.21. Image A shows epicatechin, shown in grey, to be externally bound to the enzyme in close proximity to the active site entrance. Image B is a magnification of the binding interaction of image A, depicting polarity regions such as blue for positively charged and red for negatively charged, ionic charged interactions between Asn469 Thr466 and Tyr238 with hydroxyl groups of epicatechin. The grey shading indicates hydrophobic regions. Image C is the removal of the surface representation, which depicts the ligand and interacting side chains involved more clearly

An overview of observations and findings of PrAO modulation with crude green tea extract and a number of green tea catechins and related compounds is shown in Figure 3.23.

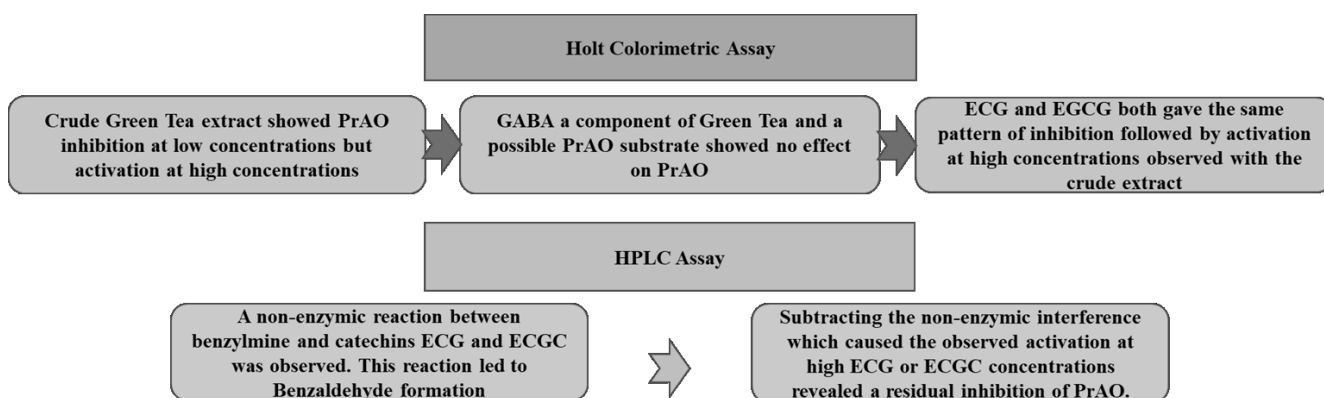


**Fig. 3.23** Overview of methods employed, and main findings observed with testing crude green tea extract and green tea catechins as PrAO inhibitors.

A summary table is shown below detailing inhibition and binding interactions between catechins and PrAO (Table 3.1).

**Table 3.1.** Summary of binding interactions for selected catechins with PrAO as predicted by AutoDock.

Docked Compound	Experimental PrAO Inhibition	Docking Score ( $\Delta G_{\text{bind}}$ )	Hydrogen Bonding	Hydrophobic Interactions	Ionic Interactions
Epicatechin gallate	Yes	-5.76	Asn231, Asn469 Thr466	Leu468 Pro237	-----
Epigallocatechin gallate	Yes	-6.91	Thr466 Tyr238	Pro237	-----
Epicatechin	No	-5.30	-----	Pro237	Thr466 Tyr238

### 3.3.3 Octopamine Inhibition of PrAO

Octopamine is a primary amine that is ubiquitously found in nature (Fig. 3.24).

Figure 3.25 shows octopamine at two concentrations, compared against a control for activity as a PrAO inhibitor.

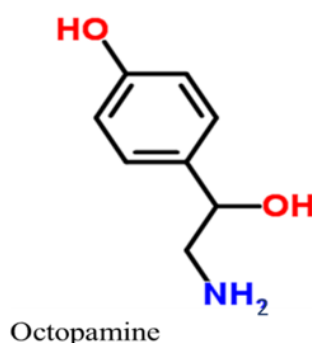


**Fig. 3.24.** Structure of octopamine. <http://www.chemspider.com/Chemical-Structure>

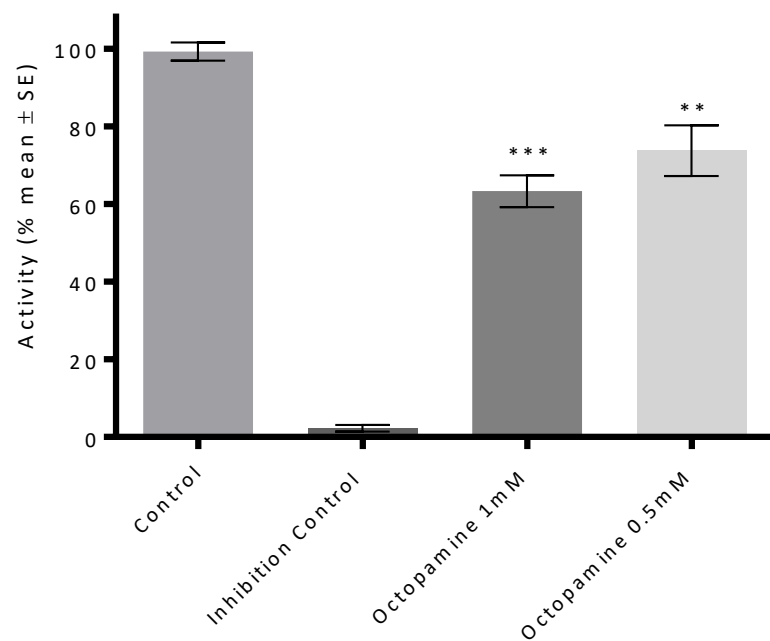


**Fig. 3.25.** Inhibition of PrAO by 1mM and 0.5mM concentrations of Octopamine. Assays were performed by HPLC at 250nM monitoring aldehyde production and in triplicate. Positive controls with PrAO and substrate and negative inhibition controls with PrAO, substrate and 1 mM semicarbazide were included. An asterisk indicates a significant difference using ANOVA was (\*\*P ≤ 0.01; \*\*\*P ≤ 0.001).

Since Octopamine showed significant inhibition of PrAO its kinetics were explored further. Figure 3.26 is an IC<sub>50</sub> plot for inhibition of PrAO by Octopamine.

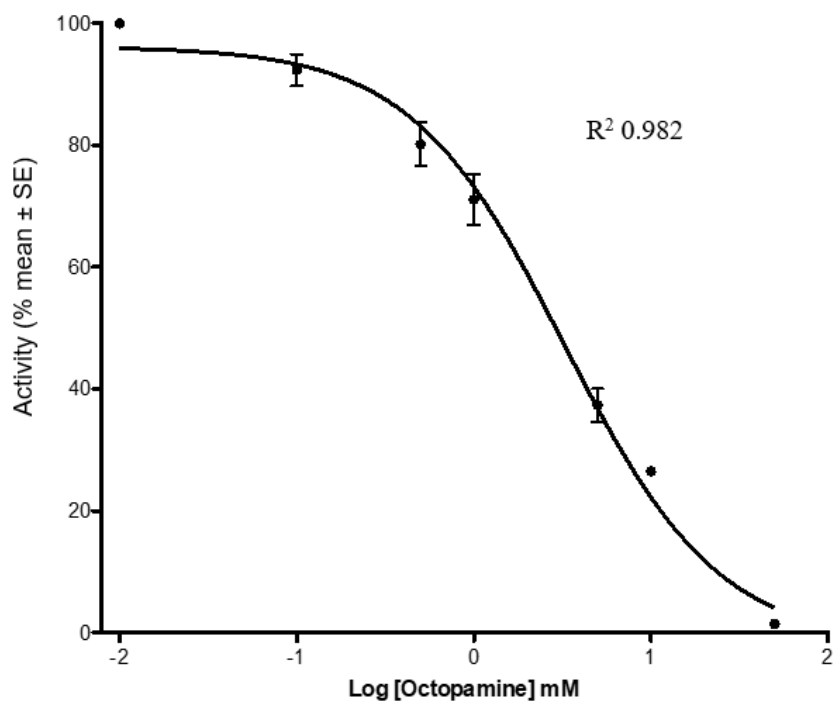


**Fig. 3.26.** Octopamine IC<sub>50</sub> plot of log concentration of inhibitor Vs % activity. , A IC<sub>50</sub> of 3.26mM  $\pm$  0.8mM was estimated. Inhibitor concentrations ranged from 0.1mM to 100mM. Data shown are the mean values  $\pm$  SEM. Assays were performed in triplicate using the plate reader based colourimetric assay at 37°C and pH 7.2. Data were fitted by non-linear regression analysis with the aid of computer software GraphPad Prism, 5.0.

Figure 3.27 shows the effect of Octopamine on the  $K_m$  for benzylamine. The resulting plot shows a mixed pattern of inhibition.

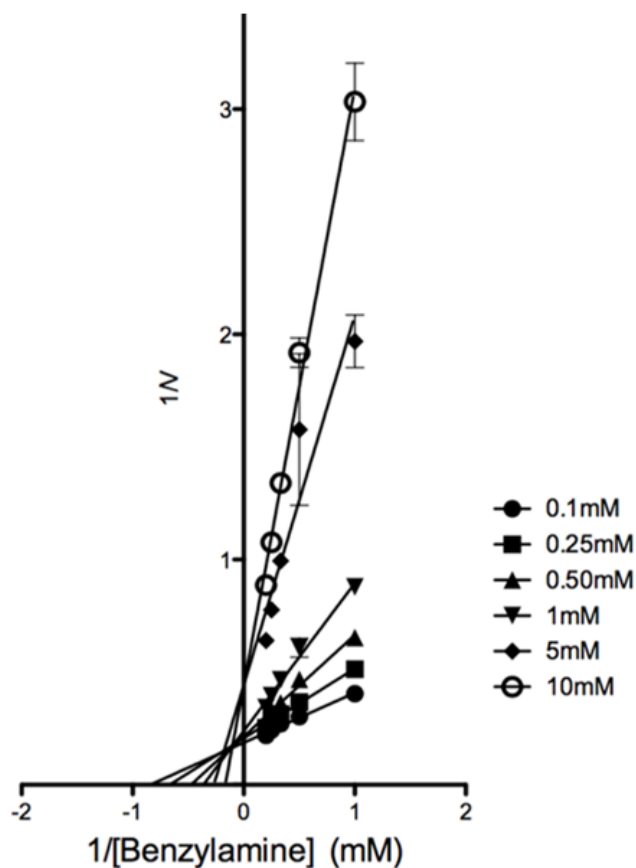


**Fig. 3.27.** Substrate (benzylamine) pattern of inhibition of PrAO by octopamine. A mixed type pattern of inhibition is observed. All samples contained increasing concentrations of octopamine (from 0.1mM to 10mM) and benzylamine from 1 to 5 mM. Data shown are the mean values  $\pm$  SEM, error bars not evident were less than the representation of the points. The initial rates ( $v = \text{abs } 498 \text{ nm} \times 10^{-3} \text{ min}$ ) of hydrogen peroxide formation were determined at 37°C and pH 7.2. Data were fitted to the Michaelis–Menten equation with the aid of GraphPad Prism, 5.0 software.

### 3.3.4 Quercetin

Quercetin is the most abundant plant polyphenol in the human diet - it belongs to the flavanoid group. This molecule has many reported beneficial health properties that are associated with many of the diseases associated with raised PrAO activity as discussed in Chapter 1, Section 1.8. Figure 3.28 is the chemical structure of quercetin. Figure 3.29 depicts quercetin being screened at two concentrations. Fig. 3.30 depicts an  $IC_{50}$  graph of Quercetin inhibition of PrAO while Figure 3.31 depicts a Lineweaver Burk plot.

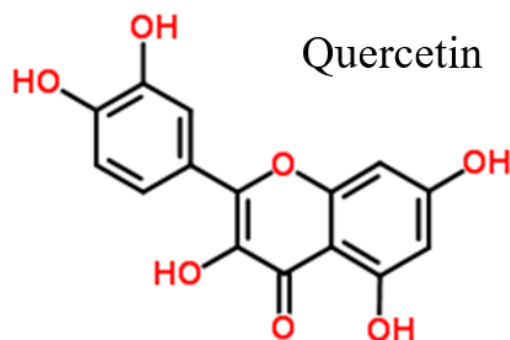


**Fig. 3.28.** Chemical structure of quercetin. <http://www.chemspider.com/Chemical-Structure>



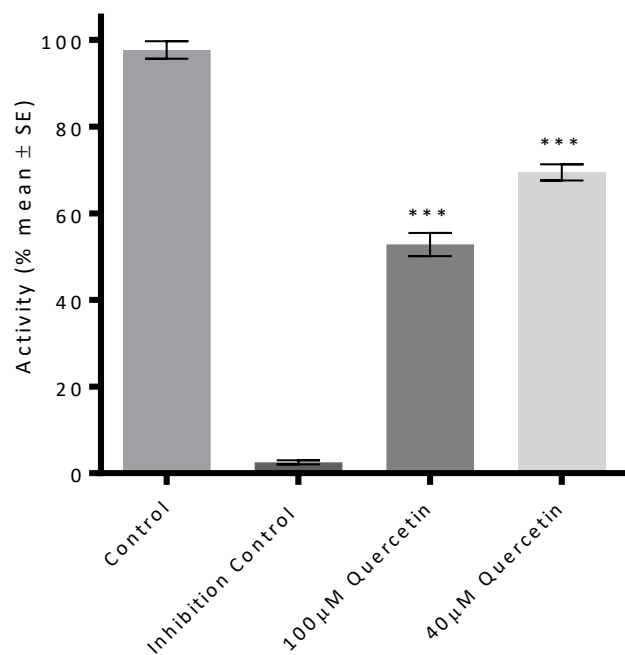


**Fig. 3.29.** Quercetin inhibition assay of PrAO with control, inhibition control and experimental assay with 100μM and 40μM concentrations. Assays were performed at 498nm monitoring H<sub>2</sub>O<sub>2</sub> production in triplicate. Positive controls with PrAO and substrate and negative inhibition controls with PrAO, substrate and 1 mM semicarbazide were included. An asterisk denotes a significant difference between treatments and the control (\*\*\*P ≤ 0.001) using ANOVA and Dunnett's test.

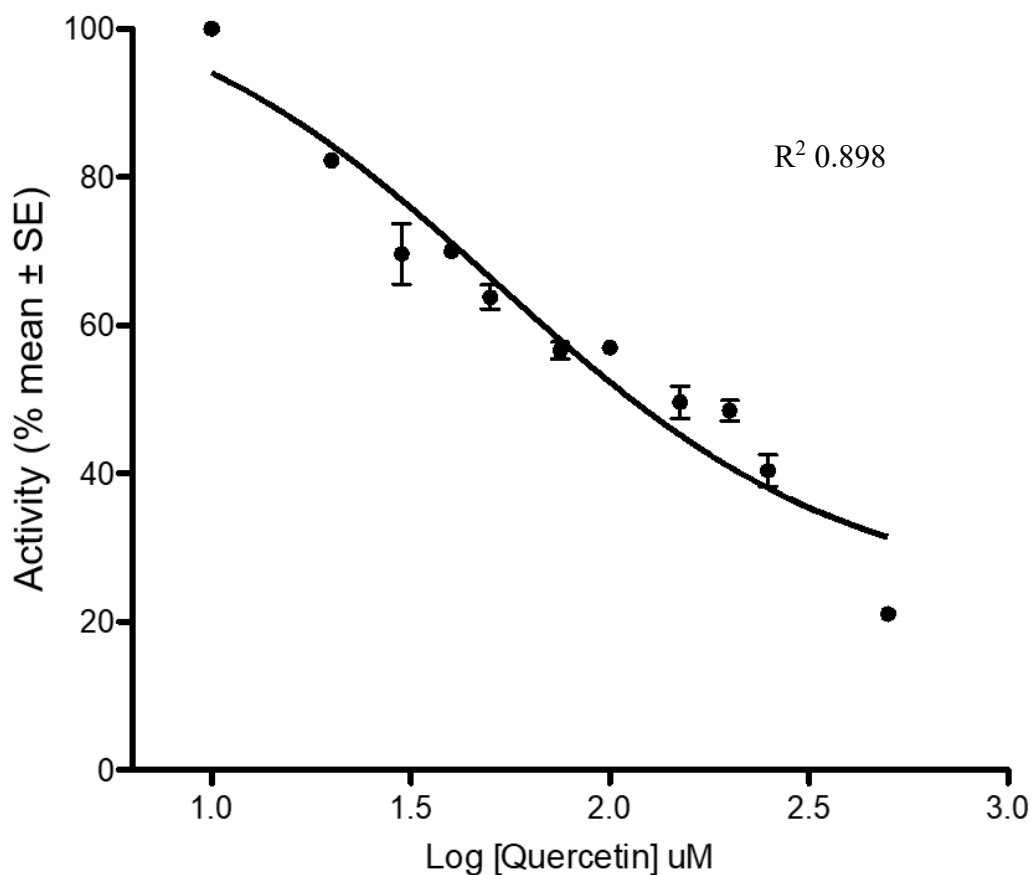


**Fig. 3.30.** Quercetin IC<sub>50</sub> inhibition plot showing log concentration of inhibitor Vs % activity, giving an IC<sub>50</sub> of 52.20µM ± 33.75µM. Inhibitor concentration ranged from 10µM to 500µM and substrate concentration of 5mM benzylamine. Data shown are the mean values ± SEM, error bars not evident were less than the representation of the points. Assays were performed in triplicate and IC<sub>50</sub> readings gained at 498nm at 37°C and pH 7.2. Data were fitted with non-linear regression analysis with the aid of computer soft- ware GraphPad Prism, 5.0.

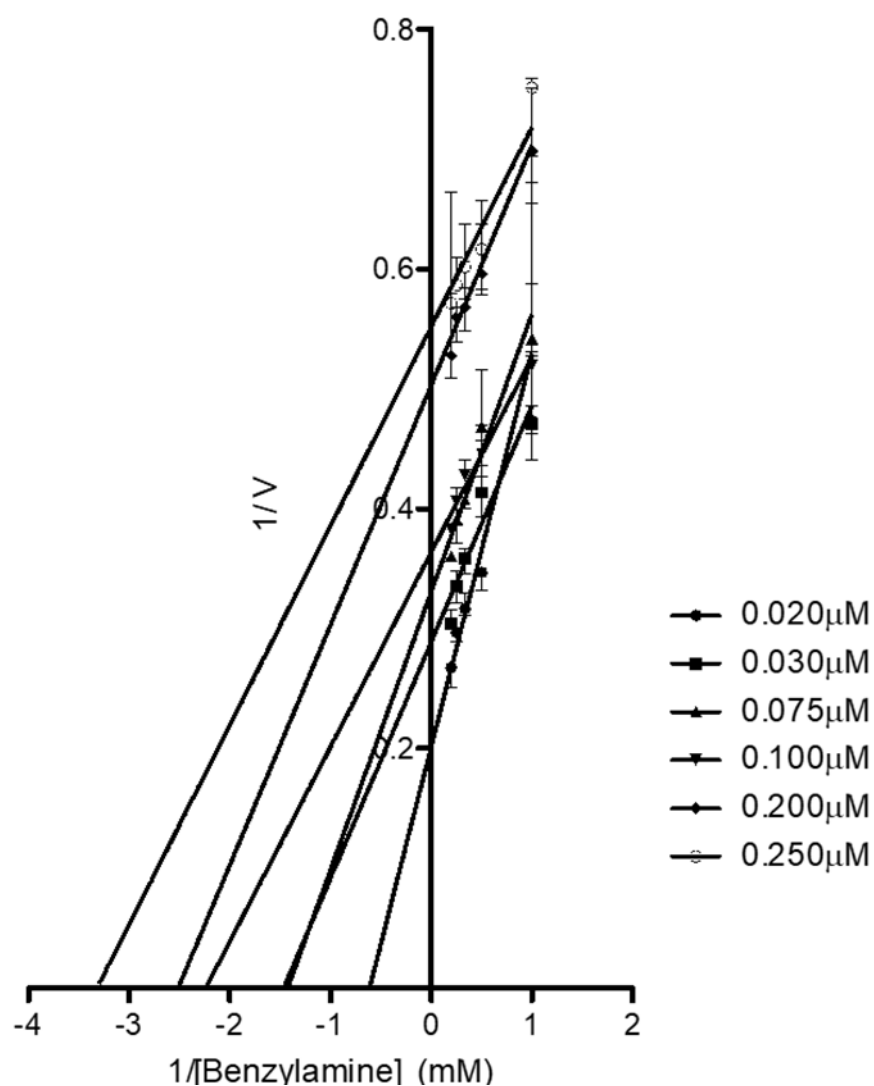


**Fig. 3.31.** Substrate (benzylamine) patterns of inhibition of PrAO by quercetin. An uncompetitive pattern of inhibition is observed. All samples contained increasing concentrations of quercetin (from 0.02  $\mu\text{M}$  to 0.250  $\mu\text{M}$ ) and benzylamine 1 to 5 mM. Data shown are the mean values  $\pm$  SEM, error bars not evident were less than the representation of the points. The initial rates ( $v = \text{abs}498 \text{ nm} \times 10^{-3} \text{ min}^{-1}$ ) of hydrogen peroxide formation were determined at 37°C and pH 7.2. Data were fitted to the Michaelis–Menten equation with the aid of computer software GraphPad Prism 5.0.

### 3.3.5 Umbelliferone

Umbelliferone is a natural product of the coumarin family. Like quercetin, it is a phenolic metabolite found ubiquitously in plants. Figure 3.32 depicts the structure of umbelliferone. In Fig. 3.33, umbelliferone was screened for inhibition at two concentrations. There was a significant difference between both treatments and the control using ANOVA ( $P \leq 0.001$ ).

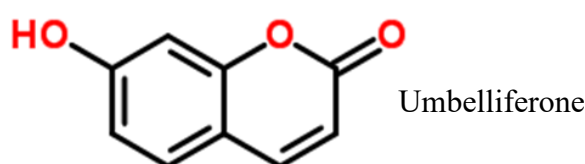


**Fig. 3.32.** Chemical structure of umbelliferone. <http://www.chemspider.com/Chemical-Structure>

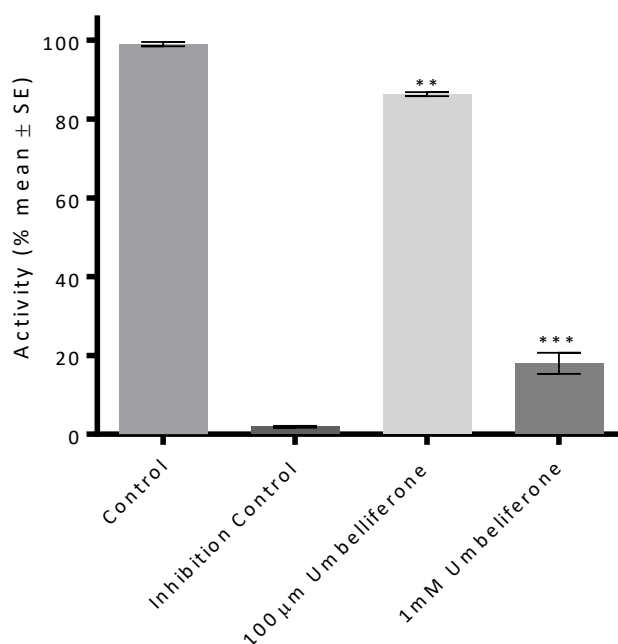


**Fig. 3.33.** Umbelliferone inhibition assay of PrAO with blank, control, inhibition control with semicarbazide and experimental assay with 1mM and 100 $\mu$ M concentrations. Assays were performed at 250nM monitoring aldehyde production and in triplicate. Positive controls with PrAO and substrate and negative inhibition controls with PrAO, substrate and 1 mM semicarbazide were included. An asterisk denotes a significant difference between treatments and the control (\*\* $P \leq 0.01$ ; \*\*\* $P \leq 0.001$ ) using ANOVA and Dunnett's test.

### 3.4 Methylxanthines and related compounds as PrAO inhibitors

Previous work in our laboratory had shown caffeine, a methylxanthine was an inhibitor of PrAO. We decided to extend this work to examine related methylxanthine structures found in the diet as PrAO inhibitors. The structures of the methylxanthines screened in this study are shown in Figure 3.34. The effect of caffeine, paraxanthine, theophylline, theobromine and 7-methylxanthine on PrAO at fixed concentrations of 500  $\mu$ M and 1.0 mM were examined using the HPLC assay as outlined above (Section 3.2).

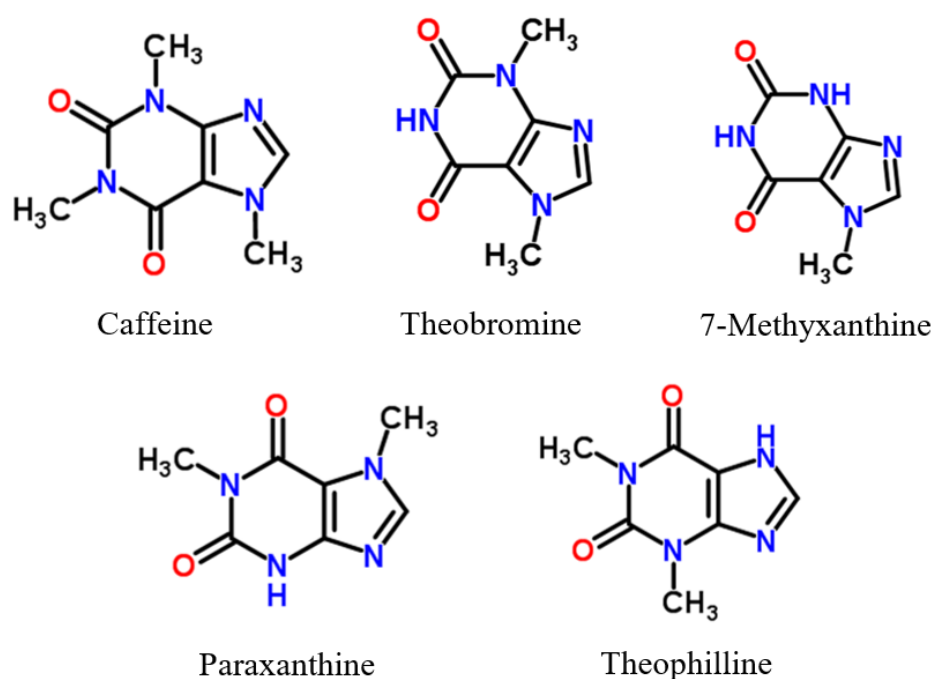


**Fig. 3.34.** Structures of the caffeine related methylxanthines considered in this study. These naturally occurring compounds are all N-methylated derivatives of xanthine. <http://www.chemspider.com/Chemical-Structure>.

Of the five methylxanthines screened only caffeine and theobromine showed substantial inhibition of PrAO. This was a highly significant finding and showed that a specific pattern of methylation was required for inhibition. Surprisingly, the other compounds tested, theophylline, paraxanthine and 7-methylxanthine, had

relatively little effect (Fig. 3.35) despite their structural similarity to caffeine and theobromine.

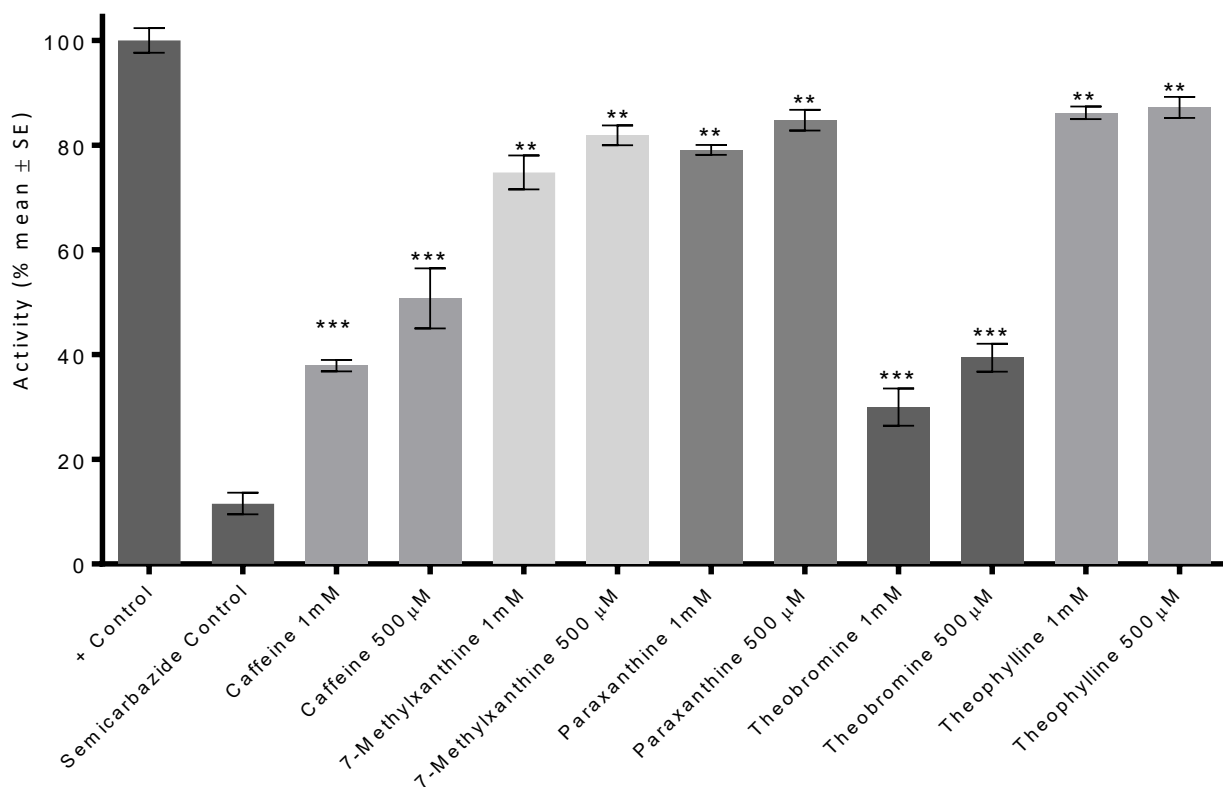


**Fig. 3.35.** Effect of selected methylxanthines at 500µM and 1 mM concentrations on PrAO activity. Activity was measured at 254 nm for benzaldehyde detection. Assays were performed using the HPLC assay described in materials and methods section 2.5.3. Positive controls with PrAO and substrate and negative inhibition controls with PrAO, substrate and 1 mM semicarbazide were included. All assays were carried out in triplicate. An asterisk denotes a significant difference between treatments and the control (\* $P \leq 0.05$ ; \*\* $P \leq 0.01$ ; \*\*\* $P \leq 0.001$ ) using ANOVA and Dunnett's test.

Since caffeine is a derivative of xanthine, several related compounds were tested as PrAO inhibitors. Figure 3.36 shows that neither xanthine nor a range of similar compounds had a significant inhibitory effect on PrAO activity at the concentrations used herein. The structures of these compounds are shown in Fig 3.37.

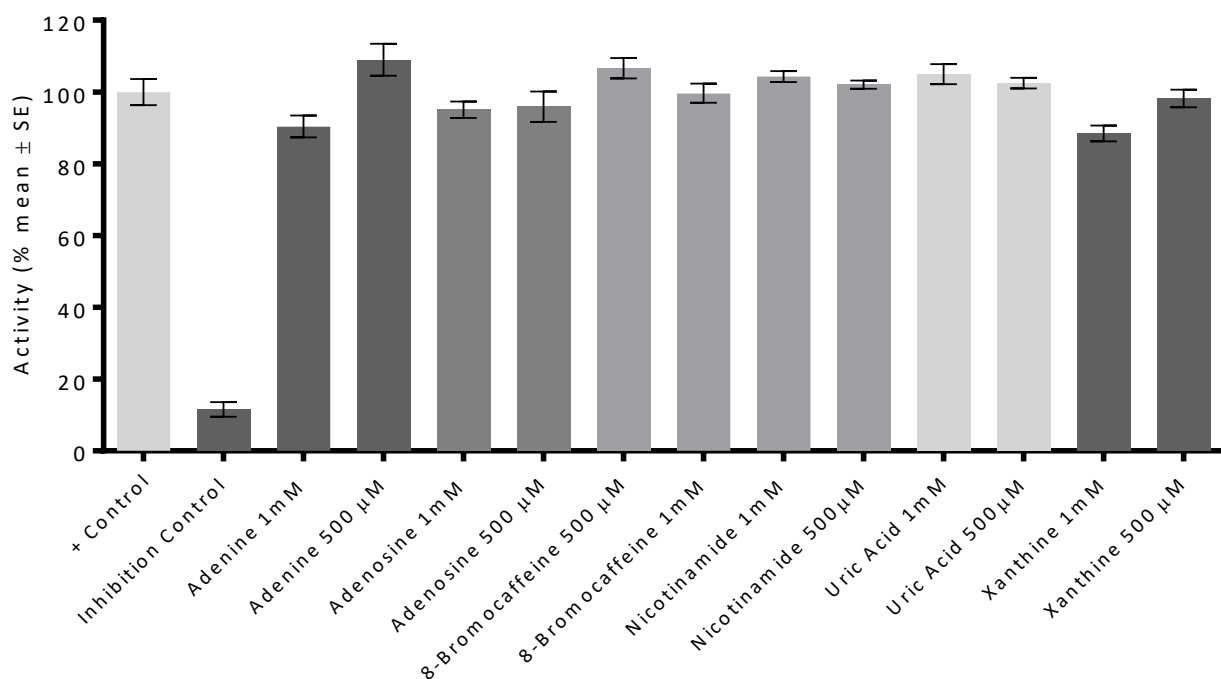


**Fig. 3.36.** Effect of selected xanthines and related compounds at 500 $\mu$ M and 1 mM concentrations on PrAO activity. Benzaldehyde formation was measured at 254 nm using the HPLC method. Assays were performed as described in materials and methods Section 2.5.3 Positive controls with PrAO and substrate and negative inhibition controls with PrAO, substrate and 1 mM semicarbazide were included and results carried out in triplicate.

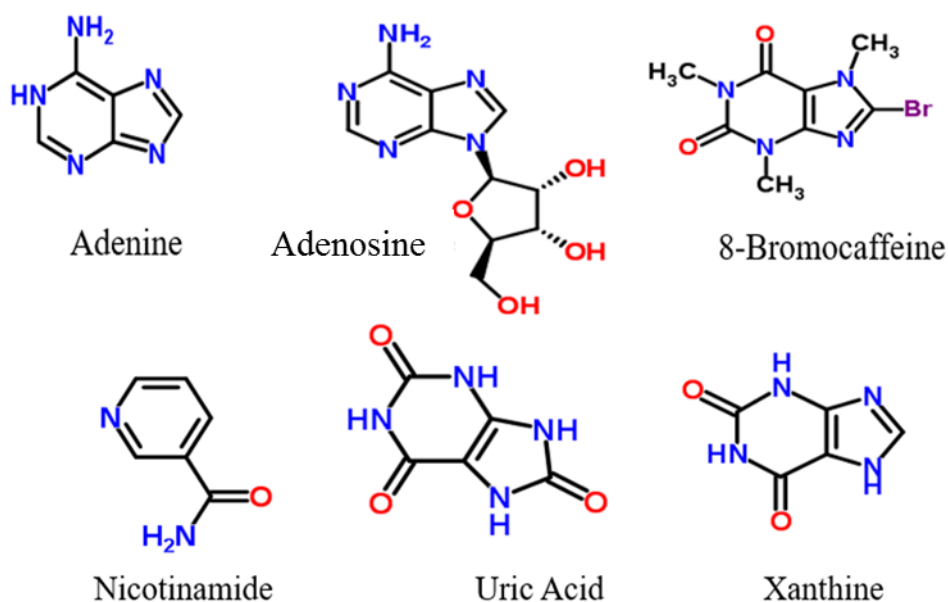


**Fig. 3.37.** Structures of selected compounds structurally related to caffeine: adenine, adenosine, 8-bromocaffeine, nicotinamide, uric acid and xanthine screened for PrAO inhibition. <http://www.chemspider.com/Chemical-Structure>

Caffeine contains an imidazole ring attached to a pyrimidinedione ring structure. Therefore, a range of diazoles were tested for PrAO inhibition (Fig. 3.38). Imidazole was the only compound of this group to show significant albeit modest inhibition ( $P \leq 0.05$ ), but at a higher concentration than caffeine or theobromine, so further testing was not pursued. Structures of the diazoles are given in Fig. 3.38.

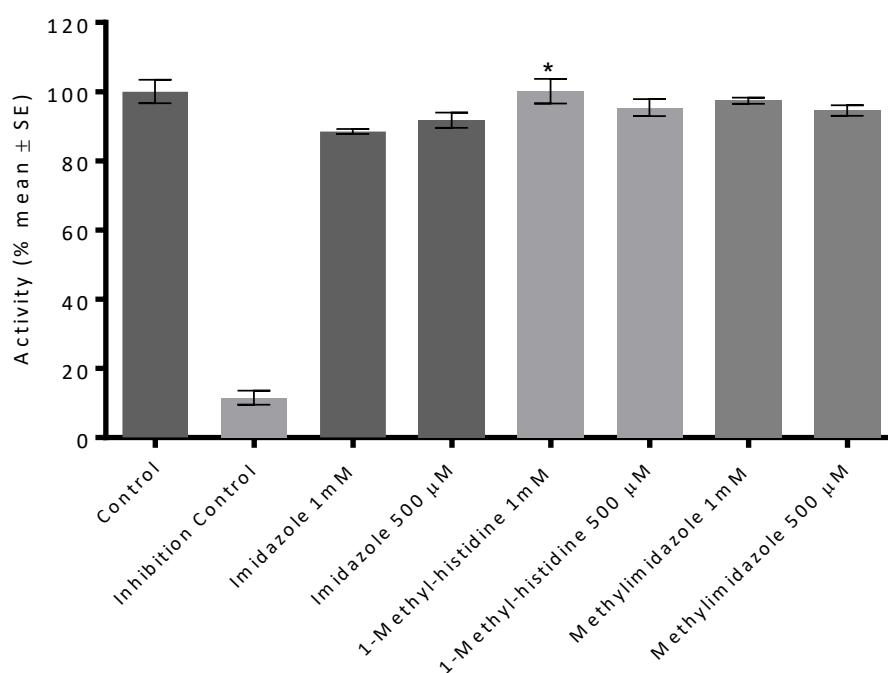


**Fig. 3.38.** Effect of selected diazoles screened at 500μM and 1 mM for inhibition of PrAO. Assays were performed using the HPLC assay described in materials and methods Section 2.5.3. Positive controls with PrAO and substrate and negative inhibition controls with PrAO, substrate and 1 mM semicarbazide were included and results carried out in triplicate. An asterisk denotes a significant difference between a treatment and the control ( $*P \leq 0.05$ ) using ANOVA and Dunnett's Test.

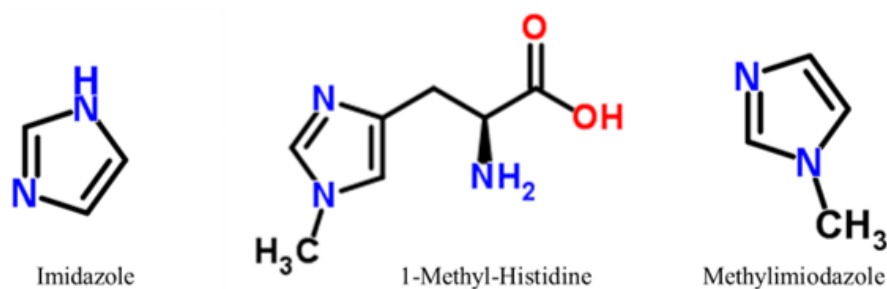


**Fig. 3.39.** Structures of Imidazole, 1-Methyl-Histidine and Methylimidazole diazole compounds selected for PrAO inhibition. <http://www.chemspider.com/Chemical-Structure>



As shown in Figures 3.35, 3.36 and 3.38, theobromine is the most potent inhibitor of PrAO of all the caffeine-related compounds tested. An  $IC_{50}$  plot (Fig 3.40) showed that theobromine had an  $IC_{50}$  of  $427.9 \mu\text{M} \pm 108 \mu\text{M}$  for the oxidation of benzylamine by PrAO.

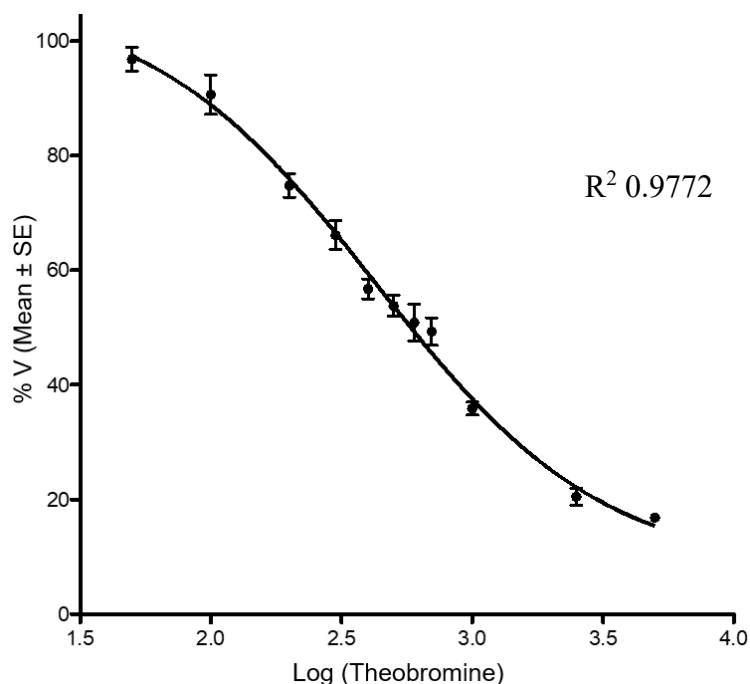


**Fig. 3.40.** Theobromine  $IC_{50}$  inhibition plot showing log concentration of inhibitor vs % activity. From this data an  $IC_{50}$  of  $427.9 \mu\text{M} \pm 108 \mu\text{M}$  was estimated. Inhibitor concentrations ranged from 0.1 mM to 5 mM using concentration 5 mM benzylamine as substrate. Data shown are the mean values  $\pm$  SEM, error bars not evident were less than the representation of the points. Assays were performed in triplicate and  $IC_{50}$  readings obtained at 498 nm at 37°C and pH 7.2 using the colorimetric assay described in Chapter 2. Data were fitted with non-linear regression analysis with the aid of GraphPad Prism, 5.0 software.

The nature of PrAO inhibition by Theobromine was further explored by examining its effect on kinetic parameters for benzylamine oxidation. (Fig. 3.41).

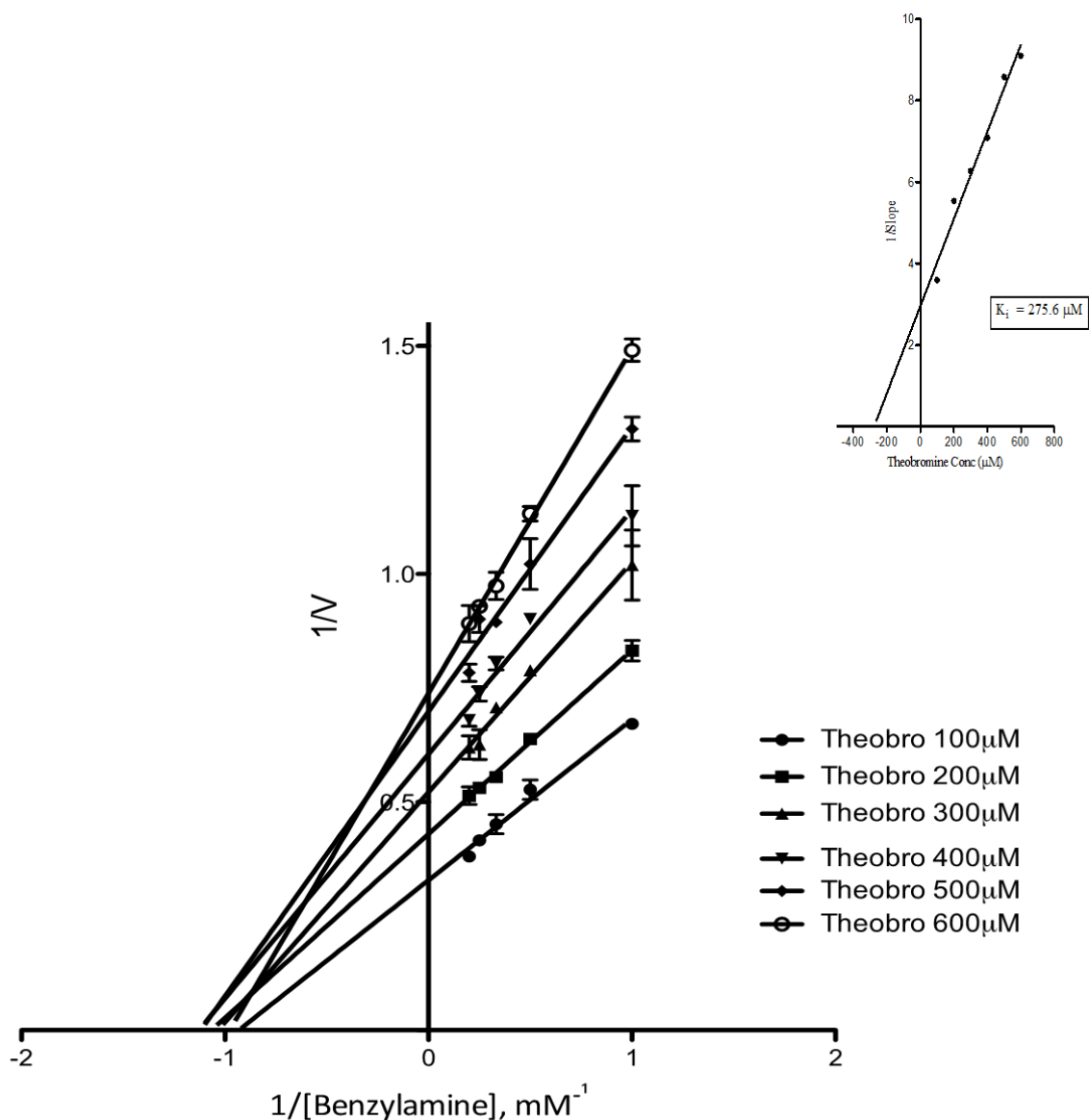


**Fig. 3.41.** Pattern of inhibition of PrAO catalysed benzylamine oxidation by theobromine. A Non-competitive pattern of inhibition is observed. Concentrations of theobromine were varied from 100 to 600  $\mu\text{M}$  and benzylamine from 1 to 5 mM. Data shown are the mean values  $\pm$  SEM, where error bars are not evident they were less than the representation of the points. The initial rates ( $v = \text{abs}_{498 \text{ nm}} \times 10^{-3} \text{ min}$ ) of hydrogen peroxide formation were determined at 37°C and pH 7.2. Data were fitted to the Michaelis–Menten equation with the aid of computer software GraphPad Prism, 5.0. The values of  $1/V_{\text{max app}}$  were plotted against the concentration of inhibitor to obtain a  $K_i$  estimate ( $-K_i = \text{intercept on the } X \text{ axis of the plot on the right}$ ) of approximately 275.6  $\mu\text{M}$  ( $\pm 63 \mu\text{M}$ ) as shown in the inset graph.

### 3.4.1 Testing of Lisofylline as an inhibitor of PrAO

Lisofylline, a therapeutic used for the treatment of diabetes and inflammation, two diseases associated with raised PrAO activity, was examined due to its close similarity in structure to methylxanthines. The mechanism of action for this drug is not clearly understood and testing was performed (Fig. 3.42) to probe PrAO inhibition. There was a statistical significance between treatments and the control ( $P \leq 0.001$ ), although the effect was not dramatic. The structure of lisofylline is shown in Fig. 3.43.

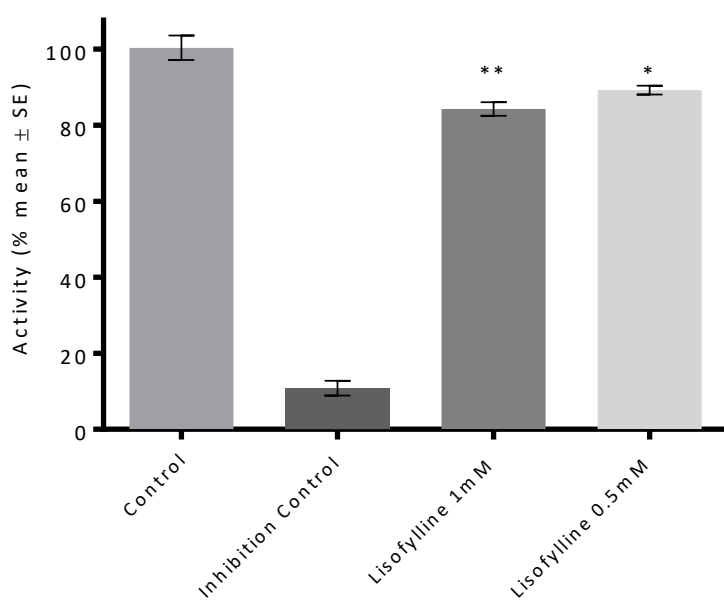
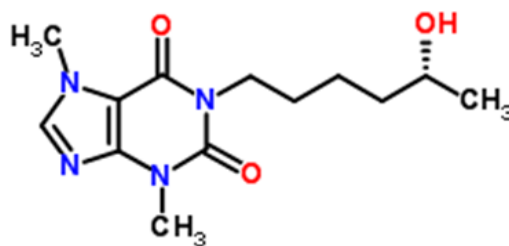


**Fig. 3.42.** Lisofylline inhibition of PrAO at 1 mM and 0.5 mM concentrations. Assays were carried out at a wavelength of 498 nm using the Holt method as described in the methods section 2.5.1 monitoring  $H_2O_2$  production. Positive controls with PrAO and substrate and negative inhibition controls with PrAO, substrate and 1 mM semicarbazide were included. All assays were carried out in triplicate. Data shows a small but significant difference (\* $P \leq 0.05$ ; \*\* $P \leq 0.01$ ) value according to ANOVA and Dunnett's test.



**Lisofylline**

**Fig. 3.43.** Structure of lisofylline. This compound was screened for PrAO inhibition.  
<http://www.chemspider.com/Chemical-Structure>

The degree of inhibition by Lisofylline was not found to be similar to that of Caffeine or Theobromine. This finding indicates that the 5-Hydroxyhexyl substituent on Lisofylline substantially reduces binding to PrAO.

### **3.4.2 Modelling of Caffeine, Theobromine and Theophylline interactions with PrAO**

In view of the noncompetitive pattern of binding observed in this study for Theobromine (Fig 3.41) and by Olivieri and Tipton (2011) for caffeine it was of interest to investigate their binding site(s) on PrAO. A computational approach was employed using AutoDock software 4.0 in an attempt to identify possible methylxanthine binding sites. A computational model for Bovine PrAO was constructed as described in Section 2.9. The top ranking scores (the more negative the ranking value the more energetically favorable the binding) and binding interactions between molecule and PrAO residue side chains are detailed.

Computational docking of theobromine, caffeine and theophylline were investigated to broaden our understanding of the binding interaction between these compounds and PrAO. Figure 3.44 is a molecular surface computational model

showing predicted binding of theobromine near the active site entrance of PrAO. Figure 3.45 is a stick model representation showing potential binding interactions between theobromine and PrAO residues in greater detail. Figures 3.46 and 3.47 show a similar exercise carried out for binding of caffeine to PrAO while Figures 3.48 and 3.49 show theophylline binding depicted in the same manner. Caffeine has not been previously computationally modeled for its binding with PrAO and is a useful comparison to theobromine for binding interactions. Theophylline is a useful comparator here since it did not inhibit PrAO to the same degree as either theobromine or caffeine.

For each compound, a surface molecular image is shown to illustrate binding interactions and show the location of the ligand on the enzyme surface. Also shown is a stick model image to illustrate the binding interactions with PrAO side chains. Relevant amino acid side chains are labelled to highlight the active site entrance location and binding interactions. The software computes binding affinity at different sites as a numerical score. A summary table can be found below detailing inhibition and binding interactions (see Table 3.2).

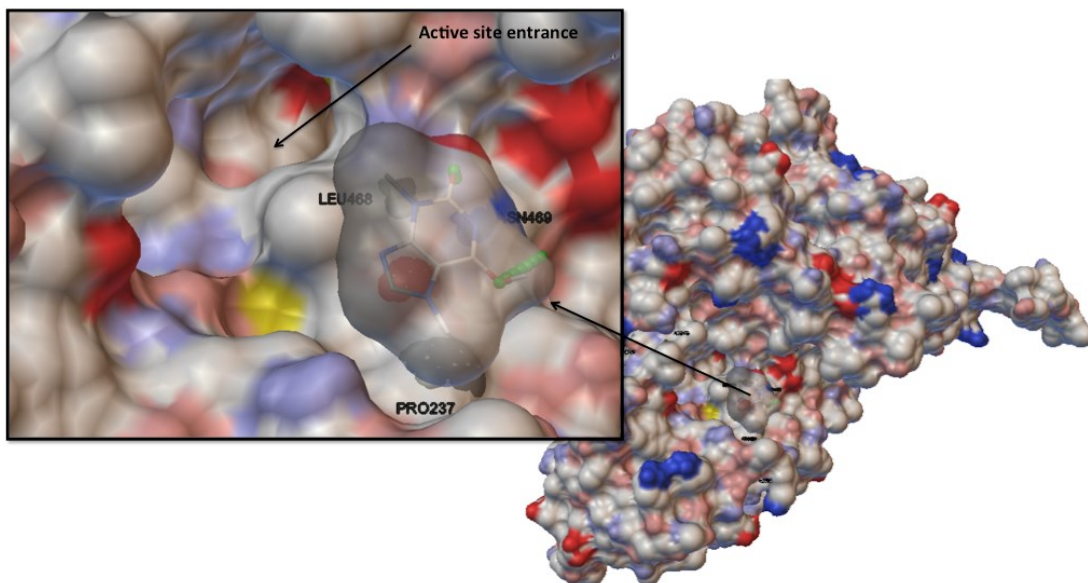


**Fig. 3.44.** A molecular surface representation with polarity shading is depicted for the docking interaction of Theobromine and PrAO. Theobromine is shown as a stick structure binding to the surface of PrAO. Docking of Theobromine had a top rank docking score of  $-2.59$  ( $\Delta G_{\text{bind}}$ ) as calculated by AutoDock Tools 1.5.6. The diagram indicates the active site entrance of PrAO and binding location of theobromine. Gate-acting Leu468, Asn469 and Pro237 residues are highlighted at or near the active site entrance. Polar regions are indicated in blue for positively charged, and red for negatively charged residues. Hydrophobic residues are indicated in in grey.

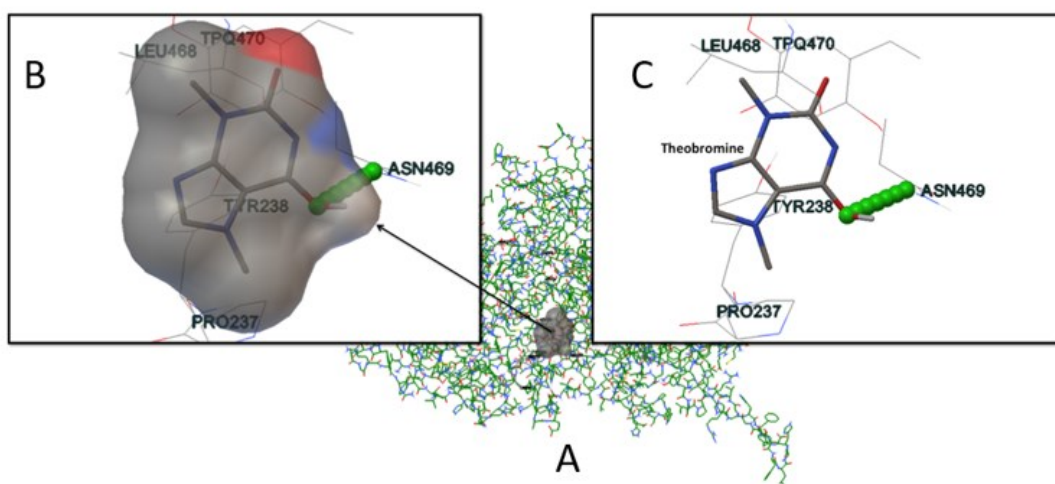


**Fig. 3.45.** A computational stick model representation of Figure 3.44. Image A (center) depicts theobromine, shown in grey, bound to the enzyme in close proximity to the active site entrance. Image B is a magnification of the binding interaction of image A showing polar regions in blue for positively charged and red for negatively charged residues. The grey shading indicates hydrophobic regions. Image C shows the removal of the surface which better depicts potential hydrogen bonding between the carbonyl group of theobromine and the amine group of Asn469 by a green line of spheres.

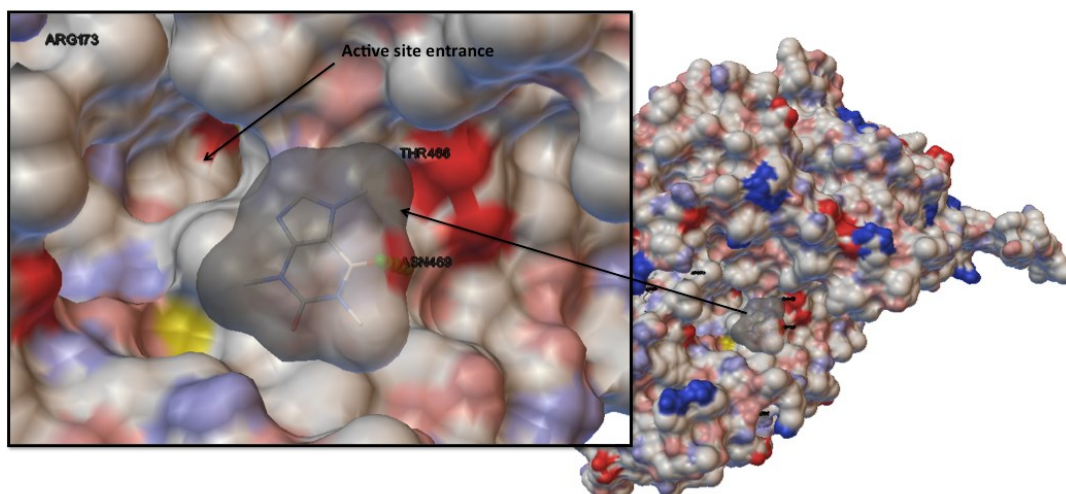


**Fig. 3.46.** Caffeine had a top rank docking score of  $-2.30$  ( $\Delta G_{\text{bind}}$ ) as calculated by AutoDock Tools 1.5.6 when bound to PrAO. A molecular surface representation with polarity shading is depicted for the docking interaction of ligand and macromolecule, indicating the active site entrance of PrAO and binding location of caffeine. Asn469, Thr466 and Arg173 are highlighted at or near the active site entrance. Polar regions are indicated by blue, positively charged and red negatively charged, binding interactions. The grey shading depicts hydrophobic interactions.

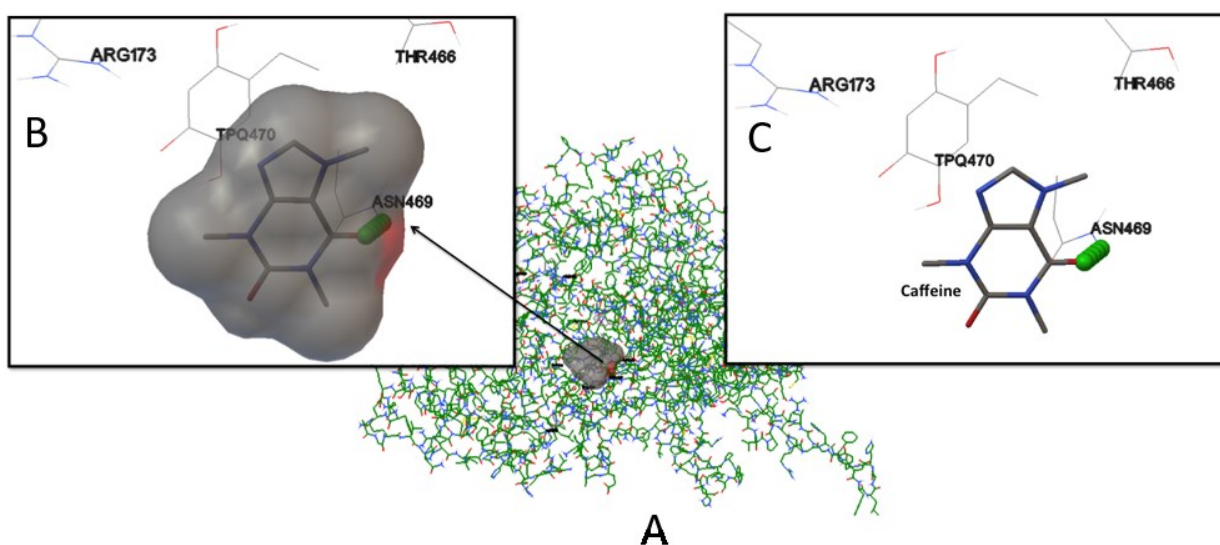


**Fig. 3.47.** A computational stick model representation of Figure 3.46. Image A depicts caffeine, shown in grey, to be externally bound to the enzyme in close proximity to the active site entrance. Image B is a magnification of the binding interaction of image A, depicting polarity regions as blue for positively charged and red for negatively charged binding interactions. The grey indicates hydrophobic regions. Image C is the removal of the surface representation, which better depicts hydrogen bonding between the carbonyl group of caffeine and the amine group of Asn469 by a green line of spheres.



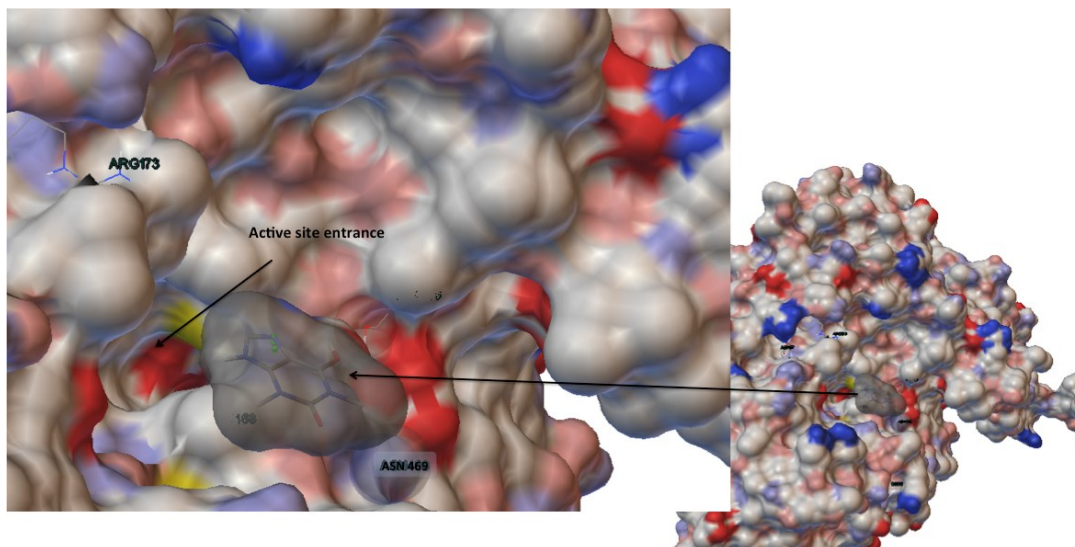


**Fig. 3.48.** Theophylline had a top rank docking score of  $-2.75$  ( $\Delta G_{\text{bind}}$ ) as calculated by AutoDock Tools 1.5.6 when bound to PrAO. A molecular surface representation with polarity shading is depicted for the docking interaction of ligand and macromolecule, indicating the active site entrance of PrAO and binding location of theophylline. Asn469 and Arg173 are highlighted at or near the active site entrance. Polar regions are indicated by blue for positively charged, red for negatively charged binding interactions.

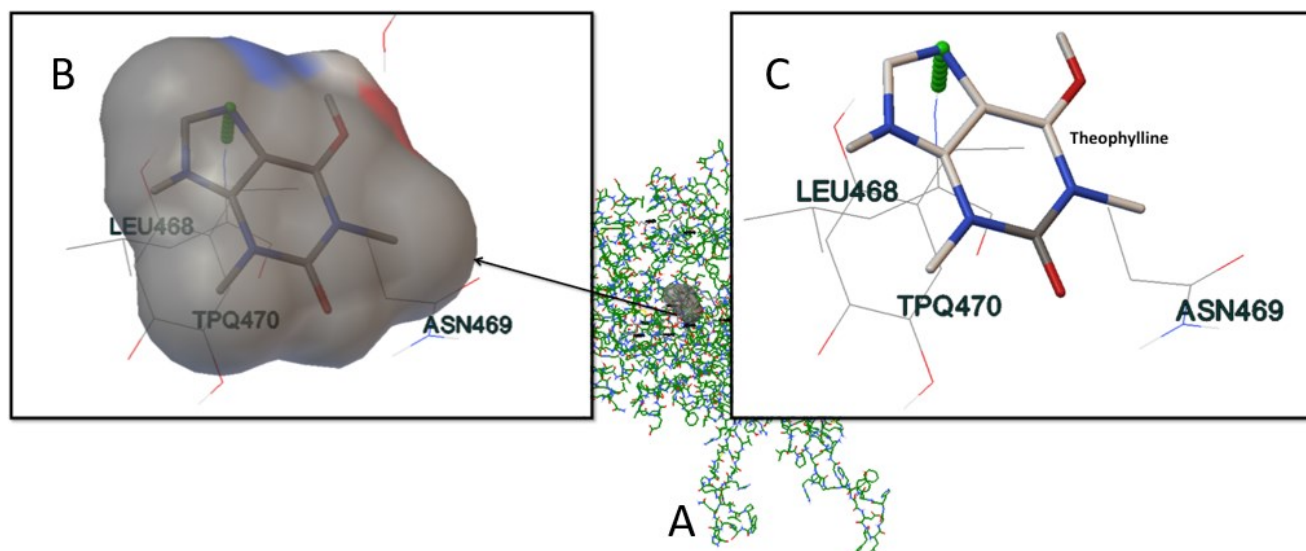


**Fig. 3.49.** A computational stick model of Fig. 3.48. Image A shows theophylline, shown in grey, to be externally bound to the enzyme in close proximity to the active site entrance. Image B is a magnification of the binding interaction of image A, depicting polarity regions such as blue for positively charged and red for negatively charged binding interactions. The grey indicates hydrophobic regions. Image C is the removal of the surface representation, which better depicts hydrogen bonding shown by a green line of spheres between the amine group of theophylline and the amine group of Leu468, while giving a better visual of the ligand and interacting side chains involved.



**Table 3.2.** Summary of binding interactions for selected Methylxanthines with PrAO, predicted by AutoDock.

<b>Docked Compound</b>	<b>Observed PrAO Inhibition</b>	<b>Docking Score (<math>\Delta G_{\text{bind}}</math>)</b>	<b>Hydrogen Bonding</b>	<b>Hydrophobic Interactions</b>
Theobromine	Yes	-2.59	Asn469	Tyr238 Leu468 Pro237
Caffeine	Yes	-2.30	Asn469	Leu468 Pro237
Theophylline	No	-2.75	Leu468	Leu468

An overview of methods and findings of methylxanthines and related structures that were tested for PrAO modulation can be found below (see Figure 3.50).

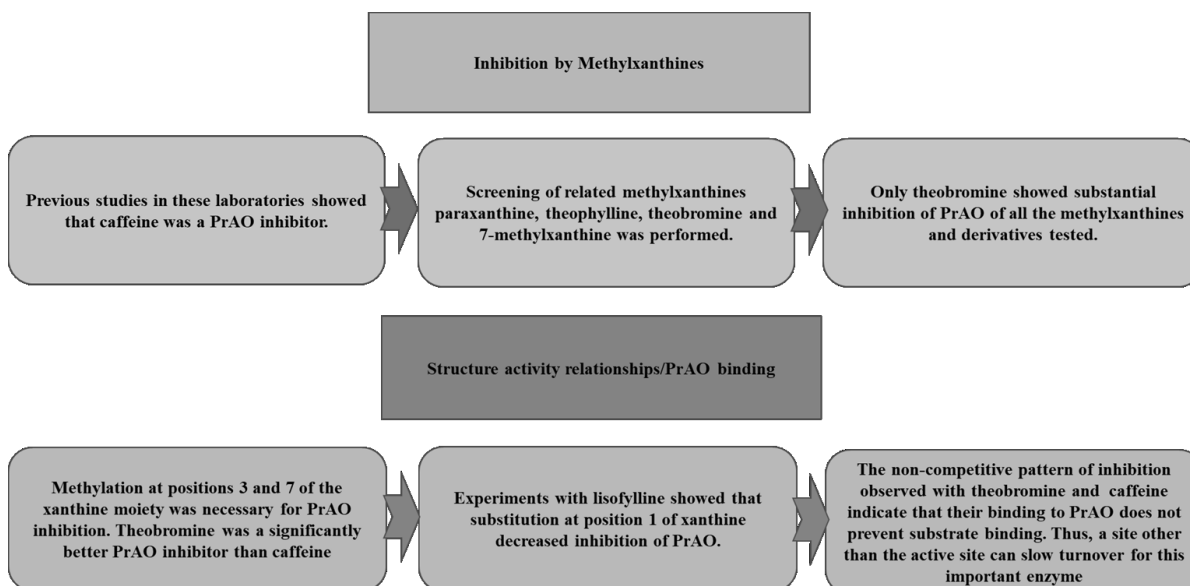


**Fig. 3.50.** Overview of main findings observed and methods used in the testing of methylxanthine and related compounds assayed for PrAO modulation.

### 3.5 Amino Acids

An interest in screening amino acids was based upon previous work in this lab, namely the inhibition of PrAO by lysine in the presence of H<sub>2</sub>O<sub>2</sub>. As lysine inhibited PrAO structurally related amino acids such as ornithine and L-arginine (Fig. 3.54 and 3.56) were screened for similar inhibitory effects. Cysteine, an amino acid with a thiol group yielded significant inhibition (Fig. 3.52), *D*-ethionine also having a thiol group (Fig. 3.55) was screened with no inhibition evident. Other similar short chained amino acids were appropriate to screen, for example; the thiol group of cysteine was replaced with a hydroxyl group of *D*-serine (Fig. 3.57.) or methyl groups of *D*-norvaline (Fig. 3.53.). In an aligned sub-study, alanine, iso-leucine, threonine and phenylalanine were also tested. A full list of test results can be found in Table 3.3. These amino acid structures are depicted in Fig. 3.51. All data were obtained using the UV plate reader spectrophotometric assay (see section 2.5) monitoring the product benzaldehyde. The concentrations of amino acids tested for inhibition were 1.0 mM and 100 μM to verify potential physiologically relevant inhibition.

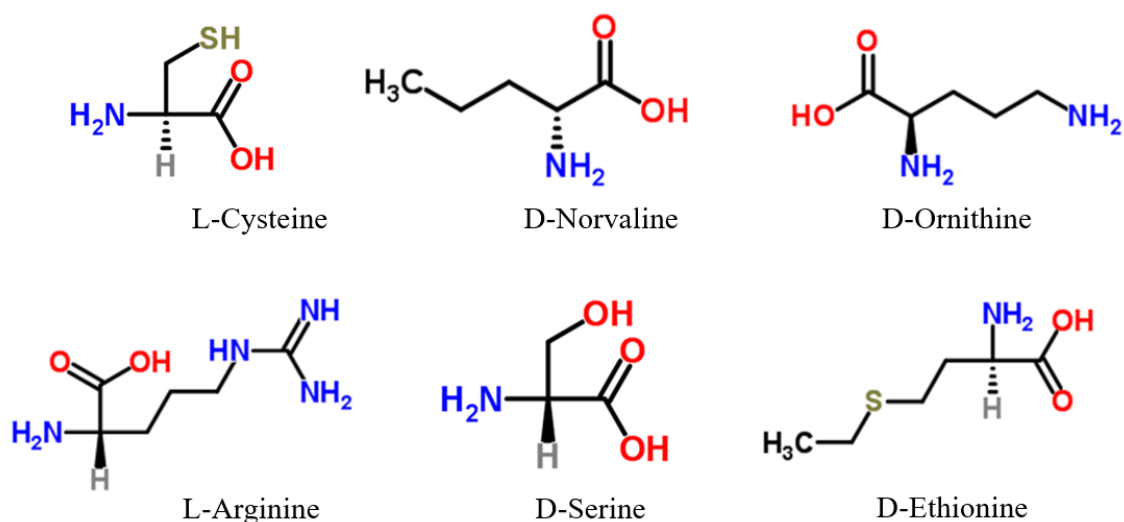
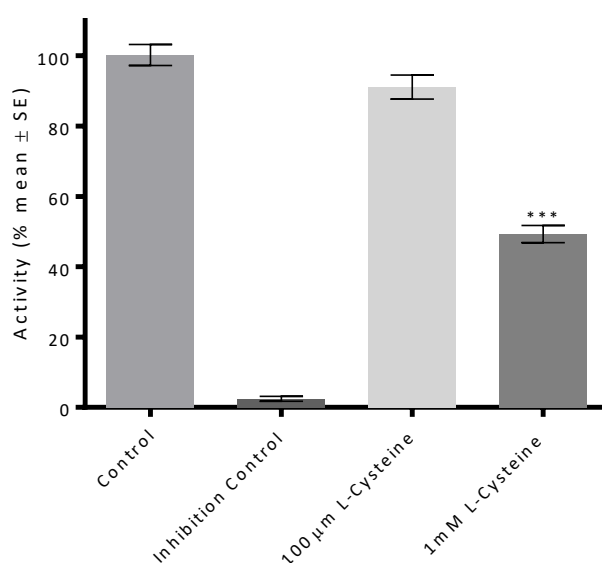


Fig. 3.51. Chemical structures of selected amino acids. <http://www.chemspider.com/Chemical-Structure>.

### 3.5.1 L-cysteine

*L*-cysteine inhibition assay of PrAO (Fig. 3.50) revealed a significant difference between treatments and the control using ANOVA ( $P \leq 0.001$ ). Although there was a significant difference between the lower concentration of *L*-cysteine (100  $\mu\text{M}$ ) and the control, the higher concentration (100 mM) was not significantly different to the control ( $P > 0.05$ ; Fig. 3.50).



**Fig. 3.52.** *L*-cysteine inhibition assay of PrAO with blank, control, inhibition control and experimental assay with 1 mM and 100  $\mu\text{M}$  concentrations. Assays were performed at 254 nm monitoring benzaldehyde production in triplicate. Positive controls with PrAO and substrate and negative inhibition controls with PrAO, substrate and 1 mM semicarbazide were included. An asterisk denotes a significant difference between treatments and the control (\*\*\*)  $P \leq 0.001$  using ANOVA and Dunnett's test.

### 3.5.2 D-norvaline

D-norvaline significantly inhibited at a concentration of 1.0mM ( $*P \leq 0.05$ ) PrAO (Fig. 3.51).

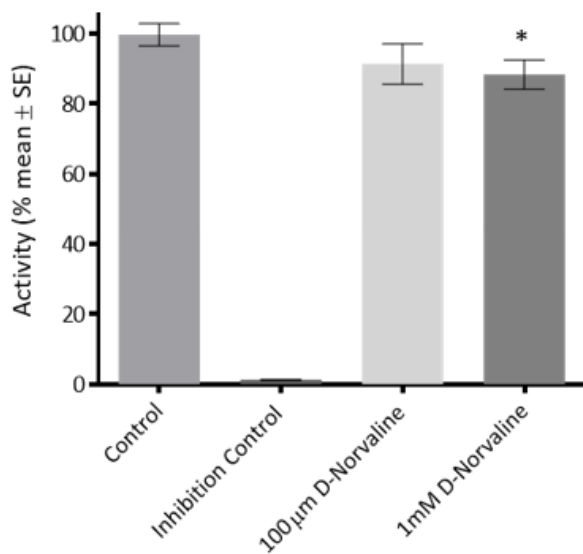


**Fig. 3.53.** *D*-norvaline inhibition assay of PrAO with blank, control, inhibition control and experimental assay with 1 mM and 100 μM concentrations of. Assays were performed at 254 nm monitoring aldehyde production and in triplicate. Positive controls with PrAO and substrate and negative inhibition controls with PrAO, substrate and 1 mM semicarbazide were included. An asterisk denotes a significant difference between treatments and the control ( $*P \leq 0.05$ ) using ANOVA and Dunnett's test.

### 3.5.3 Ornithine

Ornithine inhibition assay of PrAO (Fig. 3.52) revealed a slight decrease in the activity rate (mAbs/min); however, neither the 100  $\mu$ m or 1 mM of ornithine significantly inhibited PrAO ( $P > 0.05$ ; Fig. 3.52).

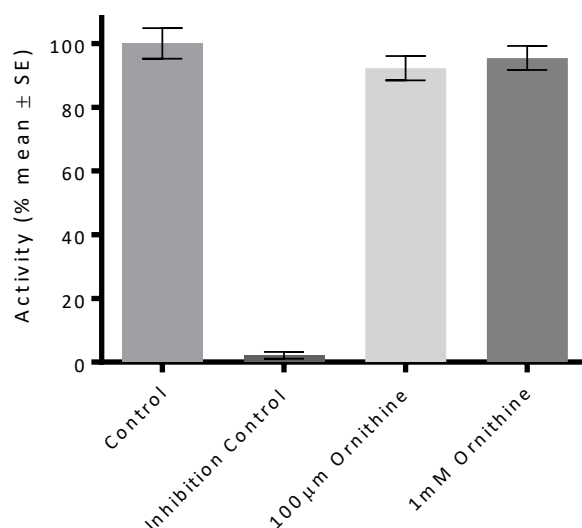


**Fig. 3.54.** Ornithine inhibition assay of PrAO with blank, control, inhibition control and experimental assay with 1 mM and 100  $\mu$ m concentrations. Assays were performed at 254 nm monitoring aldehyde production and in triplicate.

### 3.5.4 D-ethionine

*D*-ethionine did not significantly inhibit PrAO ( $P > 0.05$ ; Fig. 3.53).

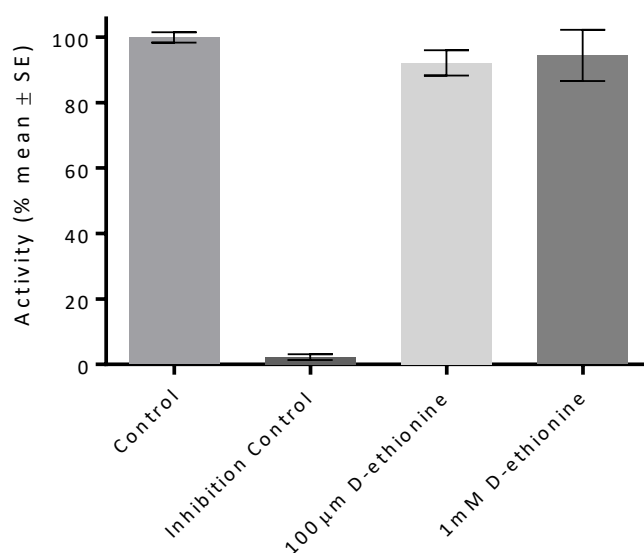


**Fig. 3.55.** *D*-ethionine inhibition assay of PrAO with blank, control, inhibition control and experimental assay with 1 mM and 100  $\mu$ m concentrations of *D*-ethionine. Assays were performed at 254 nm monitoring aldehyde production and in triplicate. Positive controls with PrAO and substrate and negative inhibition controls with PrAO, substrate and 1 mM semicarbazide were included.

### 3.5.5 L-arginine

*L*-arginine did not significantly inhibit PrAO ( $P > 0.05$ ; Fig. 3.54).

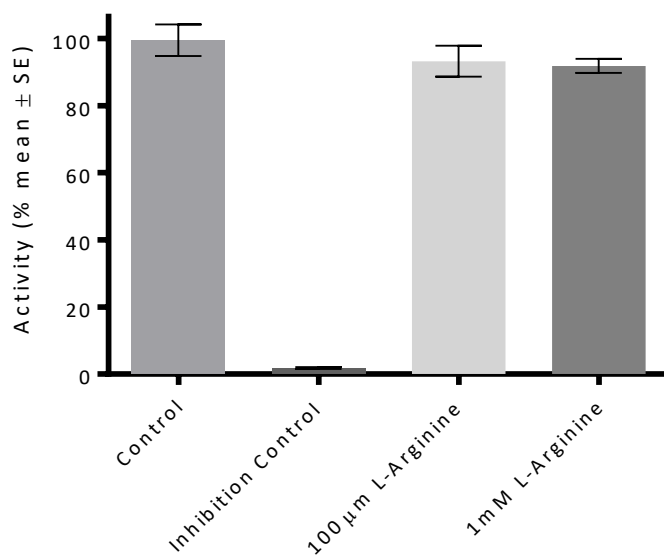


**Fig. 3.56.** *L*-arginine inhibition assay of PrAO with blank, control, inhibition control and experimental assay with 1 mM and 100 µM concentrations. Assays were performed at 254 nm monitoring aldehyde production and in triplicate. Positive controls with PrAO and substrate and negative inhibition controls with PrAO, substrate and 1 mM semicarbazide were included.

### 3.5.6 D-serine

The D-serine inhibition assay of PrAO (Fig. 3.55) exhibited a slight decrease in PrAO activity (mAbs/min) but did not significantly inhibit PrAO ( $P > 0.05$ ; Fig. 3.55).

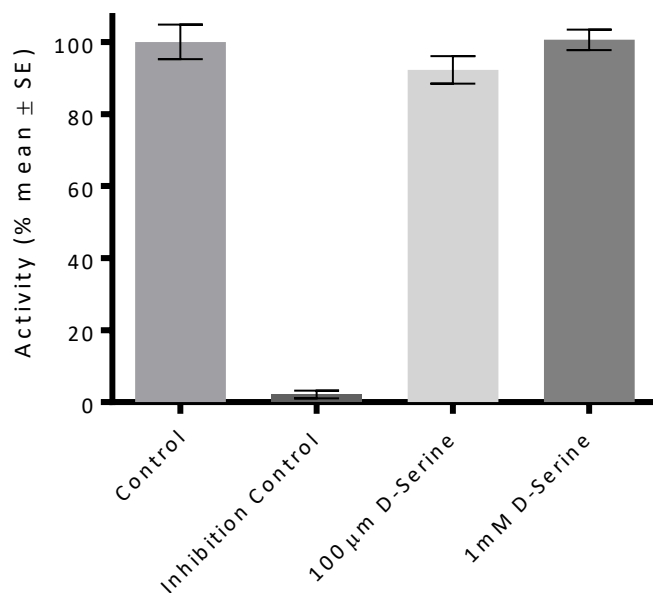


**Fig. 3.57.** D-serine inhibition assay of PrAO with blank, control, inhibition control and experimental assay with 1 mM and 100 µM concentrations. Positive controls with PrAO and substrate and negative inhibition controls with PrAO, substrate and 1 mM semicarbazide were included.

### 3.6 Vitamins as PrAO modulators

As discussed in Chapter 1 Section 1.8, vitamins are being actively researched for their specific health benefits in numerous diseases such as cancer and diabetes, and therefore have relevance in being tested as natural dietary inhibitors for PrAO modulation. Thiamine (Vitamin B1) and Pyridoxine (Vitamin B6) (Fig. 3.58) showed statistically significant inhibition when tested using the Holt method monitoring  $\text{H}_2\text{O}_2$  production as described in Section 2.5.1.  $\text{IC}_{50}$  values, patterns of inhibition and  $K_i$  values were determined for each inhibitor. A full list and results of all vitamins tested can be found in Table 3.3.

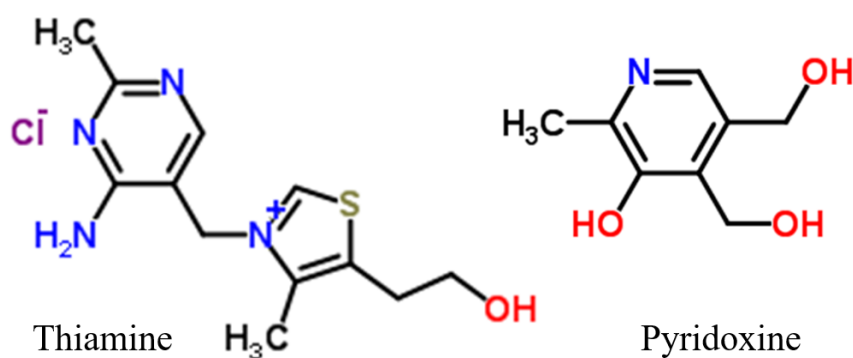


**Fig. 3.58.** Chemical structure of thiamine and pyridoxine.

<http://www.chemspider.com/Chemical-Structure>



### 3.6.1 Thiamine

The thiamine inhibition of PrAO (Fig. 3.57) revealed a significant difference between treatments using ANOVA ( $P \leq 0.01$ ). Fig. 3.58 exhibits the  $IC_{50}$  inhibition of thiamine and Fig. 3.59 depicts the Lineweaver Burk plots of thiamine.

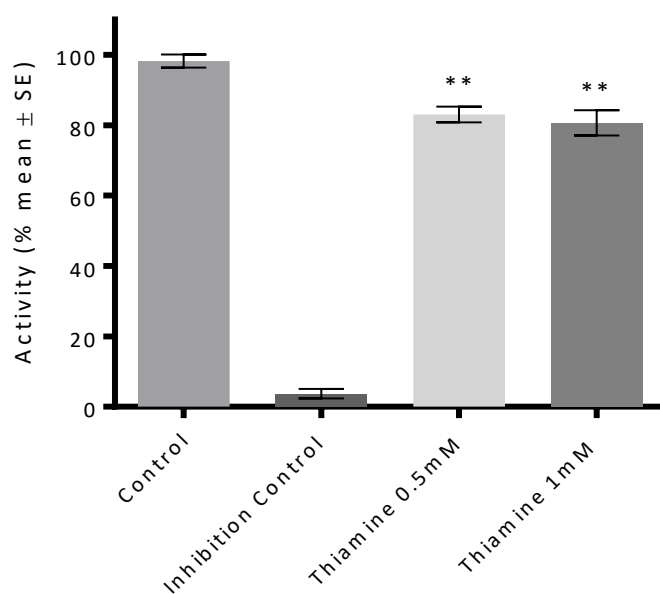


**Fig. 3.59.** Thiamine inhibition assay of PrAO with blank, control, inhibition control and experimental assay with 1 mM and 0.5 mM concentrations. Assays were performed at 498 nm monitoring  $H_2O_2$  production in triplicate. Positive controls with PrAO and substrate and negative inhibition controls with PrAO, substrate and 1 mM semicarbazide were included. An asterisk denotes a significant difference between treatments and the control (\*\* $P \leq 0.01$ ) using ANOVA and Dunnett's test.

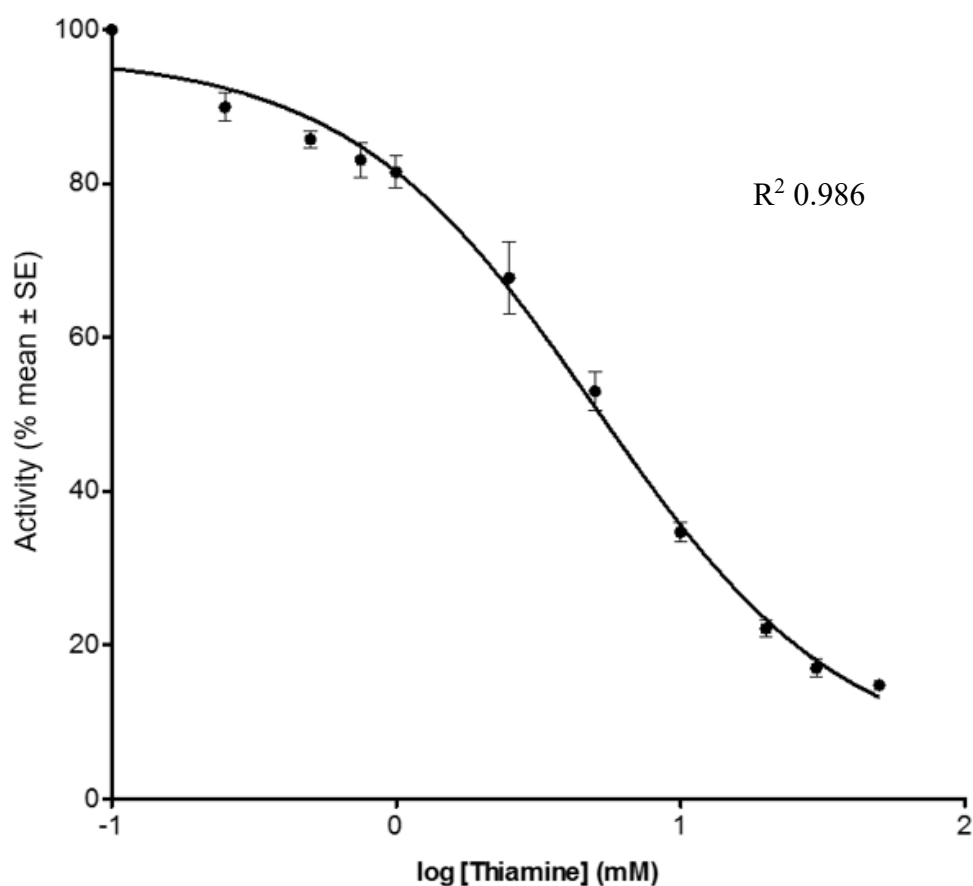


**Fig. 3.60.** Thiamine IC<sub>50</sub> inhibition plot showing log concentration of inhibitor Vs % activity, giving an IC<sub>50</sub> of 5.046 mM ± 1.15 mM. Inhibitor concentration ranged from 0.1 mM to 50 mM and substrate concentration of 5 mM benzylamine. Data shown are the mean values ± SEM, error bars not evident were less than the representation of the points. Assays were performed in triplicate and IC<sub>50</sub> readings gained at 498 nm at 37°C and pH 7.2. Data were fitted with non-linear regression analysis with the aid of computer software GraphPad Prism, 5.0.

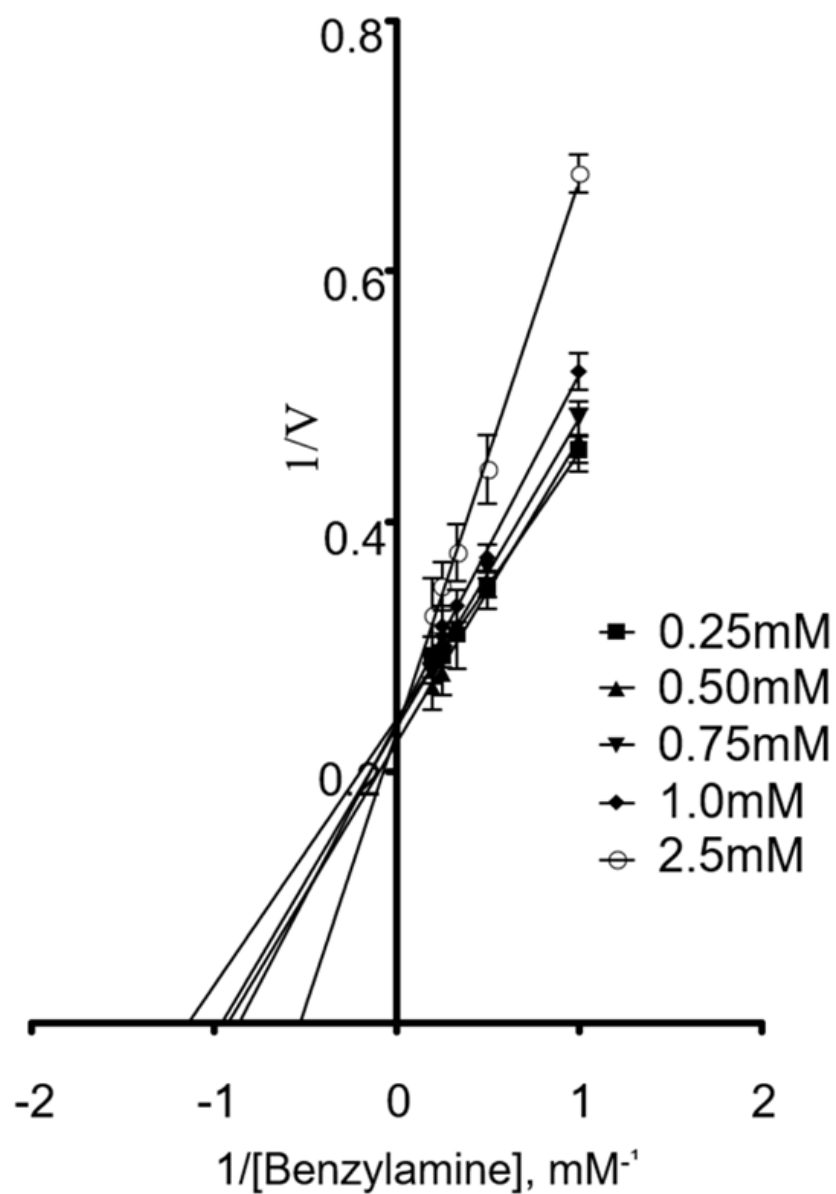


**Fig. 3.61.** Substrate (benzylamine) patterns of inhibition of PrAO by thiamine. A competitive type pattern of inhibition is observed. All samples contained increasing concentrations of thiamine (from 0.25 mM to 2.5 mM) and benzylamine (from 1 to 5 mM). Data shown are the mean values  $\pm$  SEM, error bars not evident were less than the representation of the points. The initial rates ( $v = \text{abs}498 \text{ nm} \times 10^{-3} \text{ min}$ ) of hydrogen peroxide formation were determined at  $37^\circ\text{C}$  and pH 7.2. Data were fitted to the Michaelis–Menten equation with the aid of computer software GraphPad Prism, 5.0.

### 3.6.2 Pyridoxine

Pyridoxine significantly inhibited PrAO at 0.5 mM ( $P \leq 0.01$ ) and 1 mM ( $P \leq 0.001$ ; Fig. 3.62). Fig. 3.63 exhibits the  $IC_{50}$  inhibition plot of pyridoxine and Fig. 3.64 depicts the pyridoxine Lineweaver Burk plots.

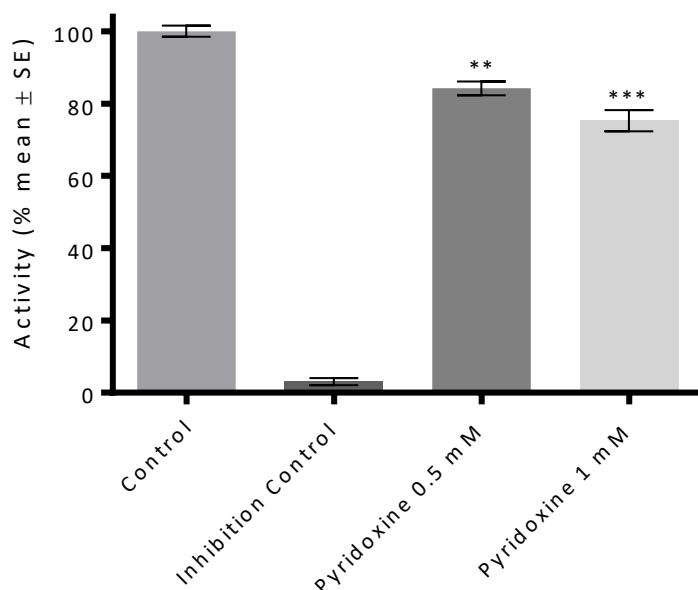


**Fig. 3.62.** Pyridoxine inhibition of PrAO with a control, inhibition control and experimental assay with 1.0 mM and 0.5 mM concentrations. Assays were performed at 498 nm monitoring  $H_2O_2$  production in triplicate. Positive controls with PrAO and substrate and negative inhibition controls with PrAO, substrate and 1 mM semicarbazide were included. An asterisk denotes a significant difference between treatments and the control (\*\* $P \leq 0.01$ ; \*\*\* $P \leq 0.001$ ) using ANOVA and Dunnett's test.

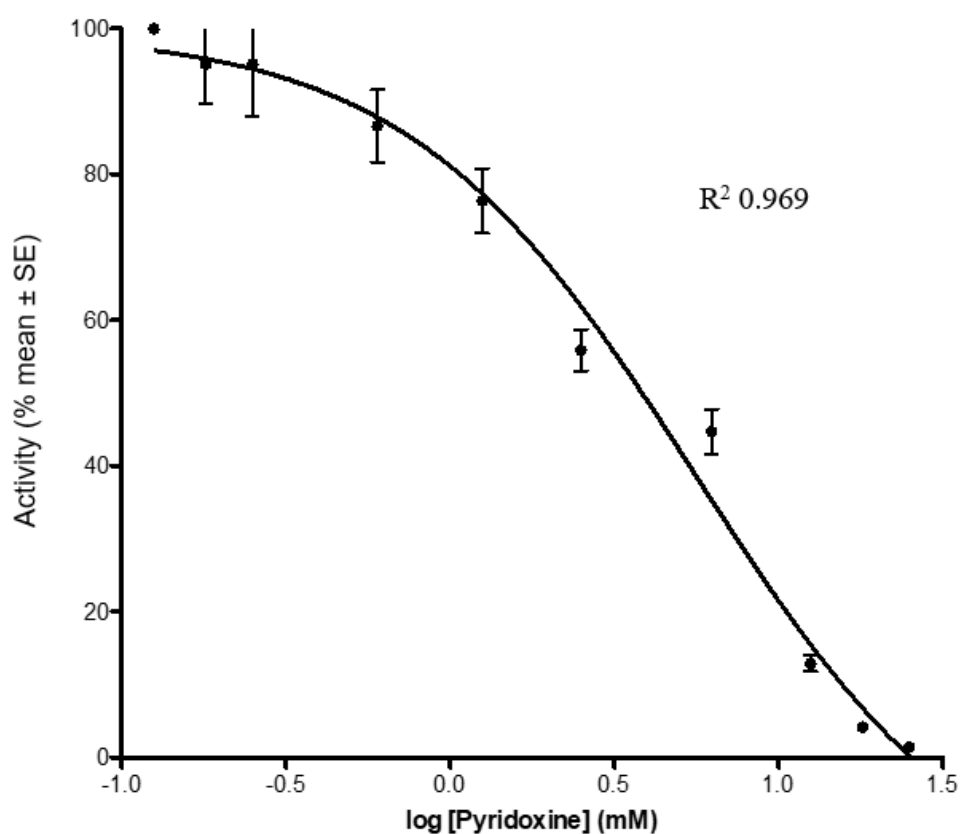


**Fig. 3.63.** Pyridoxine IC<sub>50</sub> inhibition plot showing log concentration of inhibitor Vs % activity, giving an IC<sub>50</sub> of 5.55 mM ± 2.81 mM. Inhibitor concentration ranged from 125 mM to 25 mM and substrate concentration of 5 mM benzylamine. Data shown are the mean values ± SEM, error bars not evident were less than the representation of the points. Assays were performed in triplicate and IC<sub>50</sub> readings gained at 498 nm at 37°C and pH 7.2. Data were fitted with non-linear regression analysis with the aid of computer software GraphPad Prism, 5.0.

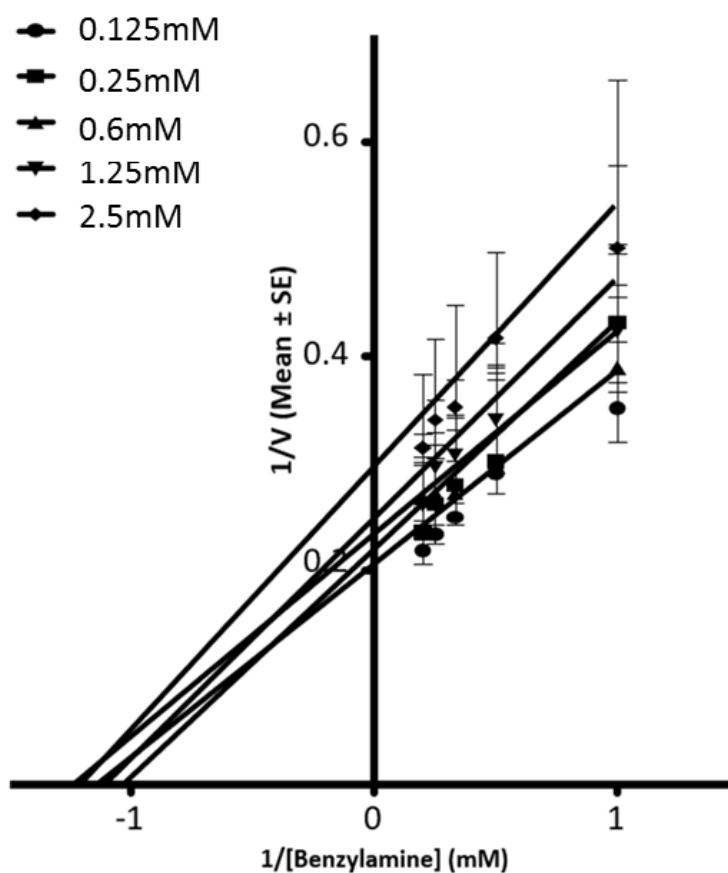
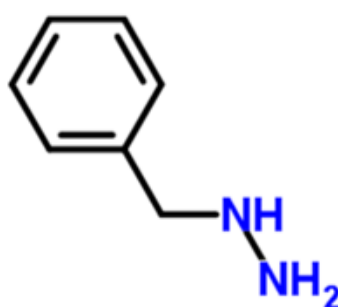


**Fig. 3.64.** Substrate (benzylamine) pattern of inhibition of PrAO by pyridoxine. An un-competitive type pattern of inhibition is observed. All samples contained increasing concentrations of pyridoxine (from 0.125 mM to 2.5 mM) and benzylamine (from 1 to 5 mM). Data shown are the mean values  $\pm$  SEM, error bars not evident were less than the representation of the points. The initial rates ( $v = \text{abs}498 \text{ nm} \times 10^{-3} \text{ min}^{-1}$ ) of hydrogen peroxide formation were determined at 37°C and pH 7.2. Data were fitted to the Michaelis–Menten equation with the aid of computer software GraphPad Prism, 5.0.

### 3.8 Non-dietary Xenobiotics as PrAO inhibitors

A selection of xenobiotic compounds such as benzylhydrazine, 4-amino-phenol and acrylamide were tested to further the knowledge of structures that may inhibit PrAO. These compounds were selected due to either having primary amines or being structurally similar to other compounds with some potential to be PrAO modulators. A summary these results can be found in Table 3.4. Benzylhydrazine (Fig. 3.65) was the only compound tested that showed statistically significant inhibition (Fig. 3.66). Additional experimentation was performed on this compound and the corresponding results are detailed below in bar graph form with  $IC_{50}$  values, patterns of inhibition. Benzylhydrazine significantly inhibited PrAO at 1.0 nM and 4.0 nM ( $P \leq 0.001$ ; Fig. 3.66).  $IC_{50}$  inhibition plot of benzylhydrazine is displayed in Fig. 3.67, the Lineweaver Burk plot of benzylhydrazine is exhibited depicting probable mode of inhibition in Fig. 3.68.



Benzylhydrazine

Fig. 3.65. Chemical structure of benzylhydrazine.

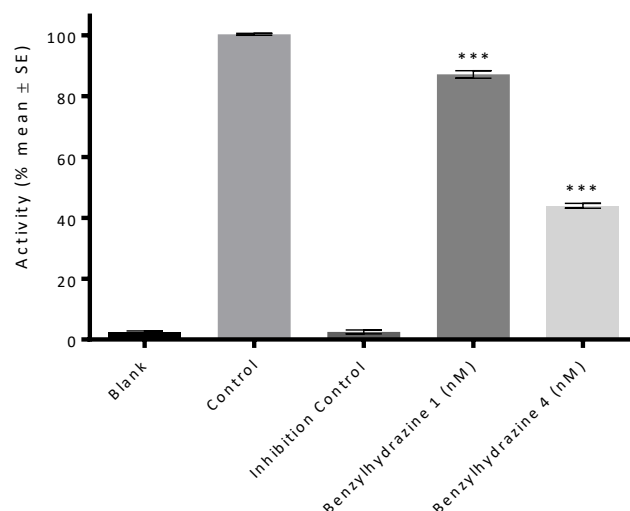


**Fig. 3.66.** Benzylhydrazine inhibition assay of PrAO with blank, control, inhibition control and experimental assay with 1 nM and 4 nM concentrations. Assays were performed at 254 nm monitoring aldehyde production in triplicate. Positive controls with PrAO and substrate and negative inhibition controls with PrAO, substrate and 1 mM semicarbazide were included. Result show a significant difference, denoted by an asterisk (\*\*\*)  $P \leq 0.001$  using ANOVA and Dunnett's post hoc analyses.

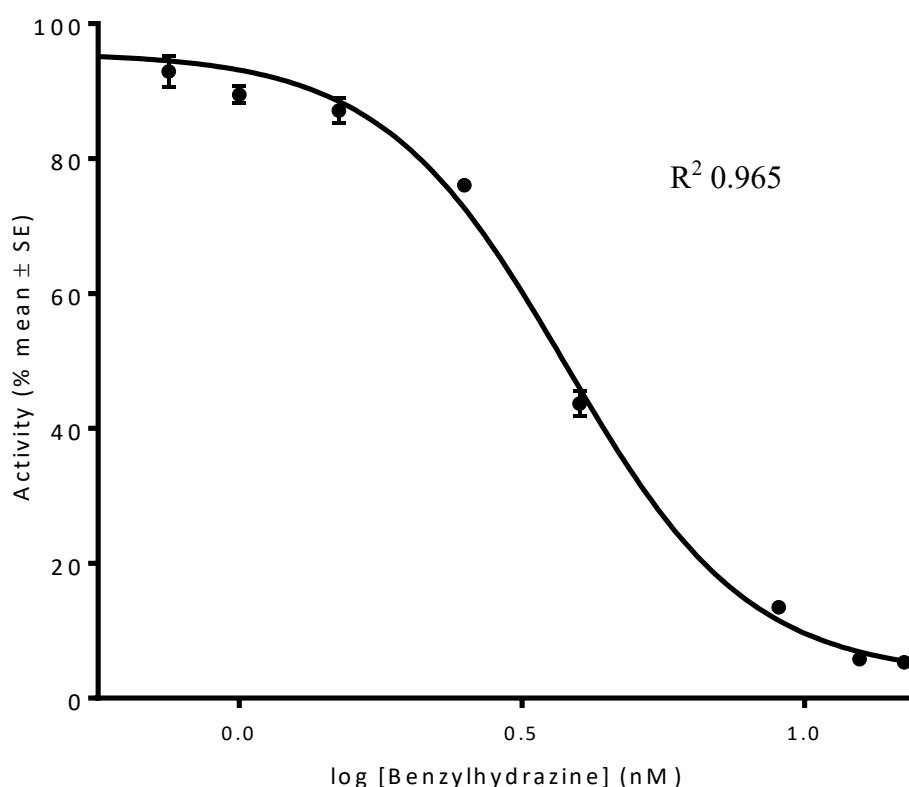


**Fig. 3.67.** Benzylhydrazine  $IC_{50}$  inhibition plot showing log concentration of inhibitor Vs % activity, giving an  $IC_{50}$  of  $6.628 \text{ nM} \pm 3.2 \text{ nM}$ . Inhibitor concentration ranged from 0.5 nM to 25 nM 25 mM and substrate concentration of 5 mM benzylamine. Data shown are the mean values  $\pm$  SEM, error bars not evident were less than the representation of the points. Assays were performed in triplicate and  $IC_{50}$  readings gained at 498 nm at  $37^\circ\text{C}$  and pH 7.2. Data were fitted with non-linear regression analysis with the aid of computer software GraphPad Prism, 5.0.



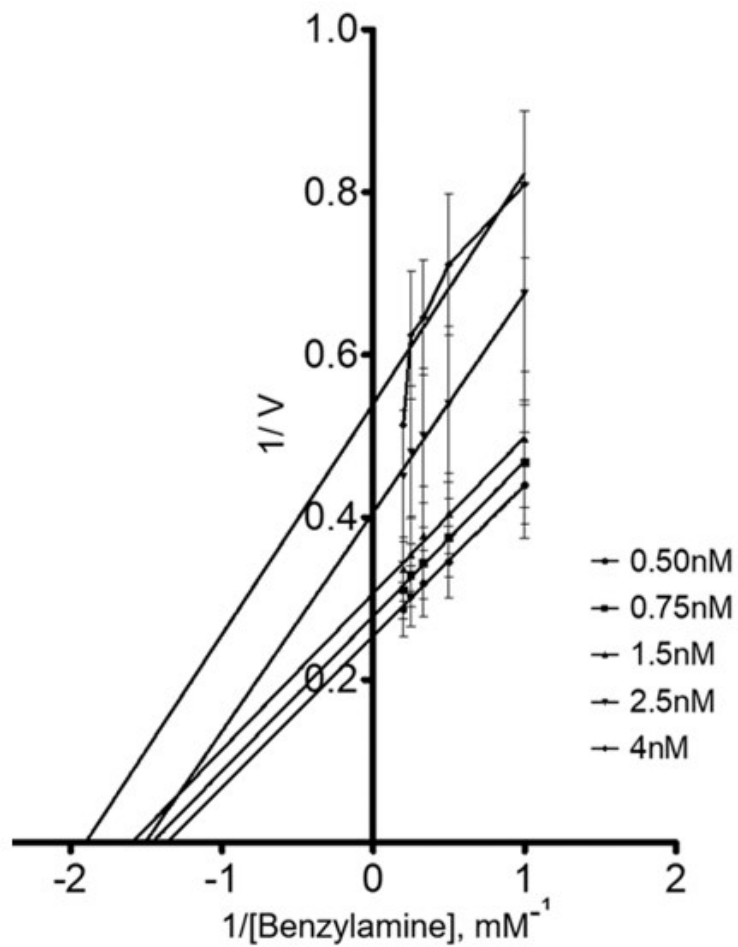


**Fig. 3.68.** Substrate (benzylamine) patterns of inhibition of PrAO by benzylhydrazine. An uncompetitive type pattern of inhibition is observed. All samples contained increasing concentrations of benzylhydrazine (from 0.125 mM to 2.5 mM) and benzylamine (from 1 to 5 mM). Data shown are the mean values  $\pm$  SEM, error bars not evident were less than the representation of the points. The initial rates ( $v = \text{abs}498 \text{ nm} \times 10^{-3} \text{ min}^{-1}$ ) of hydrogen peroxide formation were determined at 37°C and pH 7.2. Data were fitted to the Michaelis–Menten equation with the aid of computer software GraphPad Prism, 5.0.

**Table 3.3.** Summary table of various compounds tested for significance of inhibition of PrAO at 254 nm for benzaldehyde production. Compounds in each category are presented in order of significance with P values attached.

Compound	Type	Concentration (mM)	Significance of inhibition vs. control	P value
<b>Caffeine Analogs</b>				
Caffeine	Endogenous	1.00	***	≤ 0.001
Theobromine	Endogenous	1.00	***	≤ 0.001
Caffeic acid	Endogenous	1.00	***	≤ 0.001
Theophylline	Endogenous	1.00	**	≤ 0.01
7-Methylxanthine	Endogenous	1.00	**	≤ 0.01
§Lisofylline	Xenobiotic	1.00	**	≤ 0.01
Paraxanthine	Endogenous	1.00	**	≤ 0.01
Xanthine	Endogenous	1.00	N/S	≤ 0.05
Tryptamine	Endogenous	1.00	**	≤ 0.01
8-Bromocaffeine	Endogenous	1.00	N/S	> 0.05
Adenine	Endogenous	1.00	N/S	> 0.05
Uric acid	Endogenous	1.00	N/S	≤ 0.05
Nicotinamide	Endogenous	1.00	N/S	> 0.05
Adenosine	Endogenous	1.00	N/S	> 0.05
Diazole				
Imidazole	Endogenous	1.00	*	≤ 0.01
1-Methyl-L-histidine	Endogenous	1.00	N/S	> 0.05
1-Methylimidazole	Endogenous	1.00	N/S	> 0.05
<b>Phenols</b>				
Epigallocatechin gallate	Endogenous	0.02	***	≤ 0.001
Epicatechin gallate	Endogenous	0.025	***	≤ 0.001
§ Quercetin	Endogenous	0.05	***	≤ 0.001
Epicatechin	Endogenous	0.68	N/S	> 0.05
Catechol	Endogenous	0.68	N/S	> 0.05
Rutin	Endogenous	1.00	N/S	≤ 0.05
Methyl gallate	Endogenous	0.05	N/S	≤ 0.05
Gallic acid	Endogenous	0.05	N/S	≤ 0.05

<b>Amino acids</b>				
L-cysteine	Endogenous	1.00	***	≤ 0.001
D-norvaline	Endogenous	1.00	*	≤ 0.05
L-ornithine	Endogenous	1.00	N/s	≤ 0.05
D-ethionine	Endogenous	1.00	N/s	> 0.05
L-arginine	Endogenous	1.00	N/S	> 0.05
Pyrocatechol	Endogenous	1.00	N/S	> 0.05
Phenylalanine	Endogenous	1.00	N/S	> 0.05
L-alanine	Endogenous	1.00	N/S	> 0.05
D-serine	Endogenous	1.00	N/S	> 0.05
D-Iso-leucine	Endogenous	1.00	N/S	> 0.05
Cystic acid	Endogenous	1.00	N/S	> 0.05
<b>Vitamins</b>				
§Pyridoxine	Endogenous	1.00	**	≤ 0.01
§Thiamine (B1)	Endogenous	1.00	**	≤ 0.01
§Ascorbic Acid	Endogenous	1.00	N/S	> 0.05
§Vitamin B12	Endogenous	1.00	N/S	> 0.05
§Riboflavin (B2)	Endogenous	1.00	N/S	> 0.05
<b>Dietary Endogenous</b>				
Umbelliferone	Endogenous	1.00	***	≤ 0.001
Octopamine	Endogenous	1.00	**	≤ 0.01
GABA	Endogenous	1.00	N/S	> 0.05
§Trigonelline	Endogenous	1.00	N/S	> 0.05
Ethanolamine	Endogenous	1.00	N/S	> 0.05
<b>Non-dietary Xenobiotic</b>				
Benzyldiazine	Xenobiotic	0.004	***	≤ 0.001
4-amino-phenol	Xenobiotic	1.00	N/S	> 0.05
2 Chloromethyl benzimidazole	Xenobiotic	1.00	N/S	> 0.05
Sulphanilamide	Xenobiotic	1.00	N/S	> 0.05
4-acetoamidophenol	Xenobiotic	1.00	N/S	> 0.05
Tetrabenzine	Xenobiotic	1.00	N/S	> 0.05
Acrylamide	Xenobiotic	1.00	N/S	> 0.05

Note: § represents activity being monitored at 498 nm.

**Table 3.4.** Summary table of various inhibitors tested using the standard plate reader colourimetric assay at 498 nm, where IC<sub>50</sub> and K<sub>i</sub> values were obtained.

<b>Compound</b>	<b>Type</b>	<b>Concentration Range</b>	<b>IC<sub>50</sub> Value</b>	<b>Mode of Inhibition</b>	<b>K<sub>i</sub> Value</b>
Benzylhydrazine	Non-endogenous primary amine	0.5 – 25 nM	6.628 nM	non-competitive	N/A
Quercetin	Endogenous flavonoid	10 – 500 µM	52.2 µM	N/A	N/A
Theobromine	Xanthine	0.1 – 5 mM	427.9 µM	uncompetitive	275.6 µM
Octopamine	Endogenous trace amine	0.1 – 100 mM	3.26 mM	mixed mode	N/A
Thiamine	Endogenous dietary supplement (Vit-B <sub>1</sub> )	0.1 – 50 mM	5.046 mM	competitive	N/A
Pyridoxine	Endogenous dietary supplement (Vit-B <sub>6</sub> )	0.125 – 25 mM	5.55 mM	non-competitive	N/A

### **3.7 Summary**

In summary, the most significant findings were that theobromine and caffeine were the only methylxanthines to inhibit in the micromole range from the selection of methylxanthines and related compounds tested. Potential binding site and residue interactions were modelled with the aid of computational modelling software and showed a possible interaction at the base of the active site entrance funnel. Epigallocatechin gallate and epicatechin gallate could not be excluded as PrAO inhibitors but their assessment was complicated by non-enzymatic reactions that gave rise to ill-defined products.

A selection of amino acids, vitamins and xenobiotics were screened showing lysine and cysteine being the only significant inhibitors of PrAO. Other significant inhibition was observed with pyridoxine and thiamine, octopamine and quercetin along with the xenobiotic benzylhydrazine.

# **CHAPTER 4**

## *Discussion*

#### **4.0 General Introduction**

In Chapter 1 the important role played by PrAO in a wide range of diseases such as diabetes, cancer and vascular disease was described in depth. There are few proteins in the body that play a key role in such a wide range of disease processes. A large number of studies in animals have shown that inhibition of this enzyme has the ability to positively affect inflammation, cancer progression and vascular damage (Becchi *et al.*, 2017; Kinemuchi *et al.*, 2004a; Wang *et al.*, 2018). In the present study we explored the possibility that components present in the diet might influence PrAO activity. Therefore, we decided to look at bioactive compounds in plants that might have a protective effect on health through their inhibition of PrAO. Dietary methylxanthines and phytochemicals from green tea were the main focus of our efforts along with selected amino acids and vitamins.

The location of PrAO on the vascular endothelium (Hafezi-Moghadam, 2018) means it will come in contact with absorbed dietary compounds and their breakdown products as well as endogenous effectors and xenobiotics. This research focused on identifying molecules with known bioactive properties that could modulate PrAO activity.

#### **4.1 Methylxanthines in PrAO Inhibition**

Previous work in this laboratory, in collaboration with a group in Trinity College Dublin, showed caffeine to be a modulator of bovine PrAO although not a potent inhibitor with a  $K_i$  of 1.0mM (Olivieri and Tipton, 2011). This work was followed up by a laboratory in China who looked at the effect of caffeine consumption on PrAO activity *in vivo* using a rat model. They showed that caffeine could reduce PrAO activity *in vivo* and suggested that caffeine might be useful as a therapeutic for

lowering PrAO activity. This finding prompted us to explore the possibility that other, structurally related, methylxanthines might inhibit PrAO. Caffeine is one of several methylxanthines present in the diet and it is metabolized to a range of metabolites whose action against PrAO had not been explored. Caffeine analogs that were examined in this study were theophylline, theobromine, 7 methylxanthine and paraxanthine as well as a variety of related compounds that represented components of those structures. The objective was to attempt to identify structural features required for inhibition of PrAO.

Methylxanthines structurally contain two coupled rings: a pyrimidinedione ring and an imidazole ring (Zacharis *et al.*, 2013).

Theophylline (1,3-dimethylxanthine; Fig. 3.34) is a metabolite of caffeine (1,3,7-trimethylxanthine; Santos *et al.*, 2015) and is found in cocoa and tea (Martínez-López *et al.*, 2014). Theophylline has been used as a therapeutic for asthma, acting as a bronchodilator (Cosío *et al.*, 2016) and is used in the treatment of respiratory diseases such as chronic obstructive pulmonary disease (Kirkham *et al.*, 2014). This compound inhibited PrAO by approximately 20%, at 1.0 mM compared to caffeine which inhibited PrAO by *ca.* 60% at the same concentration (see Fig. 3.35).

Since theophylline and caffeine differ only by a single methyl group at position 7 on the imidazole ring it was clear that methylation at this point was important for inhibition and that the diazole moiety of xanthine could play a role in PrAO inhibition. We examined a number of diazoles (imidazole, 1-methyl-L-histidine and 1-methylimidazole; see Fig. 3.39) at a 1.0 mM concentration and they showed little or no inhibition of PrAO (Fig. 3.38). These observations indicated that the entire xanthine



molecule was required for inhibition with the position and number of methyl groups playing an important role.

The methylxanthines; 7-methylxanthine, theobromine, and paraxanthine (Fig 3.34) along with xanthine nucleus (Fig. 3.37) were examined for inhibition of PrAO (see below Fig. 4.1). Of these, it was found that theobromine inhibited PrAO activity to approximately 30% at 1 mM. The theobromine data showed that N-methyl groups were critical for inhibition (see Fig. 3.35 and Fig. 3.36). It was clear that a methylxanthine with N-methylation at positions 3 and 7 was required for significant inhibition of PrAO. The presence of a methyl group in position 1, as in caffeine, seemed to decrease the inhibitory effect presumably for reasons of steric hindrance.

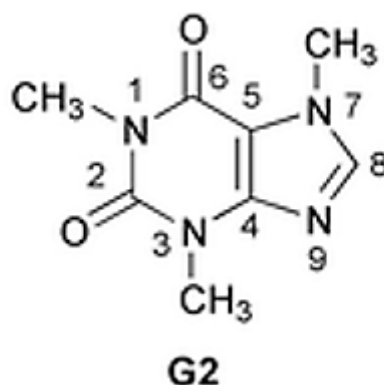


**Fig. 4.1.** Caffeine structure showing the N-methyl groups numbered around the xanthine nucleus.

Theobromine showed an  $IC_{50}$  value of  $427.9 \mu\text{M} \pm 100 \mu\text{M}$  (Fig. 3.40) and a  $K_i$  of  $276 \mu\text{M} \pm 32 \mu\text{M}$  (Fig. 3.41). Thus, it was clear that Theobromine was a more potent inhibitor than caffeine with a reported  $IC_{50}$  value of  $800 \mu\text{M} \pm 300 \mu\text{M}$  and a  $K_i$  value of 1.0 mM. Of the methylxanthines we examined, theobromine was the only one more potent than caffeine for PrAO inhibition. This is of particular interest since

theobromine, as well as being present in high amounts in dark chocolate among other sources, is a metabolite of caffeine (See Fig. 4.2).

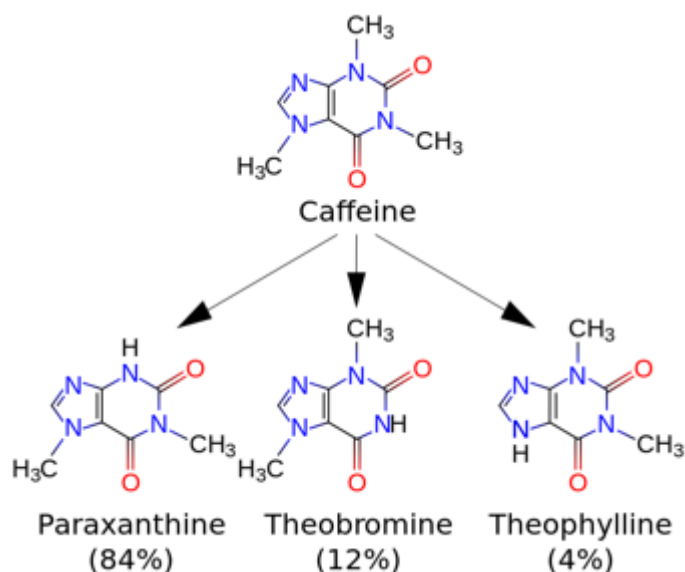


**Fig. 4.2.** The metabolites of caffeine *in vivo* are shown. These metabolites are generated by removal of a methyl group from caffeine.

Since theobromine was the most potent methylxanthine found to date associated with PrAO inhibition we looked at the pattern of inhibition by measuring the  $K_m$  for benzylamine in the presence of increasing concentrations of theobromine. A noncompetitive pattern was observed (Fig. 3.41). This pattern consists of a series of lines all intersecting on the horizontal axis. Such a pattern shows that the  $K_m$  for the substrate benzylamine was not changed by the presence of the inhibitor but  $V_{max}$  was altered. This type of inhibition is interpreted as indicating that the presence of the inhibitor does not influence the binding of substrate but does influence the catalytic rate (Fig. 4.3).

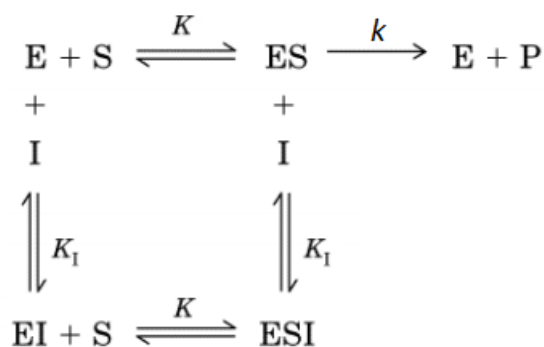


**Fig. 4.3.** Mechanism of noncompetitive Inhibition. The Enzyme (E) can bind substrate (S) to form an ES complex which, after catalysis, releases product (P). The scheme also shows that inhibitor (I) can bind to *both* the enzyme (E) and the ES complex. Thus, the binding of substrate does not prevent the binding of inhibitor (their binding sites do not overlap). Such a mechanism will give rise to a pattern of lines intersecting on the horizontal axis.

A similar inhibition pattern was observed for caffeine with benzylamine as substrate (Olivieri and Tipton, 2011). Therefore, this inhibition pattern clearly shows there is a site on the surface of PrAO that can interact with both of the methylated nitrogen moieties of theobromine and caffeine.

In humans the plasma concentration of theobromine has been reported to be as high as 63  $\mu\text{M}$  following the consumption of chocolate (Oñatibia-Astibia *et al.*, 2017). Taking the  $K_i$  as 276  $\mu\text{M}$  we can calculate the effect on PrAO of levels of theobromine as high as 63  $\mu\text{M}$  using the relationship between  $K_i$  and inhibitor concentration for a noncompetitive inhibitor given by equation 1:

$$V_{max\ app} = \frac{V_{max}}{1 + \frac{I}{K_i}}$$

**Equation 1.** Noncompetitive inhibition: The relationship between maximum velocity ( $V_{max\ app}$ , - the apparent maximum velocity) in the presence of an inhibitor (I) and the maximum velocity in the absence of an inhibitor ( $V_{max}$ ). The term  $K_i$  refers to the inhibitor binding constant.

Using a figure of 63  $\mu\text{M}$  for [I] and 276  $\mu\text{M}$  for  $K_i$  we can calculate that the maximum rate in the presence of this concentration of inhibitor is reduced by approximately 20%. This suggests that a plasma concentration of theobromine of 63  $\mu\text{M}$  could reach levels *in vivo* sufficient to inhibit PrAO by roughly 20%, which may be sufficient to influence associated diseases (see chapter 1, section 1.6 and 1.7).

The finding that Theobromine and caffeine bind at a site other than the active site on PrAO was particularly interesting. This meant that there was a site that could influence activity that was separate to the active site. This had not been reported before. These studies showed that the N-methylation at positions 3 and 7 were important for inhibition.

Interestingly, imidazoline binding sites for PrAO have been described through X-ray crystallography of two bound molecules: clonidine (Holt *et al.*, 2008) and imidazole (Elovaara *et al.*, 2011). Clonidine an inhibitor of bovine PrAO, is shown to undergo pi-stacking with the aromatic rings of TPQ and Tyr472 forcing TPQ into an inactive “on state” bound to the copper atom in the active site whereby the deamination of primary amines cannot occur (Holt *et al.*, 2008b). It seems unlikely that the N-methyl groups described here would interact in the same manner but cannot be fully excluded. In another study it was found that imidazole could form hydrogen bonds to TPQ in the inactive on-state conformation (see Fig. 1.6). A second imidazoline binding location was also identified in the substrate channel where imidazole bound to Tyr394 and Thr212 (Elovaara *et al.*, 2011). It is possible that this site might be involved in theobromine binding but the interaction with imidazole was much weaker than that for

theobromine. Additionally, computational modeling of theobromine binding to PrAO in this study did not indicate any involvement in binding (see Section 4.2).

None of the other related caffeine-related compounds tested showed significant inhibition (Chapter 3, Fig. 3.36). For example, neither 8-bromocaffeine, nor Uric Acid could significantly inhibit PrAO, despite structural similarity to xanthine (one more carboxyl group on the imidazole ring). Closely related purine molecules adenine and adenosine were also examined since they have similar structures to caffeine except for having no amides in the ring structures: these also resulted in no significant inhibition of PrAO. These findings all indicate that the xanthine structure alone cannot be the main cause of PrAO inhibition. Inhibition requires specific methyl groups at specific locations around the structure to have maximum inhibitory effect.

#### 4.1.2. PrAO inhibition by Lisofylline

Lisofylline is a methylxanthine-derived small molecule with anti-inflammatory properties that may be useful in treatment of type 1 diabetes (Fig. 4.4).

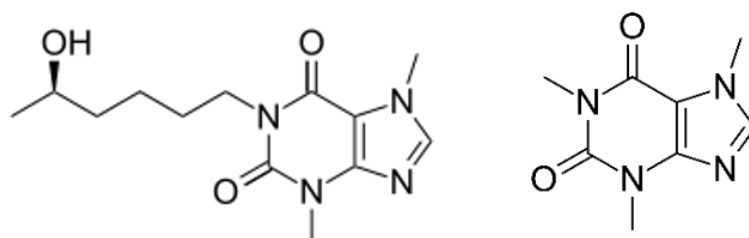


**Fig. 4.4.** The structure of lisofylline (left) compared to caffeine (right). Lisofylline is similar to caffeine but where caffeine has a methyl group (CH<sub>3</sub>) at position 1 lisofylline has a bulky hydroxyhexyl group.

The exact mechanism of action of lisofylline is not known. Given its structural similarity to caffeine it seemed likely that it might inhibit PrAO. We reasoned that if

it were a PrAO inhibitor it would provide a link between this drug and a molecular target. At a concentration of 1 mM, Lisofylline yielded significant inhibition (25%, Fig. 3.42). However, it was a poorer inhibitor than caffeine. We can conclude that the increased bulk at position 1 is leading to this loss in potency. Thus, theobromine with no substituent at position 1 is a better inhibitor than caffeine which has a methyl group at position 1. Lisofylline, with an even larger substituent at position 1, is even poorer than caffeine as a PrAO inhibitor. Thus, it is unlikely that the mechanism of action of this drug *in vivo* involves modulation of PrAO activity.

#### **4.2 Computational Docking of Methylxanthines to PrAO**

In an attempt to get a better understanding of the site of interaction between PrAO and inhibitors we constructed an *in silico* model of PrAO and looked at molecular docking of methylxanthines onto the enzyme. The software output ranks candidate dockings assigning a docking score to each binding mode.

The computational docking findings for caffeine, theobromine and theophylline all produced a rank-1 binding docking score for these compounds to a site at the base of the PrAO active site entrance funnel. Docking poses are computed for the most energy efficient binding per docking pose interaction as explained in chapter 2, section 2.9. The more negative the docking score the more efficient binding is predicted for that particular docking location.

#### **4.2.1 Computational Docking Interactions with Theobromine, Caffeine and Theophylline**

Theobromine had a rank 1 docking score of -2.59 ( $\Delta G_{\text{bind}}$ ). Hydrogen bonding is predicted between the carbonyl group of theobromine the heterocyclic aromatic amine of Asn469 on PrAO (Fig. 3.45). Hydrophobic interactions are predicted between Tyr238, Leu468 and Pro237. Caffeine had a rank 1 docking score of -2.30 ( $\Delta G_{\text{bind}}$ ) and is similarly involved in a hydrogen bond formation with amide group of Asn469 (Fig. 3.47). Hydrophobic interactions were predicted between Leu468 and Pro237.

Theophylline, which also bound near the active site, had the most energetically favourable docking score of -2.75 ( $\Delta G_{\text{bind}}$ ). Hydrogen bonding was predicted between the heterocyclic aromatic amine of theophylline and the carbonyl group of the side chain residue Leu468 (Fig. 3.49). Table 3.2 highlights the important residues involved in hydrogen binding with methylxanthines, Asn469 and Leu468, while for hydrophobic interactions residues Pro237 and Leu468 are prominent along with Tyr238.

#### **4.2.2 Computational modelling of PrAO Inhibition by Theobromine, Caffeine and Theophylline**

*In vitro* assays had shown that caffeine and theobromine inhibited PrAO, while theophylline had little or no inhibition. Common hydrogen binding patterns predicted for the two most significant methylxanthines (caffeine and theobromine) showed an interaction with Asn469 and with both carbonyl groups of these methylxanthines in the same position, showing the importance of this group in hydrogen bonding interactions with Asn469 of PrAO. Asn469 is located internally in the active site, but is also part of the external wall structure.

Asn469 has significance in bovine PrAO catalysis where it is required to rotate away from the internal pocket and face the mouth of the entrance channel to permit substrate docking (Holt *et al.*, 2008b). The binding of caffeine and theobromine to Asn469 may hinder this rotation, preventing substrate from interacting with the TPQ co-factor.

Leu468 is understood to act like a gate-controlling side chain as discussed in chapter 1, section 1.3.1. It is located at the active site entrance and therefore has a significant effect on substrate access. From the computational modelling data for theophylline, it is possible that binding to Leu468 may keep the side chain in the open position and therefore not interfere with substrate access or catalysis in the active site.

Theobromine has greater hydrophobicity than caffeine (see Section 1.8.1); theobromine displays a 0.5mg/mL solubility concentration in H<sub>2</sub>O (<https://pubchem.ncbi.nlm.nih.gov/compound.ncbi.nlm.nih.gov/compound/2519#section=Melting-Point>), which could indicate that theobromine might preferentially bind in the hydrophobic pocket at the base of the PrAO active site funnel. Docking studies for theobromine and caffeine (Fig. 3.44 and 3.46) show that these ligands are bound near the active site entrance in a predominantly hydrophobic pocket. Hydrophobic interactions for both caffeine and theobromine in this pocket are reported to be with Tyr238, Leu468 and Pro237 (See Table 3.2). These interactions may account for the greater affinity and potency observed in the docking score for these compounds and help to explain the experimental findings for theobromine inhibition compared to caffeine.



### 4.2.3 Methylxanthines Summary

We have shown for the first time that theobromine is an inhibitor of PrAO. It is more effective than caffeine. Comparing the structures of compounds that significantly inhibited PrAO against those that did not, we were able to identify N-methylation at positions 3 and 7 of the xanthine nucleus as necessary for inhibition. We further showed that the presence of bulky substituents at position 1 caused inhibition to decrease. Both caffeine and theobromine were found to inhibit PrAO significantly in the micromole range: computational docking predicted the importance of positions 3 and 7 containing methyl groups thereby allowing the carbonyl group contained between these positions to be involved in hydrogen bonding to Asn469.

Theophylline with methyl groups at positions 1 and 3, hydrogen bonding occurred with the free amine at position 7 and with the amino group of the PrAO residue Leu468. This then leads to the hypothesis that it is crucial for positions 3 and 7 on the xanthine structure to have methyl or possibly other functional groups to have a notable inhibitory effect on PrAO.

### 4.3 Inhibition of PrAO by polyphenols

Polyphenols have shown great potential in treating diseases such as cancer, diabetes, inflammation and obesity (Chen *et al.*, 2011; Chacko *et al.*, 2010; Wang *et al.*, 2014). Our interest in screening polyphenols as potential inhibitors of PrAO was underpinned by reported health benefits for these compounds especially the correlation noted between the health benefits of dietary polyphenols and PrAO-associated disease. Many of the diseases correlated with abnormal PrAO activity such as cancer, diabetes, inflammation, heart disease, Parkinson's disease and obesity (Chacko *et al.*, 2010;

Hara, 2001; Schneider and Segre, 2009; Sinija and Mishra, 2008) are also targets of polyphenols.

#### **4.3.1 Green Tea**

A crude extract of undiluted green tea was initially assayed to explore any modulatory effects that green tea might have on PrAO activity. In our initial trial experiments green tea extract resulted in a large *increase* in PrAO activity rates. When the extract was diluted 1:100 instead of a leveling of rates compared to the control, which would have been expected, inhibition of PrAO was evident (Fig. 3.7). Inhibition at low concentrations of an inhibitor followed by activation at high concentrations was an obviously anomalous finding. There is no simple mechanism whereby binding at a single site on an enzyme can give rise to inhibition at low concentrations and activation at high concentrations.

One possibility was that individual components of the Green tea extracts might have competing effects. We initially looked at amines in green tea. Green tea contains GABA (gamma-aminobutyric acid) with a dry weight content in leaves of approx. 50µg/g (Syu *et al.*, 2008). GABA was a possible modulator of PrAO as discussed in chapter 1, section 1.5 and 1.7. In plants, GABA plays a metabolic role and in mammals acts as a potent neurotransmitter (Anju *et al.*, 2014). This small molecule has the potential to be either a substrate for PrAO which could potentially have been the cause of the increase in rates or an inhibitor. However, GABA showed no effect on PrAO activity when tested to a concentration exceeding the possible dry weight content found in green tea (see Table 3.3).

Other prominent bioactive compounds in Green tea are the green tea polyphenols. Although they lacked an amine group there was a possibility that they might react with PrAO bound copper. Epicatechin (EC), epicatechin gallate (ECG) and epigallocatechin gallate (EGCG), (Fig 3.6) were all tested due to their reported health benefits (see Section 1.8). When screened against PrAO, the three catechins mimicked the findings originally found with green tea extracts (i.e. an increase in rates with higher concentrations with inhibition being observed at lower concentrations, especially with EGCG and ECG, suggesting further study was appropriate.

These findings were unusual since they were carried out using pure compounds and therefore could not be due to competing components in green tea extracts. In an attempt to further understand the observations, we used a UV spectrophotometric assay (see section 2.5) to monitor PrAO inhibition. This assay directly monitored benzaldehyde production at 254 nm. The results generated from monitoring benzaldehyde using the spectrophotometric assay showed inhibition for EGCG (Fig. 3.9) and ECG (Fig. 3.10), but not for epicatechin (Fig. 3.8).

This finding suggested that epicatechin was somehow acting as an inhibitor in the coupled Holt assay method but not when the catalysis was monitored using the direct spectrophotometric assay monitoring benzaldehyde production. Furthermore, the concentrations of EGCG and ECG required for observable inhibition were also greater when monitoring rates using the direct spectrophotometric method indicating systematic interference with the Holt colorimetric method.

Further investigation of the Holt method of PrAO inhibition monitoring resulted in clear interference by green tea catechins resulting in false inhibition of rates through H<sub>2</sub>O<sub>2</sub> sequestering. This affected all findings with catechins when monitoring PrAO activity relying on H<sub>2</sub>O<sub>2</sub> production, namely the Holt colorimetric method. This observation was confirmed by adding a low concentration of H<sub>2</sub>O<sub>2</sub> to the colorimetric dye solution, whereupon formation of the pink quinoneimine dye was not observed compared to a control equivalent.

Similar H<sub>2</sub>O<sub>2</sub> scavenging was noted with the Holt assay method by Fernando and Soya's lab (Fernando and Soysa, 2015) when testing other phenolic compounds extracted from plants as noted in chapter 1, section 1.8. Once catechin H<sub>2</sub>O<sub>2</sub> sequestering was confirmed all inhibition characterization was carried out using the direct spectrophotometric assay. Epicatechin was shown to not inhibit PrAO when assayed using the direct spectrophotometric method. The same observation was found for EGCG and ECG (except requiring higher concentrations of both compounds); these being an increase in rates at high concentrations of EGCG and ECG and at lower concentrations an inhibition effect was noted. It was noted that control experiments with both catechins and substrate without enzyme present was producing an apparent rate using the Holt *and* direct spectrophotometric method but it was unclear what metabolite was being formed. These confusing results required the need for a further change in assay method to fully elucidate what was occurring.

#### **4.3.2 HPLC Method Development**

In order to fully elucidate what the anomalous inhibition/activation profile was due to an HPLC method was developed to separate products and separately monitor

benzaldehyde production. For this method to work effectively a suitable mobile phase, separating column and flow rates were devised. A standard curve of pure benzaldehyde was prepared (Fig. 3.4). Enzyme assay times were increased from an average of 15min to 3hrs so as the production of benzaldehyde by the enzyme would fall within the standard curve range for accurate activity monitoring of PrAO. A control assay was performed to show that benzaldehyde production by PrAO was linear over this time period (Fig. 3.5).

### **4.3.3 Deamination of Benzylamine by Catechins**

It was found, with the aid of the HPLC method, that an increase in peak area for benzaldehyde production at higher EGCG or ECG concentrations was observed (see Fig. 3.11 and 3.12). At lower concentrations an inhibition effect was evident matching the results obtained with the spectrophotometric assay at 254 nm (see Fig. 3.9 and 3.10).

When the HPLC assay was run in the absence of PrAO benzaldehyde formation was *still* observed at high concentrations of EGCG and ECG. This non-enzymatic formation of benzaldehyde clearly accounted for the observed activation seen at high concentrations of EGCG and ECG (see Fig. 3.9 and 3.10). This type of non-enzymatic reaction between benzylamine and catechins was a complicating factor in measuring inhibition of PrAO by catechins.

A search of the literature revealed that Akagawa and co-workers (2005) had previously described this type of non-enzymatic reaction between polyphenols and benzylamine to produce benzaldehyde. They briefly mentioned the possibility that PrAO inhibition

testing could be compromised by catechin deamination when benzylamine was a substrate.

It was clear that the confusing activation/inhibition profile we had observed was due to a mixture of factors: firstly, there was a reaction between some catechins and the components of the colorimetric assay. More significantly there was a non-enzymatic reaction between catechins and benzylamine producing benzaldehyde. This latter reaction was more pronounced at high concentrations of catechins and was almost absent at low concentrations. This clearly interfered with the assay methodology in a manner that gave the impression of higher activity at high concentrations.

#### **4.3.4 Subtraction of the non-enzymatic Deamination Reaction by Catechins**

In this experiment, benzylamine and inhibitor (EGCG and ECG) were left to deaminate in the absence of enzyme. A parallel experiment was run using identical concentrations of benzylamine and catechin but including PrAO. Benzaldehyde formation in the non-enzymatic reaction was subtracted from that of the reaction in the presence of enzyme (see Fig. 3.11 and 3.12). Once the background deamination reaction was removed inhibition of PrAO was evident (see Fig. 3.11 and 3.12).

When comparing EGCG and ECGs ability to deaminate benzylamine, EGCG is approximately 4 times more efficient than ECG yet has similar potency of inhibition when the deamination reaction is subtracted. This would suggest that the deamination reaction neither causes nor contributes to PrAO inhibition and provides further evidence that EGCG and ECG are directly inhibiting PrAO.

Finally, we found that another polyphenol, caffeic acid, produced a deamination reaction with the substrate benzylamine. However, subtraction of the non-enzymatic rate showed no inhibition of PrAO for this polyphenol (Fig. 3.15).

While inhibition is difficult to assess when competing reactions are being examined our findings indicate that the possibility that catechins directly inhibit PrAO cannot be ruled out.

#### **4.3.5 PrAO Substrates that may deaminate**

A range of PrAO substrates were tested to explore whether the same deamination reaction would occur. Methylamine, spermine and spermidine, all known PrAO substrates (see Section 1.5) were screened. Screening was unsuccessful due to these compounds either absorbing strongly in the 254 nm region or the inability to detect product being formed, leaving only H<sub>2</sub>O<sub>2</sub> to monitor which would be affected by reacting with catechin giving rise to assay interference.

#### **4.3.6 Gallated Polyphenol Inhibition of PrAO**

Since EGCG and ECG inhibited PrAO and epicatechin did not it was hypothesized that the gallate moiety of the compound might be responsible for the inhibition observed. In order to explore this in more detail other gallate like molecules were screened such as; gallic acid, methyl gallate and a related, non-phenolic trigonelline. None of these compounds were found to inhibit (see Table 3.3) indicating the whole molecule to be necessary to have an inhibitory effect.

Gallated polyphenols have been shown to interact with and modulate a series of enzymes most probably through hydrogen bonding to the many phenolic groups

present allowing for interaction with varying hydrogen bond accepting and negatively charged amino acid side chains. Other studies add weight to this hypothesis like that of Sánchez-del-Campo and co-workers (2009) who examined how human dihydrofolate reductase (DHFR) was inhibited by EGCG and ECG but interestingly not by other non-gallated catechins. The binding of ECG and EGCG were proposed to be due to the 7 or 8 phenolic groups present and their ability to act as hydrogen bond donors (Sánchez-del-Campo *et al.*, 2009).

A study by Hara and Honda (1990) showed that  $\alpha$ -amylase was non-competitively inhibited by gallated catechins and less so by the non-gallated type as indicated by  $ID_{50}$  measurements: ECG 130 $\mu$ M, EGCG 260 $\mu$ M, other non-gallated catechins and Gallic Acid were above 1000 $\mu$ M. Additional inhibiting molecules included theaflavin, theaflavin mono-gallates and theaflavin di-gallate (Hara and Honda, 1990). Such findings align with observations in this study: the two catechin gallates of EGCG and ECG inhibit in the mid to low micro-molar range, while the non-gallate epicatechin displays little or no effect.

#### **4.4 Molecular docking of Selected Catechins with PrAO.**

##### **4.4.1 Residue Binding Interactions and Location of ECG, EGCG and Epicatechin on PrAO**

In this study, and for the first time, ECG, EGCG and epicatechin were all computationally screened to explore potential binding sites and binding interactions with PrAO. ECG had a top rank docking score of -5.76 ( $\Delta G_{\text{bind}}$ ). The predicted hydrogen bonding interactions occur with the gallate phenol group of ECG binding to the primary amine of the PrAO residue Asn231 and between other ECG phenol groups



and the PrAO primary amine of Asn469 as well as the hydroxyl group of the side chain Thr466. Hydrophobic contacts were indicated with side chains Leu468 and Pro237. Binding of ECG is shown to be externally at the base of the wide funnel near the active site where it completely blocks the active site entrance indicating steric inhibition (Fig. 3.17).

EGCG with a predicted docking score of -6.91 ( $\Delta G_{\text{bind}}$ ) had the most energetically favorable binding of all three catechins tested. Hydrogen bonding is represented via the phenol group of the gallate moiety of EGCG binding to the hydroxyl group of the PrAO side chain residue Thr466 and also the EGCG ester group to the PrAO hydroxyl group of side chain Tyr238. Hydrophobic contact was predicted with the side chain Pro237. EGCG is externally bound at the base of the funnel and partially blocks the active site entrance, indicating steric inhibition as evidenced with ECG (Fig. 3.19).

Epicatechin had a predicted docking score of -5.30 ( $\Delta G_{\text{bind}}$ ) when bound to PrAO. Ionic charged interactions were shown for both side chains Thr466 and Tyr238 via the phenol groups of epicatechin. Hydrophobic contact is with Pro237. The binding of epicatechin is shown externally at the base of the funnel but is seen not to block the active site entrance (Fig. 3.21).

As can be seen from the findings, residue side chains involved in ionic type bindings were Asn231, Asn469 Thr466 and Tyr238 while notable non-charged interactions were predicted with Pro237 and Leu468. These findings indicate that compounds with phenol group arrangements around their structure as with green tea catechins or, as shown by Hara and Honda's research, other phenolic compounds such as theaflavin,

theaflavin mono-gallates and theaflavin di-gallate (Hara and Honda, 1990) may have an improved inhibition of PrAO.

#### **4.4.2 Comparison of Computational Docking Results and Experimental Results**

The computational results for ECG, EGCG and Epicatechin correlate with the experimental inhibition screening of PrAO with the catechins examined in this study. Both EGCG and ECG inhibited PrAO in the low micromolar range while epicatechin did not. In the modeled binding of ECG and EGCG the gallates were involved in hydrogen bond interactions with PrAO with EGCG showing the ester group also being involved.

A similar study by Glisan and colleagues (2014) examined tea polyphenols ability to inhibit digestive enzymes such as pancreatic lipase. EGCG non-competitively inhibited this enzyme in the micromolar range where computational modelling studies predicted that EGCG interacted with residues around the active site and therefore, hindered substrate access and binding (Glisan *et al.*, 2014). Furthermore, the phenol groups attached to the catechins are primarily responsible for ionic binding interactions of catechins (Fig. 3.17 and 3.19). Although patterns of inhibition could not be reliably carried out in the present study due to the deamination reaction between catechins and the substrate benzylamine a competitive inhibition pattern is the most likely based on the computational models presented here.

#### **4.5 Octopamine Inhibition of PrAO**

Octopamine (Fig. 3.24) showed an  $IC_{50}$  value of  $3.26 \text{ mM} \pm 0.8 \text{ mM}$  when assayed using benzylamine as substrate. A double reciprocal plot inhibition pattern showed a

mixed inhibition pattern (Fig. 3.27). Physiological concentrations of octopamine in blood plasma of humans were found to be in the range of 0.0026 +/- 0.0014  $\mu$ M (Yonekura *et al.*, 1988), indicating that this compound to have little physiological effect. In the literature there is conflict as to whether octopamine is an inhibitor or substrate. In one study octopamine is reported to act as an inhibitor and in others (Castillo *et al.*, 1998; Visentin *et al.*, 2001) to act as a weak substrate. To test whether octopamine was a substrate or an inhibitor it was added to an assay mixture at a concentration of 50  $\mu$ M. The reaction was monitored for 15 minutes using the Holt colorimetric assay method at 498 nm for evidence of catalysis and production of H<sub>2</sub>O<sub>2</sub>. No rate was observed, leading to the conclusion that octopamine is not a substrate for bovine PrAO but an inhibitor.

To further investigate octopamine inhibition similar structures of 4-aminophenol and 4-acetoamidophenol were examined for inhibition of PrAO. 4-aminophenol is the first hydrolytic product of the breakdown of the mild analgesic 4-acetoamidophenol (Fan *et al.*, 2011) and is different to octopamine in having one less carbon and hydroxyl group. Conversely, 4-acetoamidophenol (paracetamol) differs from 4-aminophenol by an addition of an acid group attached to the nitrogen forming an amide bond. Neither of these two compounds showed any inhibition of PrAO suggesting that the distance of the primary amine from the main phenol structure is key to enzyme modulation.

#### **4.5.1 Inhibition of PrAO by Quercetin**

Quercetin (Fig. 3.28) is a flavonoid that is ubiquitous in foods ranging from plants and vegetables to teas and wines. It is an antioxidant that is thought to protect against various diseases including cancer, diabetes, lung and heart disease (Boots *et al.*, 2008).

Flavonoids, in general, are known to have strong antioxidant properties mainly due to their aromatic hydroxyls groups and can scavenge reactive oxygen and nitrogen species (Li *et al.*, 2007). Quercetin consists of two polyphenol rings linked by a pyranose ring structure (Day and Williamson, 2001). In this study, quercetin gave an  $IC_{50}$  of  $52.20 \mu\text{M} \pm 33.75 \mu\text{M}$ .

Previous studies (Lee *et al.*, 2002) have shown moderate PrAO inhibition by quercetin through a using zymogram staining. As part of the current study, Rutin, a glycoside of quercetin was also tested at 1 mM and 0.5 mM concentration and showed no significant inhibition.

#### **4.5.2 Additional Phenolic Compounds Screened for PrAO Inhibition.**

Other phenolic compounds examined were tetrabenzine and umbelliferone. Tetrabenzine is a xenobiotic drug used to treat a variety of hyperkinetic movement disorders by reversibly binding to the type 2 vesicular monoamine transporter tetrabenzine as an antichorea therapy in Huntington disease. This drug showed no effect on PrAO.

#### **4.6 Amino Acids**

Amino acids were of interest in this study due to being found in the diet and having primary amino groups (chapter 1, section 1.5 and 1.7). This would suggest that these compounds could be potential substrates or inhibitors of PrAO. In this study, eleven amino acids were tested at concentrations of 1 mM and 100  $\mu\text{M}$ . Only two of these eleven amino acids gave significant inhibition at 1 mM concentrations, L-cysteine and D-norvaline.

#### 4.6.1 L-lysine inhibition of PrAO and Testing of Similar Amino Acids

Previously L-lysine was reported as an uncompetitive inhibitor of bovine PrAO in the presence of H<sub>2</sub>O<sub>2</sub> with a K<sub>i</sub> value of 103 ± 14 μM with benzylamine as the substrate (Olivieri *et al.*, 2010). Ornithine and Arginine showed no inhibition of PrAO (Fig. 3.54 and 3.56).

#### 4.6.2 Cysteine inhibition of PrAO and Testing of Similar Amino Acids

Cysteine, a short chain amino acid with a thiol group showed a significant inhibitory effect ( $P \leq 0.01$ ). Cysteine is a low abundance amino acid that is highly reactive, polarizable and redox-active (Marino and Gladyshev, 2012) At a 1 mM concentration L-cysteine gave an inhibition of approximately 50% (Fig. 3.52). Cysteine contains a thiol group, which becomes reactive at neutral pH; the thiol group reacts with metals such as copper (Kim *et al.*, 2014) and may directly interact with PrAO's copper atom in the active site. Human blood plasma concentration of cysteine reported is 197.00 (+/- 56.00 μM; Pastore *et al.*, 1998), and based on the results of this study suggests that cysteine at the typical blood plasma concentration may have an effect on PrAO activity. To test if the thiol groups were significant in the inhibition of PrAO, the structurally similar amino acid, ethionine, was examined. This showed no inhibitory effect, indicating that thiol groups alone were not important (Fig. 3.55).

Alanine, having a methyl group side chain showed no inhibition. Longer chained amino acids, namely Iso-leucine and norvaline, were examined as they have one more carbon on the side chain compared to cysteine, with methyl groups attached. Iso-leucine being the same as norvaline except for an additional methyl group branching off, showed no inhibition, but norvaline displayed an approximate 12% inhibition (Fig. 3.53).

Phenylalanine showed no effect on PrAO. Serine and Threonine showed no effect on PrAO.

#### **4.7 Modulation of PrAO by selected Vitamins**

Vitamins which are naturally found in the diet and important for human health were examined for PrAO inhibition.

##### **4.7.1 Pyridoxine Inhibition of PrAO**

Pyridoxine inhibited PrAO un-competitively with an  $IC_{50}$  result of  $5.55 \text{ mM} \pm 2.81 \text{ mM}$ . Physiological concentrations of Pyridoxine found in human blood plasma were reported as  $0.025 \text{ }\mu\text{M}$  (Gori *et al.*, 2006) which may not be sufficient to have any significant physiological effect given the  $IC_{50}$  result found in this study. Interestingly, studies carried out with rabbit lung and heart membrane bound PrAO found that another form of the vitamin B complex pyridoxamine inhibited these forms of PrAO.

##### **4.7.2 Inhibition of PrAO by Thiamine (Vitamin B1)**

Thiamine (Vitamin B1) was an inhibitor of PrAO with an  $IC_{50}$  value of  $5.046 \text{ mM} \pm 1.15 \text{ mM}$ . Physiological concentrations found in blood plasma can be as high as  $0.12 \text{ }\mu\text{M}$  (Hung *et al.*, 2001). The fact that a competitive inhibition was observed indicated that this molecule binds in the active site competing with substrate binding. Interaction could be via the positive charge on the imidazole ring structure binding to the negative charge of TPQ, while the amine group on the pyrimidine ring could possibly hydrogen bond to nearby polar residues Asn469 or Tyr383.

### 4.7.3 Other Vitamins Assayed

Vitamin B12 and riboflavin (B2) were tested. Vitamin B12 was of interest based on the six primary amines attached to its structure, therefore qualifying to be a potential modulator of PrAO. Another B vitamin of interest was riboflavin (B2), due to the hydroxyl and amine groups present. However, both showed no significant inhibitory effect on PrAO (see Table 3.3).

## 4.8 A Selection of Non-Dietary Compounds Chosen for the Testing of PrAO Inhibition

### 4.8.1 Inhibition of PrAO by Benzylhydrazine

Benzylhydrazine IC<sub>50</sub> results were 6.628 nM ±3.2nM (Fig. 3.67). Lineweaver Burk plot results showed an un-competitive inhibition pattern. Studies with another species of PrAO *Arthrobacter globiformis*, showed benzylhydrazine to be covalently bonded in the active site. Findings showed a covalent bond forming a Schiff base to the C5 atom of the TPQ quinone ring whereby the reaction product is stabilized and prevented from releasing an aldehyde in the first reduced steps of the ping-pong reaction mechanism (Langley *et al.*, 2008). Small molecule phenyl-hydrazine type structures have generally been shown to bind either reversibly or irreversibly to the active site of amine oxidases (see section 1.7). Phenelzine, a known PrAO and MAO-A inhibitor (Wang *et al.*, 2006) (see chapter 1 section 1.1), is structurally similar to benzylhydrazine and was shown to be a reversible inhibitor in bovine PrAO from lung tissue (Lizcano *et al.*, 1996). Studies with similar hydrazine inhibitors have shown effects arising from additions to the molecule. For example, it was noted that any addition to the phenyl ring structure, such as a fluorine atom can effect selectivity between MAOs and PrAO (Wang *et al.*, 2006).

#### **4.8.2 Testing of Sulphanilamide for PrAO Inhibition**

Sulphanilamides have been extensively used as a bactericidal compound (Venkatesh *et al.*, 2013). This molecule having a primary amine and sulphanomide group was of particular interest in this study due to its similarity to known PrAO inhibitors.

#### **4.8.3 Testing of Acrylamide for PrAO Inhibition**

Acrylamide is a neurotoxic carcinogen that is gaining interest since it is produced by the Maillard reaction from cooking carbohydrate rich foods at high heat (Basiri *et al.*, 2016) and is therefore naturally found in the diet. This molecule was chosen as it is a small molecule with a primary amine attached and is readily found in the diet, but upon testing had no effect (see Table 3.3).

#### **4.9 Conclusion/Future work**

Key results from this study highlight the key modulating roles that theobromine and caffeine can have on PrAO. It would be of interest to examine a wider range of methylxanthines with substituents at other positions for their effect on PrAO. Moreover, there are a range of other bioactive compounds present in foods such as rutin, curcumin, thymol, lupeol as well as a host of others that might be interesting to test as PrAO inhibitors.

The extension of this work to studies on the human form of PrAO is another important next step. If the inhibition is similar or even more pronounced it would be of considerable impact. The results from this study indicate that consuming foods and beverages containing theobromine like cocoa or caffeine may have health benefits



associated with modulated PrAO. Moreover, the fact that theobromine can arise as a metabolite of caffeine shows that inhibition may be prolonged by metabolites.

The effect of these compounds on other amine oxidases would also be of interest. Thus, monoamine oxidase and plasma amine oxidase may also be inhibited by methylxanthines, for example. This is of significance since these enzymes also play critical roles in the body in the regulation of amines and especially neurotransmitter metabolism.

The potential of green tea catechins to have an inhibitory role is suggested by the data and requires future exploration. It may be that such inhibition is irreversible and it might be possible to isolate an enzyme inhibitor complex. Mass Spectrometry of native PrAO versus inhibited PrAO would be useful in this regard.

Finally, the compounds identified herein may act as potential lead compounds for the discovery of novel PrAO inhibitors.

## Bibliography

- Agarwal, S. and Mehrotra, R. (2016) 'An Overview of Molecular Docking', *JSM Chemistry*, 4(2), 1-4.
- Agostinelli, E., Tempera, G., Viceconte, N., Saccoccio, S., Battaglia, V., Grancara, S., Toninello, A. and Stevanato, R. (2010) 'Potential anticancer application of polyamine oxidation products formed by amine oxidase: a new therapeutic approach', *Amino Acids*, 38(2), 353-368.
- Ahlawat, A., Ghodasara, S., Dongre, V. and Gajbhiye, P. (2014) 'Chocolate toxicity in a dog', *Indian Journal of Veterinary and Animal Sciences Research*, 43, 452-453.
- Akagawa, M., Shigemitsu, T. and Suyama, K. (2005) 'Oxidative deamination of benzylamine and lysine residue in bovine serum albumin by green tea, black tea, and coffee', *Journal of Agricultural and Food Chemistry*, 53(20), 8019-8024.
- Alferova, V., Uzbekov, M., Shklovskii, V., Misionzhnik, E., Luk'ianiuk, E. and Gekht, A. (2010) 'Role of semicarbazide-sensitive amine oxidase in disturbances of endogenous detoxication in ischemic stroke patients', *Zhurnal nevrologii i psikhatrii imeni SS Korsakova/Ministerstvo zdravookhraneniia i meditsinskoi promyshlennosti Rossiiskoi Federatsii, Vserossiiskoe obshchestvo nevrologov [i] Vserossiiskoe obshchestvo psikiatrov*, 111(4 Pt 2), 18-22.
- Anju, P., Moothedath, I. and Shree, A. B. R. (2014) 'Gamma amino butyric acid accumulation in medicinal plants without stress', *Ancient Science of Life*, 34(2), 68.
- Arendash, G. W. and Cao, C. (2010) 'Caffeine and Coffee as Therapeutics Against Alzheimer's Disease', *Journal of Alzheimer's Disease*, 20, 117-126.
- Armenta, S. and Blanco, M. (2012) 'Ion mobility spectrometry for monitoring diamine oxidase activity', *Analyst*, 137(24), 5891-5897.
- Ashihara, H. and Crozier, A. (1999) 'Biosynthesis and Metabolism of Caffeine and Related Purine Alkaloids in Plants', *Advances in Botanical Research*, 30, 117-205.
- Autio, A., Jalkanen, S. and Roivainen, A. (2013) 'Nuclear imaging of inflammation: homing-associated molecules as targets', *EJNMMI Research*, 3(1), 1-7.
- Azam, S. S. and Abbasi, S. W. (2013) 'Molecular docking studies for the identification of novel melatonergic inhibitors for acetylserotonin-O-methyltransferase using different docking routines', *Theoretical Biology & Medical Modelling*, 10, 63-63.

- Baggott, M. J., Childs, E., Hart, A. B., De Bruin, E., Palmer, A. A., Wilkinson, J. E. and De Wit, H. (2013) 'Psychopharmacology of theobromine in healthy volunteers', *Psychopharmacology*, 228(1), 109-118.
- Baker, G. B., Sowa, B. and Todd, K. G. (2007) 'Amine oxidases and their inhibitors: what can they tell us about neuroprotection and the development of drugs for neuropsychiatric disorders?', *Journal of Psychiatry & Neuroscience*, 32(5), 313-315.
- Barone, J. and Roberts, H. (1996) 'Caffeine consumption', *Food and Chemical Toxicology*, 34(1), 119-129.
- Basiri, B., Sutton, J. M., Hanberry, B. S., Zastre, J. A. and Bartlett, M. G. (2016) 'Ion pair liquid chromatography method for the determination of thiamine (vitamin B1) homeostasis', *Biomedical Chromatography*, 30(1), 35-41.
- Becchi, S., Buson, A., Foot, J., Jarolimek, W. and Balleine, B. W. (2017) 'Inhibition of semicarbazide-sensitive amine oxidase/vascular adhesion protein-1 reduces lipopolysaccharide-induced neuroinflammation', *British Journal of Pharmacology*, 174(14), 2302-2317.
- Binda, C., Edmondson, D. E. and Mattevi, A. (2013) 'Monoamine Oxidase Inhibitors: Diverse and Surprising Chemistry with Expanding Pharmacological Potential' In Read R., Urzhumtsev A. and V., L., eds., *Advancing Methods for Biomolecular Crystallography*, Dordrecht, NL: Springer, 309-312.
- Black, J. C. and Whetstone, J. R. (2012) 'LOX out, histones: A new enzyme is nipping at your tails', *Molecular Cell*, 46(3), 243-244.
- Block, G. (1991) 'Vitamin C and cancer prevention: the epidemiologic evidence', *The American Journal of clinical Nutrition*, 53(1), 270S-282S.
- Bonaiuto, E., Lunelli, M., Scarpa, M., Vettor, R., Milan, G. and Di Paolo, M. L. (2010) 'A structure–activity study to identify novel and efficient substrates of the human semicarbazide-sensitive amine oxidase/VAP-1 enzyme', *Biochimie*, 92(7), 858-868.
- Boomsma, F., Pedersen-Bjergaard, U., Agerholm-Larsen, B., Hut, H., Dhamrait, S. S., Thorsteinsson, B. and van den Meiracker, A. H. (2005) 'Association between plasma activities of semicarbazide-sensitive amine oxidase and angiotensin-converting enzyme in patients with type 1 diabetes mellitus', *Diabetologia*, 48(5), 1002-1007.
- Boots, A. W., Haenen, G. R. and Bast, A. (2008) 'Health effects of quercetin: from antioxidant to nutraceutical', *European Journal of Pharmacology*, 585(2), 325-337.

- BRENDA (2015) '1.4.3.21: primary-amine oxidase', [online], available: [http://www.brenda-enzymes.org/all\\_enzymes.php?ecno=1.4.3.21](http://www.brenda-enzymes.org/all_enzymes.php?ecno=1.4.3.21) (accessed 10/03/2017).
- Buffoni, F. and Blaschko, H. (1964) 'Benzylamine oxidase and histaminase: purification and crystallization of an enzyme from pig plasma', *Proceedings of the Royal Society of London B: Biological Sciences*, 161(983), 153-167.
- Cabrera, C., Artacho, R. and Giménez, R. (2010) 'Beneficial Effects of Green Tea - A Review', *American College of Nutrition*, 25(2), 79-99.
- Carpéné, C., Hasnaoui, M., Balogh, B., Matyus, P., Fernández-Quintela, A., Rodríguez, V., Mercader, J. and Portillo, M. P. (2016) 'Dietary phenolic compounds interfere with the fate of hydrogen peroxide in human adipose tissue but do not directly inhibit primary amine oxidase activity', *Oxidative Medicine and Cellular Longevity*, 2016.
- Castillo, V., Lizcano, J. M., Visa, J. and Unzeta, M. (1998) 'Semicarbazide-sensitive amine oxidase (SSAO) from human and bovine cerebrovascular tissues: biochemical and immunohistological characterization', *Neurochem Int*, 33(5), 415-423.
- Chacko, S. M., Thambi, P. T., Kuttan, R. and Nishigaki, I. (2010) 'Beneficial effects of green tea: A literature review', *Chinese Medicine*, 5(1), 13.
- Chang, H.-P., Sheen, L.-Y. and Lei, Y.-P. (2015) 'The protective role of carotenoids and polyphenols in patients with head and neck cancer', *Journal of the Chinese Medical Association*, 78(2), 89-95.
- Chaudhary, K. K. and Mishra, N. (2015) 'A Review on Molecular Docking: Novel Tool for Drug Discovery', *JSM Chemistry*, 4(3), 1029.
- Che, B., Wang, L., Zhang, Z., Zhang, Y. and Deng, Y. (2012) 'Distribution and accumulation of caffeine in rat tissues and its inhibition on semicarbazide-sensitive amine oxidase', *Neurotoxicology*, 33(5), 1248-1253.
- Chen, D., Wan, S. B., Yang, H., Yuan, J., Chan, T. H. and Dou, Q. P. (2011) 'EGCG, green tea polyphenols and their synthetic analogs and prodrugs for human cancer prevention and treatment', *Advances in Clinical Chemistry*, 53, 155-77.
- Chen, K., Kazachkov, M. and Yu, P. (2007a) 'Effect of aldehydes derived from oxidative deamination and oxidative stress on  $\beta$ -amyloid aggregation; pathological implications to Alzheimer's disease', *Journal of Neural Transmission*, 114(6), 835-839.
- Chen, K., Kazachkov, M. and Yu, P. H. (2007b) 'Effect of aldehydes derived from oxidative deamination and oxidative stress on  $\beta$ -amyloid aggregation;

- pathological implications to Alzheimer's disease', *J Neural Transm*, 114, 835-839.
- Chen, X., Ghribi, O. and Geiger, J. D. (2010) 'Caffeine protects against disruptions of the blood-brain barrier in animal models of Alzheimer's and Parkinson's diseases', *Journal of Alzheimer's Disease*, 20(S1), 127-141.
- Cheng, T., Li, Q., Zhou, Z., Wang, Y. and Bryant, S. H. (2012) 'Structure-Based Virtual Screening for Drug Discovery: a Problem-Centric Review', *The AAPS Journal*, 14(1), 133-141.
- Clarke, D. E., Lyles, G. A. and Callingham, B. A. (1982) 'A comparison of cardiac and vascular clorgyline-resistant amine oxidase and monoamine oxidase: Inhibition by amphetamine, mexiletine and other drugs', *Biochemical Pharmacology*, 31(1), 27-35.
- Cosconati, S., Forli, S., Perryman, A. L., Harris, R., Goodsell, D. S. and Olson, A. J. (2010) 'Virtual screening with AutoDock: theory and practice', *Expert Opinion on Drug Discovery*, 5(6), 597-607.
- Cosío, B. G., Shafiek, H., Iglesias, A., Yanez, A., Córdova, R., Palou, A., Rodríguez-Roisin, R., Peces-Barba, G., Pascual, S. and Gea, J. (2016) 'Oral low-dose theophylline on top of inhaled fluticasone-salmeterol does not reduce exacerbations in patients with severe COPD: A pilot clinical trial', *CHEST Journal*, 150(1), 123-130.
- da Silva Pinto, M. (2013) 'Tea: A new perspective on health benefits', *Food Research International*, 53(2), 558-567.
- Daglia, M. (2012) 'Polyphenols as antimicrobial agents', *Current Opinion in Biotechnology*, 23(2), 174-181.
- Daly, J. W. (2007) 'Caffeine analogs: biomedical impact', *Cellular and Molecular Life Sciences*, 64(16), 2153-2169.
- Dangour, A. D., Whitehouse, P. J., Rafferty, K., Mitchell, S. A., Smith, L., Hawkesworth, S. and Vellas, B. (2010) 'B-vitamins and fatty acids in the prevention and treatment of Alzheimer's disease and dementia: a systematic review', *Journal of Alzheimer's Disease : JAD*, 22(1), 205-24.
- Day, A. J. and Williamson, G. (2001) 'Biomarkers for exposure to dietary flavonoids: a review of the current evidence for identification of quercetin glycosides in plasma', *British Journal of Nutrition*, 86(1), 105-110.
- Dubois, B., Feldman, H. H., Jacova, C., Hampel, H., Molinuevo, J. L., Blennow, K., DeKosky, S. T., Gauthier, S., Selkoe, D., Bateman, R., Cappa, S., Crutch, S., Engelborghs, S., Frisoni, G. B., Fox, N. C., Galasko, D., Habert, M. O., Jicha, G. A., Nordberg, A., Pasquier, F., Rabinovici, G., Robert, P., Rowe, C., Salloway, S., Sarazin, M., Epelbaum, S., de Souza, L. C., Vellas, B.,

- Visser, P. J., Schneider, L., Stern, Y., Scheltens, P. and Cummings, J. L. (2014) 'Advancing research diagnostic criteria for Alzheimer's disease: the IWG-2 criteria', *Lancet Neurol*, 13(6), 614-629.
- Eitenmiller, R. R., Landen Jr, W. and Ye, L. (2016) *Vitamin Analysis for the Health and Food Sciences*, CRC press.
- Elovaara, H., Kidron, H., Parkash, V., Nymalm, Y., Bligt, E., Ollikka, P., Smith, D. J., Pihlavisto, M., Salmi, M., Jalkanen, S. and Salminen, T. A. (2011) 'Identification of Two Imidazole Binding Sites and Key Residues for Substrate Specificity in Human Primary Amine Oxidase AOC3', *Biochemistry*, 50(24), 5507-5520.
- Elovaara, H., Parkash, V., Fair-Mäkelä, R., Salo-Ahen, O. M., Guédez, G., Bligt-Lindén, E., Grönholm, J., Jalkanen, S. and Salminen, T. A. (2016) 'Multivalent Interactions of Human Primary Amine Oxidase with the V and C22 Domains of Sialic Acid-Binding Immunoglobulin-Like Lectin-9 Regulate Its Binding and Amine Oxidase Activity', *PLoS One*, 11(11), e0166935.
- Enrique-Tarancon, G., Marti, L., Morin, N., Lizcano, J. M., Unzeta, M., Sevilla, L., Camps, M., Palacin, M., Testar, X., Carpene, C. and Zorzano, A. (1998) 'Role of semicarbazide-sensitive amine oxidase on glucose transport and GLUT4 recruitment to the cell surface in adipose cells', *J Biol Chem*, 273(14), 8025-32.
- Enzsoly, A., Marko, K., Tabi, T., Szoko, E., Zelko, R., Toth, M., Petrash, J. M., Matyus, P. and Nemeth, J. (2013) 'Lack of association between VAP-1/SSAO activity and corneal neovascularization in a rabbit model', *Journal of Neural Transmission*, 120(6), 969-975.
- Fan, Y., Liu, J.-H., Yang, C.-P., Yu, M. and Liu, P. (2011) 'Graphene–polyaniline composite film modified electrode for voltammetric determination of 4-aminophenol', *Sensors and Actuators B: Chemical*, 157(2), 669-674.
- Ferjančič, Š., Gil-Bernabé, A. M., Hill, S. A., Allen, P. D., Richardson, P., Sparey, T., Savory, E., McGuffog, J. and Muschel, R. J. (2013) 'VCAM-1 and VAP-1 recruit myeloid cells that promote pulmonary metastasis in mice', *Blood*, 121(16).
- Fernando, C. D. and Soysa, P. (2015) 'Optimized enzymatic colorimetric assay for determination of hydrogen peroxide (H<sub>2</sub>O<sub>2</sub>) scavenging activity of plant extracts', *MethodsX*, 2(1), 283-891.
- Ferreira, L., dos Santos, R., Oliva, G. and Andricopulo, A. (2015) 'Molecular Docking and Structure-Based Drug Design Strategies', *Molecules*, 20(7), 13384-13421.

- Ferrucci, L. M., Cartmel, B., Molinaro, A. M., Leffell, D. J., Bale, A. E. and Mayne, S. T. (2014) 'Tea, coffee, and caffeine and early-onset basal cell carcinoma in a case-control study', *Eur J Cancer Prev*, 23(4), 296-302.
- Floris, G. and Mondovi, B. (2009) *Copper Amine Oxidases: Structure, Catalytic Mechanisms and Role in Pathophysiology*, Boca Raton, FL: CRC Press.
- Foot, J. S., Yow, T. T., Schilter, H., Buson, A., Deodhar, M., Findlay, A. D., Guo, L., McDonald, I. A., Turner, C. I., Zhou, W. and Jarolimek, W. (2013) 'PXS-4681A, a potent and selective mechanism-based inhibitor of SSAO/VAP-1 with anti-inflammatory effects *in vivo*', *Journal of Pharmacology and Experimental Therapeutics*, 347(2), 365-374.
- Franco, R., Oñatibia-Astibia, A. and Martínez-Pinilla, E. (2013) 'Health Benefits of Methylxanthines in Cacao and Chocolate', *Nutrients*, 5(10), 4159-4173.
- Frost-Meyer, N. J. and Logomarsino, J. V. (2012) 'Impact of coffee components on inflammatory markers: A review', *Journal of Functional Foods*, 4(4), 819-830.
- Fujiki, H., Imai, K., Nakachi, K., Sueoka, E., Watanabe, T. and Suganuma, M. (2015) 'Innovative strategy of cancer treatment with the combination of green tea catechins and anticancer compounds', *Cancer Cell & Microenvironment*, 2(4).
- Fukushima, Y., Ohie, T., Yonekawa, Y., Yonemoto, K., Aizawa, H., Mori, Y., Watanabe, M., Takeuchi, M., Hasegawa, M., Taguchi, C. and Kondo, K. (2009) 'Coffee and Green Tea As a Large Source of Antioxidant Polyphenols in the Japanese Population', *Journal of Agricultural and Food Chemistry*, 57(4), 1253-1259.
- Furman, D., Chang, J., Lartigue, L., Bolen, C. R., Haddad, F., Gaudilliere, B., Ganio, E. A., Fragiadakis, G. K., Spitzer, M. H. and Douchet, I. (2017) 'Expression of specific inflammasome gene modules stratifies older individuals into two extreme clinical and immunological states', *Nature Medicine*, 23(2), 174.
- George, S. E., Ramalakshmi, K. and Mohan Rao, L. J. (2008) 'A perception on health benefits of coffee', *Crit Rev Food Sci Nutr*, 48(5), 464-86.
- Gharaghani, S., Khayamian, T. and Ebrahimi, M. (2013) 'Multitarget fragment-based design of novel inhibitors for AChE and SSAO/VAP-1 enzymes', *Journal of Chemometrics*, 27(10), 297-305.
- Glisan, S., Sae-Tan, S., Grove, K., Yennawar, N. and Lambert, J. (2014) 'Inhibition of digestive enzymes by tea polyphenols: enzymological and *in silico* studies (1045.34)', *The FASEB Journal*, 28(1), 1045.34.

- Göktürk, C., Nilsson, J., Nordquist, J., Kristensson, M., Svensson, K., Söderberg, C., Israelson, M., Garpenstrand, H., Sjöquist, M., Orelund, L. and Forsberg-Nilsson, K. (2003) 'Overexpression of semicarbazide-sensitive amine oxidase in smooth muscle cells leads to an abnormal structure of the aortic elastic laminae', *The American Journal of Pathology*, 163(5), 1921-8.
- Gong, B. and Boor, P. J. (2006) 'The role of amine oxidases in xenobiotic metabolism', *Expert Opinion on Drug Metabolism & Toxicology*, 2(4), 559-571.
- González-Castejón, M. and Rodríguez-Casado, A. (2011) 'Dietary phytochemicals and their potential effects on obesity: a review', *Pharmacological Research*, 64(5), 438-455.
- Gori, A. M., Sofi, F., Corsi, A. M., Gazzini, A., Sestini, I., Lauretani, F., Bandinelli, S., Gensini, G. F., Ferrucci, L. and Abbate, R. (2006) 'Predictors of vitamin B6 and folate concentrations in older persons: the InCHIANTI study', *Clinical Chemistry*, 52(7), 1318-1324.
- Gunter, M. J., Murphy, N., Cross, A. J., Dossus, L., Dartois, L., Fagherazzi, G., Kaaks, R., Kühn, T., Boeing, H. and Aleksandrova, K. (2017) 'Coffee drinking and mortality in 10 European countries: a multinational cohort study', *Annals of Internal Medicine*, 167(4), 236-247.
- Guo, W., Kong, E. and Meydani, M. (2009) 'Dietary Polyphenols, Inflammation, and Cancer', *Nutrition and Cancer*, 61(6), 807-810.
- Hafezi-Moghadam, A., Massachusetts Eye and Ear Infirmary, 2018. *Methods and compositions for treating conditions associated with angiogenesis using a vascular adhesion protein-1 (vap-1) inhibitor*. U.S. Patent Application 15/429, 679.
- Hara, Y. (2001) *Green tea: health benefits and applications*, 1st edn. Marcel Dekker Inc., New York. 259pp.
- Hara, Y. and Honda, M. (1990) 'The inhibition of  $\alpha$ -amylase by tea polyphenols', *Agricultural and Biological Chemistry*, 54(8), 1939-1945.
- Hernandez, M., Sole, M., Boada, M. and Unzeta, M. (2006a) 'Soluble semicarbazide sensitive amine oxidase (SSAO) catalysis induces apoptosis in vascular smooth muscle cells', *Biochimica et Biophysica Acta*, 1763(2), 164-73.
- Hernandez, M., Solé, M., Boada, M. and Unzeta, M. (2006b) 'Soluble semicarbazide sensitive amine oxidase (SSAO) catalysis induces apoptosis in vascular smooth muscle cells', *Biochimica et Biophysica Acta (BBA)-Molecular Cell Research*, 1763(2), 164-173.



- Hill, A. D. and Reilly, P. J. (2015) 'Scoring Functions for AutoDock' In Lütteke, T. and Frank, M., eds., *Glycoinformatics*, New York, NY: Springer New York, 467-474.
- Holt, A. and Palcic, M. M. (2006) 'A peroxidase-coupled continuous absorbance plate-reader assay for flavin monoamine oxidases, copper-containing amine oxidases and related enzymes', *Nature Protocols*, 1(5), 2498-2545.
- Holt, A., Smith, D. J., Cendron, L., Zanotti, G., Rigo, A. and Di Paolo, M. L. (2008a) 'Multiple binding sites for substrates and modulators of semicarbazide-sensitive amine oxidases: kinetic consequences', *Molecular Pharmacology*, 73(2), 525-38.
- Holt, A., Smith, D. J., Cendron, L., Zanotti, G., Rigo, A. and Di Paolo, M. L. (2008b) 'Multiple binding sites for substrates and modulators of semicarbazide-sensitive amine oxidases: kinetic consequences', *Molecular Pharmacology*, 73(2), 525-538.
- Hsieh, C.-E., Chen, G. S., Yeh, J.-S. and Lin, Y.-L. (2016) *Molecular Descriptors Selection and Machine Learning Approaches in Protein-Ligand Binding Affinity with Applications to Molecular Docking*, translated by IEEE, 38-43.
- Hung, S. C., Hung, S. H., Tarng, D. C., Yang, W. C., Chen, T. W. and Huang, T. P. (2001) 'Thiamine deficiency and unexplained encephalopathy in hemodialysis and peritoneal dialysis patients', *American Journal of Kidney Diseases*, 38(5), 941-947.
- Jakobsson, E., Nilsson, J., Ogg, D. and Kleywegt, G. J. (2005) 'Structure of human semicarbazide-sensitive amine oxidase/vascular adhesion protein-1', *Acta Crystallographica Section D Biological Crystallography*, 61(11), 1550-1562.
- Januszewski, A. S., Mason, N., Karschimkus, C. S., Rowley, K. G., Best, J. D., O'Neal, D. N. and Jenkins, A. J. (2014) 'Plasma semicarbazide-sensitive amine oxidase activity in type 1 diabetes is related to vascular and renal function but not to glycaemia', *Diabetes & Vascular Disease Research*, 11(4), 262-269.
- Jung, H. A., Ali, M. Y., Choi, R. J., Jeong, H. O., Chung, H. Y. and Choi, J. S. (2016) 'Kinetics and molecular docking studies of fucosterol and fucoxanthin, BACE1 inhibitors from brown algae *Undaria pinnatifida* and *Ecklonia stolonifera*', *Food and Chemical Toxicology*, 89, 104-111.
- Kargul, B., Özcan, M., Peker, S., Nakamoto, T., Simmons, W. B. and Falster, A. U. (2012) 'Evaluation of human enamel surfaces treated with theobromine: a pilot study', *Oral Health and Preventive Dentistry*, 10(3), 275-285.
- Kaserer, T., Beck, K. R., Akram, M., Odermatt, A., Schuster, D. and Willett, P. (2015) 'Pharmacophore Models and Pharmacophore-Based Virtual

Screening: Concepts and Applications Exemplified on Hydroxysteroid Dehydrogenases', *Molecules*, 20(12), 22799-22832.

- Khan, M. K., Faught, E. L., Chu, Y. L., Ekwaru, J. P., Storey, K. E. and Veugelers, P. J. (2017) 'Is it nutrients, food items, diet quality or eating behaviours that are responsible for the association of children's diet with sleep?', *Journal of Sleep Research*, 26(4), 468-476.
- Khan, N., Monagas, M., Andres-Lacueva, C., Casas, R., Urpi-Sarda, M., Lamuela-Raventos, R. and Estruch, R. (2012) 'Regular consumption of cocoa powder with milk increases HDL cholesterol and reduces oxidized LDL levels in subjects at high-risk of cardiovascular disease', *Nutrition, Metabolism and Cardiovascular Diseases*, 22(12), 1046-1053.
- Kim, H.-S., Quon, M. J. and Kim, J.-a. (2014) 'New insights into the mechanisms of polyphenols beyond antioxidant properties; lessons from the green tea polyphenol, epigallocatechin 3-gallate', *Redox Biology*, 2(1), 187-195.
- Kinemuchi, H., Sugimoto, H., Obata, T., Satoh, N. and Ueda, S. (2004a) 'Selective inhibitors of membrane-bound semicarbazide-sensitive amine oxidase (SSAO) activity in mammalian tissues', *Neurotoxicology*, 25(1-2), 325-335.
- Kirkham, P. A., Whiteman, M., Winyard, P. G., Caramori, G., Gordon, F., Ford, P. A., Barnes, P. J., Adcock, I. M. and Chung, K. F. (2014) 'Impact of theophylline/corticosteroid combination therapy on sputum hydrogen sulfide levels in patients with COPD', *European Respiratory Journal*, 43(5), 1504-1506.
- Klein, E. A., Lippman, S. M., Thompson, I. M., Goodman, P. J., Albanes, D., Taylor, P. R. and Coltman, C. (2003) 'The selenium and vitamin E cancer prevention trial', *World Journal of Urology*, 21(1), 21-27.
- Klema, V. J. and Wilmot, C. M. (2012) 'The role of protein crystallography in defining the mechanisms of biogenesis and catalysis in copper amine oxidase', *International Journal of Molecular Sciences*, 13(5), 5375-5405.
- Kozłowska, A. and Szostak-Wegierek, D. (2014) 'Flavonoids-food sources and health benefits', *Roczniki Państwowego Zakładu Higieny*, 65(2), 79-85.
- Langley, D. B., Trambaiolo, D. M., Duff, A. P., Dooley, D. M., Freeman, H. C. and Guss, J. M. (2008) 'Complexes of the copper-containing amine oxidase from *Arthrobacter globiformis* with the inhibitors benzylhydrazine and tranylcypromine', *Acta Crystallographica Section F: Structural Biology and Crystallization Communications*, 64(7), 577-583.
- Largerón, M. (2011) 'Amine oxidases of the quinoproteins family: their implication in the metabolic oxidation of xenobiotics', *Annales Pharmaceutiques Françaises*, 69(1), 53-61.

- Lee, M. H., Chuang, M. T. and Hou, W. C. (2002) 'Activity staining of plasma amine oxidase after polyacrylamide gel electrophoresis and its application to natural inhibitor screening', *Electrophoresis*, 23(15), 2369-2372.
- Li, H.-Y., Lin, H.-A., Nien, F.-J., Wu, V.-C., Jiang, Y.-D., Chang, T.-J., Kao, H.-L., Lin, M.-S., Wei, J.-N., Lin, C.-H., Shih, S.-R., Hung, C.-S. and Chuang, L.-M. (2016) 'Serum Vascular Adhesion Protein-1 Predicts End-Stage Renal Disease in Patients with Type 2 Diabetes', *PLoS One*, 11(2), e0147981-e0147981.
- Li, W., Dai, R.-J., Yu, Y.-H., Li, L., Wu, C.-M., Luan, W.-W., Meng, W.-W., Zhang, X.-S. and Deng, Y.-L. (2007) 'Antihyperglycemic effect of Cephalotaxus sinensis leaves and GLUT-4 translocation facilitating activity of its flavonoid constituents', *Biological and Pharmaceutical Bulletin*, 30(6), 1123-1129.
- Liu, J. and Wang, R. (2015) 'Classification of current scoring functions', *Journal of Chemical Information and Modeling*, 55(3), 475-482.
- Liu, Y.-H., Liang, W.-L., Lee, C.-C., Tsai, Y.-F. and Hou, W.-C. (2011) 'Antioxidant and semicarbazide-sensitive amine oxidase inhibitory activities of glucuronic acid hydroxamate', *Food Chemistry*, 129(2), 423-428.
- Liu, Y.-H., Wu, W.-C., Lu, Y.-L., Lai, Y.-J. and Hou, W.-C. (2010) 'Antioxidant and Amine Oxidase Inhibitory Activities of Hydroxyurea', *Bioscience, Biotechnology, and Biochemistry*, 74(6), 1256-1260.
- Lizcano, J. M., Fernandez de Arriba, A., Tipton, K. F. and Unzeta, M. (1996) 'Inhibition of bovine lung semicarbazide-sensitive amine oxidase (SSAO) by some hydrazine derivatives', *Biochemical Pharmacology*, 52(2), 187-195.
- Lotan, R. (1980) 'Effects of vitamin A and its analogs (retinoids) on normal and neoplastic cells', *Biochimica et Biophysica Acta (BBA)-Reviews on Cancer*, 605(1), 33-91.
- Lourida, I., Soni, M., Thompson-Coon, J., Purandare, N., Lang, I. A., Ukoumunne, O. C. and Llewellyn, D. J. (2013) 'Mediterranean Diet, Cognitive Function, and Dementia', *Epidemiology*, 24(4), 479-489.
- Luo, W., Xie, F., Zhang, Z. and Sun, D. (2013) 'Vascular adhesion protein 1 in the eye', *Journal of Ophthalmology*, 2013(925267), 1-8.
- Mak, J. C. W. (2012) 'Potential role of green tea catechins in various disease therapies: Progress and promise', *Clinical and Experimental Pharmacology and Physiology*, 39(3), 265-273.
- Marinho, C., Arduino, D., Falcão, L. M. and Bicho, M. (2010) 'Alterations in plasma semicarbazide-sensitive amine oxidase activity in hypertensive heart disease with left ventricular systolic dysfunction', *Revista portuguesa de cardiologia: orgao oficial da Sociedade Portuguesa de Cardiologia= Portuguese journal*

*of cardiology: an official journal of the Portuguese Society of Cardiology*, 29(1), 37-47.

- Marino, S. M. and Gladyshev, V. N. (2012) 'Analysis and functional prediction of reactive cysteine residues', *Journal of Biological Chemistry*, 287(7), 4419-4425.
- Martínez-López, S., Sarriá, B., Gómez-Juaristi, M., Goya, L., Mateos, R. and Bravo-Clemente, L. (2014) 'Theobromine, caffeine, and theophylline metabolites in human plasma and urine after consumption of soluble cocoa products with different methylxanthine contents', *Food Research International*, 63, 446-455.
- Martínez-Pinilla, E., Oñatibia-Astibia, A. and Franco, R. (2015) 'The relevance of theobromine for the beneficial effects of cocoa consumption', *Frontiers in Pharmacology*, 6(30), 1-5.
- Mátyus, P., Magyar, K., Pihlavisto, M., Gyires, K., Haider, N., Wang, Y., Woda, P., Dunkel, P., Tóth-Sarudy, É. and Túrós, G. (2013) *Compounds for inhibiting semicarbazide-sensitive amine oxidase (SSAO)/vascular adhesion protein-1 (VAP-1) and uses thereof for treatment and prevention of diseases*, US Patent 8536210.
- McDonald, A., Tipton, K., O'Sullivan, J., Olivieri, A., Davey, G., Coonan, A.-M. and Fu, W. (2007) 'Modelling the roles of MAO and SSAO in glucose transport', *Journal of Neural Transmission*, 114(6), 783-786.
- Mercader, J., Iffiú-Soltész, Z., Bour, S. and Carpené, C. (2011) 'Oral Administration of Semicarbazide Limits Weight Gain together with Inhibition of Fat Deposition and of Primary Amine Oxidase Activity in Adipose Tissue', *Journal of Obesity*, 2011(10), 1-10.
- Mercier, N. (2009) 'The role of "semicarbazide-sensitive amine oxidase" in the arterial wall', *Artery Research*, 3(4), 141-147.
- Mercier, N., Moldes, M., El Hadri, K. and Fève, B. (2003) 'Regulation of semicarbazide-sensitive amine oxidase expression by tumor necrosis factor- $\alpha$  in adipocytes: Functional consequences on glucose transport', *Journal of Pharmacology and Experimental Therapeutics*, 304(3), 1197-1208.
- Monteiro, J. P., Alves, M. G., Oliveira, P. F. and Silva, B. M. (2016) 'Structure-bioactivity relationships of methylxanthines: Trying to make sense of all the promises and the drawbacks', *Molecules*, 21(8), 974.
- Morris, G. M., Huey, R., Lindstrom, W., Sanner, M. F., Belew, R. K., Goodsell, D. S. and Olson, A. J. (2009) 'AutoDock4 and AutoDockTools4: Automated docking with selective receptor flexibility', *Journal of Computational Chemistry*, 30(16), 2785-2791.

- Naz, F., Qamarunnisa, S., Shinwari, Z. K., Azhar, A. and Ali, S. I. (2013) 'Phytochemical investigations of *Tamarix indica* Willd. and *Tamarix passernioides* Del. ex Desv. leaves from Pakistan', *Pak. J. Bot*, 45(5), 1503-1507.
- Nehlig, A. (2015) 'Effects of coffee/caffeine on brain health and disease: What should I tell my patients?', *Practical Neurology*, practneurol-2015-001162.
- Ness, R. A., Miller, D. D. and Wei, L. (2015) 'The role of vitamin D in cancer prevention', *Chinese Journal of Natural Medicines*, 13(7), 481-497.
- Nunes, S. F., Figueiredo, I. V., Pereira, J. S., Soares, P. J., Caramona, M. M. and Callingham, B. (2010) 'Changes in the activities of semicarbazide-sensitive amine oxidase in inferior mesenteric artery segments and in serum of patients with type 2 diabetes', *Acta Diabetologica*, 47(2), 179-182.
- O'Keefe, J. H., Bhatti, S. K., Patil, H. R., DiNicolantonio, J. J., Lucan, S. C. and Lavie, C. J. (2013) 'Effects of Habitual Coffee Consumption on Cardiometabolic Disease, Cardiovascular Health, and All-Cause Mortality', *Journal of the American College of Cardiology*, 62(12), 1043-1051.
- O'Sullivan, J., Unzeta, M., Healy, J., O'Sullivan, M. I., Davey, G. and Tipton, K. F. (2004) 'Semicarbazide-sensitive amine oxidases: enzymes with quite a lot to do', *Neurotoxicology*, 25(1), 303-15.
- Olivieri, A., O'Sullivan, J., Fortuny, L. R. A., Vives, I. L. and Tipton, K. F. (2010) 'Interaction of l-lysine and soluble elastin with the semicarbazide-sensitive amine oxidase in the context of its vascular-adhesion and tissue maturation functions', *Biochimica et Biophysica Acta (BBA) - Proteins and Proteomics*, 1804(4), 941-947.
- Olivieri, A., Rico, D., Khiari, Z., Henehan, G., O'Sullivan, J. and Tipton, K. (2011) 'From caffeine to fish waste: amine compounds present in food and drugs and their interactions with primary amine oxidase', *Journal of Neural Transmission*, 118(7), 1079-1089.
- Olivieri, A. and Tipton, K. (2011) 'Inhibition of bovine plasma semicarbazide-sensitive amine oxidase by caffeine', *Journal of Biochemical and Molecular Toxicology*, 25(1), 26-27.
- Olivieri, A., Tipton, K. and O'Sullivan, J. (2007) 'L-lysine as a recognition molecule for the VAP-1 function of SSAO', *Journal of Neural Transmission*, 114(6), 747-749.
- Oñatibia-Astibia, A., Franco, R. and Martínez-Pinilla, E. (2017) 'Health benefits of methylxanthines in neurodegenerative diseases', *Molecular Nutrition & Food Research*, 61(6), p1600670.

- Pastore, A., Massoud, R., Motti, C., Lo Russo, A., Fucci, G., Cortese, C. and Federici, G. (1998) 'Fully automated assay for total homocysteine, cysteine, cysteinylglycine, glutathione, cysteamine, and 2-mercaptopropionylglycine in plasma and urine', *Clinical Chemistry*, 44(4), 825-832.
- Peet, G. W., Lukas, S., Hill-Drzewi, M., Martin, L., Rybina, I. V., Roma, T., Shoultz, A., Zhu, X., Cazacu, D., Kronkaitis, A., Baptiste, A., Raudenbush, B. C., August, E. M. and Modis, L. K. (2011) 'Bioluminescent method for assaying multiple semicarbazide-sensitive amine oxidase (SSAO) family members in both 96- and 384-well formats', *Journal of Biomolecular Screening*, 16(9), 1106-1111.
- Rashidinejad, A., Birch, E., Sun-Waterhouse, D. and Everett, D. (2015) 'Total phenolic content and antioxidant properties of hard low-fat cheese fortified with catechin as affected by in vitro gastrointestinal digestion', *LWT-Food Science and Technology*, 62(1), 393-399.
- Rogers, P. J., Heatherley, S. V., Hayward, R. C., Seers, H. E., Hill, J. and Kane, M. (2005) 'Effects of caffeine and caffeine withdrawal on mood and cognitive performance degraded by sleep restriction', *Psychopharmacology*, 179(4), 742-752.
- Salmi, M. and Jalkanen, S. (2011) 'Homing-associated molecules CD73 and VAP-1 as targets to prevent harmful inflammations and cancer spread', *FEBS Letters*, 585(11), 1543-1550.
- Salter-Cid, L. M., Wang, E. Y., MacDonald, M. T. and Zhao, J. (2012) *Amine-based and amide-based inhibitors of semicarbazide-sensitive amine oxidase (SSAO) enzyme activity and vap-1 mediated adhesion useful for treatment of diseases*, U.S. Patent Application 11/602,565.
- Sánchez-del-Campo, L., Sáez-Ayala, M., Chazarra, S., Cabezas-Herrera, J. and Rodríguez-López, J. N. (2009) 'Binding of natural and synthetic polyphenols to human dihydrofolate reductase', *International Journal of Molecular Sciences*, 10(12), 5398-5410.
- Sang, L.-X., Chang, B., Li, X.-H. and Jiang, M. (2013) 'Consumption of coffee associated with reduced risk of liver cancer: a meta-analysis', *BMC Gastroenterology*, 13(1), 1-34.
- Sanner, M. F. (1999) 'Python: a programming language for software integration and development', *Journal of Molecular Graphics*, 17(1), 57-61.
- Santos-Martins, D., Forli, S., Ramos, M. J. and Olson, A. J. (2014) 'AutoDock4Zn: An Improved AutoDock Force Field for Small-Molecule Docking to Zinc Metalloproteins', *Journal of Chemical Information and Modeling*, 54(8), 2371-2379.

- Santos, R., Cotta, K., Jiang, S. and Lima, D. (2015) 'Does CYP1A2 genotype influence coffee consumption', *Austin J. Pharmacol. Ther.*, 3, 1065.
- Sarriá, B., Martínez-López, S., Sierra-Cinos, J. L., Garcia-Diz, L., Goya, L., Mateos, R. and Bravo, L. (2015) 'Effects of bioactive constituents in functional cocoa products on cardiovascular health in humans', *Food Chemistry*, 174, 214-218.
- Schneider, C. and Segre, T. (2009) 'Green tea: potential health benefits', *American Family Physician*, 79(7).
- Shepard, E. M. and Dooley, D. M. (2015) 'Inhibition and oxygen activation in copper amine oxidases', *Accounts of Chemical Research*, 48(5), 1218-1226.
- Silvola, J. M., Virtanen, H., Siitonen, R., Hellberg, S., Liljenbäck, H., Metsälä, O., Ståhle, M., Saanijoki, T., Käckelä, M. and Hakovirta, H. (2016) 'Leukocyte trafficking-associated vascular adhesion protein 1 is expressed and functionally active in atherosclerotic plaques', *Scientific Reports*, 6, 35089.
- Singh, B., Parsaik, A. K., Mielke, M. M., Erwin, P. J., Knopman, D. S., Petersen, R. C. and Roberts, R. O. (2014) 'Association of Mediterranean Diet with Mild Cognitive Impairment and Alzheimer's Disease: A Systematic Review and Meta-Analysis', *Journal of Alzheimer's Disease*, 39(2), 271-282.
- Sinija, V. R. and Mishra, H. N. (2008) 'Green tea: Health benefits', *Journal of Nutritional and Environmental Medicine*, 17(4), 232-242.
- Sisecioglu, M., Gulcin, I., Cankaya, M., Atasever, A. and Ozdemir, H. (2010) 'The effects of norepinephrine on lactoperoxidase enzyme (LPO)', *Scientific Research and Essays*, 5(11), 1351-1356.
- Smith, A. (2002) 'Effects of caffeine on human behavior', *Food and Chemical Toxicology*, 40(9), 1243-1255.
- Smith, D. J., Salmi, M., Bono, P., Hellman, J., Leu, T. and Jalkanen, S. (1998) 'Cloning of vascular adhesion protein 1 reveals a novel multifunctional adhesion molecule', *Journal of Experimental Medicine*, 188(1), 17-27.
- Steinmann, J., Buer, J., Pietschmann, T. and Steinmann, E. (2013) 'Anti-infective properties of epigallocatechin-3-gallate (EGCG), a component of green tea', *British Journal of Pharmacology*, 168(5), 1059-73.
- Sugimoto, N., Miwa, S., Katakura, M., Matsuzaki, K., Shido, O., Tsuchiya, H. and Yachie, A. (2014) 'Theobromine, the primary methylxanthine found in Theobroma cacao, inhibits malignant glioblastoma cell growth by negatively regulating Akt/mammalian target of rapamycin kinase (LB836)', *The FASEB Journal*, 28(1 Supplement), LB836.
- Sun, P., Sole, M. and Unzeta, M. (2014) 'Involvement of SSAO/VAP-1 in oxygen-glucose deprivation-mediated damage using the endothelial hSSAO/VAP-1-

- expressing cells as experimental model of cerebral ischemia', *Cerebrovasc Dis*, 37(3), 171-180.
- Suzuki, M., Willcox, D. C. and Willcox, B. (2016) 'Okinawa Centenarian Study: Investigating Healthy Aging among the World's Longest-Lived People' In Pachana, N. A., ed. *Encyclopedia of Geropsychology*, Springer Singapore, 1-5.
- Syu, K.-Y., Lin, C.-L., Huang, H.-C. and Lin, J.-K. (2008) 'Determination of Theanine, GABA, and Other Amino Acids in Green, Oolong, Black, and Pu-erh Teas with Dabsylation and High-Performance Liquid Chromatography', *Journal of Agricultural and Food Chemistry*, 56(17), 7637-7643.
- Takata, Y., Xiang, Y.-B., Yang, G., Li, H., Gao, J., Cai, H., Gao, Y.-T., Zheng, W. and Shu, X.-O. (2013) 'Intakes of fruits, vegetables, and related vitamins and lung cancer risk: results from the Shanghai Men's Health Study (2002–2009)', *Nutrition and Cancer*, 65(1), 51-61.
- Thakur, K., Tomar, S. K., Singh, A. K., Mandal, S. and Arora, S. (2017) 'Riboflavin and health: A review of recent human research', *Critical Reviews in Food Science and Nutrition*, 57(17), 3650-3660.
- Tomitori, H., Nakamura, M., Sakamoto, A., Terui, Y., Yoshida, M., Igarashi, K. and Kashiwagi, K. (2012) 'Augmented glutathione synthesis decreases acrolein toxicity', *Biochemical and Biophysical Research Communications*, 418(1), 110-115.
- Ullah, K., Xie, B., Iqbal, J., Rasool, A., Qing, H. and Deng, Y. (2013) 'Arterial vascular cell line expressing SSAO: a new tool to study the pathophysiology of vascular amine oxidases', *Journal of Neural Transmission*, 120(6), 1005-1013.
- Unzeta, M., Sole, M., Boada, M. and Hernandez, M. (2007) 'Semicarbazide-sensitive amine oxidase (SSAO) and its possible contribution to vascular damage in Alzheimer's disease', *Journal of Neural Transmission*, 114(6), 857-862.
- Valente, T., Gella, A., Solé, M., Durany, N. and Unzeta, M. (2012) 'Immunohistochemical study of semicarbazide-sensitive amine oxidase/vascular adhesion protein-1 in the hippocampal vasculature: Pathological synergy of Alzheimer's disease and diabetes mellitus', *Journal of Neuroscience Research*, 90(10), 1989-1996.
- Vayalil, P. K. (2012) 'Date fruits (*Phoenix dactylifera* Linn): an emerging medicinal food', *Critical Reviews in Food Science and Nutrition*, 52(3), 249-271.
- Venkatesh, G., Sivasankar, T., Karthick, M. and Rajendiran, N. (2013) 'Inclusion complexes of sulphanilamide drugs and  $\beta$ -cyclodextrin: a theoretical approach', *Journal of Inclusion Phenomena and Macrocyclic Chemistry*, 77(1), 309-318.



- Visentin, V., Morin, N., Fontana, E., Prevot, D., Boucher, J., Castan, I., Valet, P., Grujic, D. and Carpene, C. (2001) 'Dual action of octopamine on glucose transport into adipocytes: inhibition via beta3-adrenoceptor activation and stimulation via oxidation by amine oxidases', *Journal of Pharmacology and Experimental Therapeutics*, 299(1), 96-104.
- Voet, A., Qing, X., Lee, X. Y., De Raeymaecker, J., Tame, J., Zhang, K. and De Maeyer, M. (2014) 'Pharmacophore modeling: advances, limitations, and current utility in drug discovery', *Journal of Receptor, Ligand and Channel Research*, 7, 81-81.
- Wang, E. Y., Gao, H., Salter-Cid, L., Zhang, J., Huang, L., Podar, E. M., Miller, A., Zhao, J., O'Rourke, A. and Linnik, M. D. (2006) 'Design, synthesis, and biological evaluation of semicarbazide-sensitive amine oxidase (SSAO) inhibitors with anti-inflammatory activity', *Journal of Medicinal Chemistry*, 49(7), 2166-2173.
- Wang, S.H., Yu, T.Y., Tsai, F.C., Weston, C. J., Lin, M.-S., Hung, C.S., Kao, H.L., Li, Y.-I., Solé, M. and Unzeta, M. (2018) 'Inhibition of semicarbazide-sensitive amine oxidase reduces atherosclerosis in apolipoprotein E-deficient mice', *Translational Research* 7, 12-31
- Wang, S., Moustaid-Moussa, N., Chen, L., Mo, H., Shastri, A., Su, R., Bapat, P., Kwun, I. and Shen, C.-L. (2014a) 'Novel insights of dietary polyphenols and obesity', *The Journal of Nutritional Biochemistry*, 25(1), 1-18.
- Wang, Y., Zhang, G., Yan, J. and Gong, D. (2014b) 'Inhibitory effect of morin on tyrosinase: insights from spectroscopic and molecular docking studies', *Food Chemistry*, 163, 226-233.
- Willcox, D. C., Scapagnini, G. and Willcox, B. J. (2014) 'Healthy aging diets other than the Mediterranean: A focus on the Okinawan diet', *Mechanisms of Ageing and Development*, 136, 148-162.
- Williams, K., Bilsland, E., Sparkes, A., Aubrey, W., Young, M., Soldatova, L. N., De Grave, K., Ramon, J., de Clare, M. and Sirawaraporn, W. (2015) 'Cheaper faster drug development validated by the repositioning of drugs against neglected tropical diseases', *Journal of the Royal Society Interface*, 12(104), 1-9.
- Wong, M., Saad, S., Zhang, J., Gross, S., Jarolimek, W., Schilter, H., Chen, J. A., Gill, A. J., Pollock, C. A. and Wong, M. G. (2014) 'Semicarbazide-sensitive amine oxidase (SSAO) inhibition ameliorates kidney fibrosis in a unilateral ureteral obstruction murine model', *American Journal of Physiology-Renal Physiology*, 307(8), 908-916.

- Wong, M. Y., Saad, S., Pollock, C. and Wong, M. G. (2013) 'Semicarbazide-sensitive amine oxidase and kidney disease', *American Journal of Physiology-Renal Physiology*, 305(12), 1637-1644.
- Wu, G. (2009) 'Amino acids: metabolism, functions, and nutrition', *Amino acids*, 37(1), 1-17.
- Wu, G. (2013) 'Functional amino acids in nutrition and health', 45(3), 407–411.
- Wu, G. (2014) 'Dietary requirements of synthesizable amino acids by animals: a paradigm shift in protein nutrition', *Journal of Animal Science and Biotechnology*, 5(1), 34.
- Yang, F., De Villiers, W. J. S., McClain, C. J. and Varilek, G. W. (1998) 'Biochemical and Molecular Roles of Nutrients Green Tea Polyphenols Block Endotoxin-Induced Tumor Necrosis Factor- Production and Lethality in a Murine Model 1,2', *Journal of Nutrition*, 128, 2334-2340.
- Yonekura, T., Kamata, S., Wasa, M., Okada, A., Yamatodani, A., Watanabe, T. and Wada, H. (1988) 'Simultaneous determination of plasma phenethylamine, phenylethanolamine, tyramine and octopamine by high-performance liquid chromatography using derivatization with fluorescamine', *Journal of Chromatography B: Biomedical Sciences and Applications*, 427, 320-325.
- Yraola, F., Garcia-Vicente, S., Fernandez-Recio, J., Albericio, F., Zorzano, A., Marti, L. and Royo, M. (2006) 'New efficient substrates for semicarbazide-sensitive amine oxidase/VAP-1 enzyme: analysis by SARs and computational docking', *Journal of Medicinal Chemistry*, 49(21), 6197-6208.
- Yraola, F., Zorzano, A., Albericio, F. and Royo, M. (2009) 'Structure–Activity Relationships of SSAO/VAP-1 Arylalkylamine-Based Substrates', *ChemMedChem*, 4(4), 495-503.
- Yuriev, E. and Ramsland, P. A. (2013) 'Latest developments in molecular docking: 2010-2011 in review', *Journal of Molecular Recognition*, 26(5), 215-239.
- Zacharis, C. K., Kika, F. S., Tzanavaras, P. D. and Fytianos, K. (2013) 'Development and validation of a rapid ultra high pressure liquid chromatographic method for the determination of methylxanthines in herbal infusions', *Journal of Chromatography B*, 927, 218-222.
- Zhang, X. and McIntire, W. S. (1996) 'Cloning and sequencing of a copper-containing, topa quinone-containing monoamine oxidase from human placenta', *Gene*, 179(2), 279-286.